

**SEASONAL AND SPATIAL VARIABILITY OF THE CO<sub>2</sub> SYSTEM IN  
THE DELAWARE ESTUARY**

by

Andrew A. Joesoef

A thesis submitted to the Faculty of the University of Delaware in partial fulfillment  
of the requirements for the degree of Master of Science in Marine Studies

Winter 2016

© 2016 Andrew A. Joesoef  
All Rights Reserved

ProQuest Number: 10055519

All rights reserved

INFORMATION TO ALL USERS

The quality of this reproduction is dependent upon the quality of the copy submitted.

In the unlikely event that the author did not send a complete manuscript and there are missing pages, these will be noted. Also, if material had to be removed, a note will indicate the deletion.



ProQuest 10055519

Published by ProQuest LLC (2016). Copyright of the Dissertation is held by the Author.

All rights reserved.

This work is protected against unauthorized copying under Title 17, United States Code  
Microform Edition © ProQuest LLC.

ProQuest LLC.  
789 East Eisenhower Parkway  
P.O. Box 1346  
Ann Arbor, MI 48106 - 1346

**SEASONAL AND SPATIAL VARIABILITY OF THE CO<sub>2</sub> SYSTEM IN  
THE DELAWARE ESTUARY**

by

Andrew A. Joesoef

Approved: \_\_\_\_\_  
Wei-Jun Cai, Ph.D.  
Professor in charge of thesis on behalf of the Advisory Committee

Approved: \_\_\_\_\_  
Mark A. Moline, Ph.D.  
Director of the School of Marine Science and Policy

Approved: \_\_\_\_\_  
Mohsen Badiy, Ph.D.  
Acting Dean of the College of Earth, Ocean, and Environment

Approved: \_\_\_\_\_  
Ann L. Ardis, Ph.D.  
Interim Vice Provost for Graduate and Professional Education

## **ACKNOWLEDGMENTS**

I would like to express my sincere gratitude to my advisor Dr. Wei-Jun Cai for his guidance and assistance throughout the entirety of this project. I am extremely grateful for everything he has taught me, the opportunities he has given me, and the never-ending encouragement. Special thanks to Dr. Wei-Jen Huang for his continuous support and professionalism. His mentorship has truly shaped my career. I thank my committee members Dr. David Kirchman and Dr. Christopher Sommerfield for their help and guidance throughout this project. I am extremely thankful for my lab mates. All your help is tremendously appreciated. I would also like to thank Dr. Najid Hussain for his hard work and leadership in maintaining the lab. Lastly, I thank my family and friends for all of their support.

## TABLE OF CONTENTS

LIST OF TABLES .....	vi
LIST OF FIGURES .....	vii
ABSTRACT .....	ix
Chapter	
1 INTRODUCTION .....	1
2 AIR-WATER FLUXES AND SOURCES OF CARBON DIOXIDE IN THE DELAWARE ESTUARY: SPATIAL AND SEASONAL VARIABILITY .....	5
Introduction .....	5
Methods .....	8
Field Measurements .....	8
Air-water CO <sub>2</sub> Flux Estimation .....	9
Temperature-normalized <i>p</i> CO <sub>2</sub> Estimation .....	12
Estuarine and River CO <sub>2</sub> Contributions .....	14
Results .....	17
Hydrographic Conditions .....	17
Surface Water <i>p</i> CO <sub>2</sub> .....	18
Air-water CO <sub>2</sub> Fluxes .....	19
CO <sub>2</sub> Distribution across the Salinity Gradient .....	20
Seasonal Variations in Temperature-normalized <i>p</i> CO <sub>2</sub> .....	21
Discussion .....	21
Temperature vs. Biological Effects on <i>p</i> CO <sub>2</sub> .....	22
Influence of River-borne CO <sub>2</sub> on Estuarine Degassing .....	23
Internal Estuarine Production vs. River CO <sub>2</sub> Input .....	25
Assumptions and Limitations .....	26
Summary and Concluding Remarks .....	29
TABLES .....	32
FIGURES .....	35

3	SEASONAL VARIABILITY OF THE INORGANIC CARBON SYSTEM IN THE DELAWARE ESTUARY .....	44
	Introduction .....	44
	Methods .....	46
	Study Area .....	46
	Field Measurements .....	47
	Analytical Methods .....	48
	Results .....	48
	Spatial Distributions of DIC, TA, and pH .....	48
	DIC and TA Riverine Flux .....	49
	DIC and TA Export Flux .....	49
	Discussion .....	50
	Influence of River Discharge and Weathering Intensity .....	50
	Influence of River Mixing .....	53
	Seasonal Variation in DIC .....	55
	CO <sub>2</sub> Mass Balance .....	56
	Summary and Concluding Remarks .....	58
	TABLES .....	59
	FIGURES .....	62
4	CONCLUSION .....	69
	BIBLIOGRAPHY .....	71
	Appendix	
A	TEMPERATURE DERIVED COEFFICIENTS .....	91
B	TEMPERATURE AND BIOLOGICAL EFFECT .....	94

## LIST OF TABLES

Table 1. Area-averaged, standard deviation, and range of $p\text{CO}_2$ and $\text{CO}_2$ flux ( $F_{\text{CO}_2}$ ) in five of the six zones in the Delaware Estuary during each cruise. ....	32
Table 2. Flushing time in five of the six zones in the Delaware Estuary during each cruise. ....	33
Table 3. Calculated $\Delta p\text{CO}_{2\text{thermal}}$ , $\Delta p\text{CO}_{2\text{non-thermal}}$ , $T - B$ , and $T/B$ values for each salinity interval in the Delaware Estuary. ....	34
Table 4: Sampling dates, average discharge, pH, DIC, TA, and DIC to TA ratio measured at the Delaware (Trenton), Schuylkill, and Christina River. ..	59
Table 5: TA and DIC in the Delaware (Trenton), Schuylkill, and Christina River and their input fluxes in the Delaware Estuary. ....	60
Table 6: Effective TA and DIC values extrapolated from the high salinity section and their export fluxes to the ocean. ....	61
Table A1: Averaged temperature coefficients ( $\partial \ln p\text{CO}_2 / \partial T$ ) for each salinity bin. ....	92

## LIST OF FIGURES

Figure 1: Map of the Delaware Estuary divided into six zones from the head of the tide in Trenton, NJ to the mouth of the bay.....	35
Figure 2. Concentrations of (A) DIC, (B) TA, and (C) dissolved CO <sub>2</sub> in the Delaware Estuary during March 2014.....	36
Figure 3. Measured (A) surface water temperatures and (B) Delaware River discharge in the Delaware Estuary during each sampling month. ....	37
Figure 4. Spatial distributions of surface water salinity in the Delaware Estuary measured during each sampling month. ....	38
Figure 5. Spatial distributions of surface water pCO <sub>2</sub> in the Delaware Estuary measured during each sampling month. ....	39
Figure 6. Measured surface water pCO <sub>2</sub> against the salinity gradient during each sampling month in the Delaware Estuary.....	40
Figure 7. Salinity-binned intervals of temperature-normalized observed pCO <sub>2</sub> values at 13.3°C, annual mean, area-averaged pCO <sub>2</sub> values at in situ temperature, and observed pCO <sub>2</sub> values in the Delaware Estuary over the year. ....	41
Figure 8: Air-water CO <sub>2</sub> fluxes against river-borne CO <sub>2</sub> fluxes in the urban river and turbidity maximum zone of the Delaware Estuary .....	42
Figure 9: Dissolved CO <sub>2</sub> concentrations (normalized to 13.3 °C, area-averaged) due to river inputs and internal estuarine sources in each region of the Delaware Estuary. ....	43
Figure 10: Map of the Delaware Estuary and river end-members. ....	62
Figure 11: Discharge at the Delaware (Trenton), Schuylkill, and Christina River from March to October 2015.....	63
Figure 12: Salinity distributions of DIC, TA, and pH in the Delaware Estuary .....	64
Figure 13: TA and DIC versus log discharge at the Delaware (Trenton), Schuylkill, and Christina River.....	65
Figure 14: The relationship between TA and discharge (A), TA flux and discharge (B), as well as the time series of the Delaware River discharge and TA values (C) and TA flux (D) at Trenton, NJ (1998 – 2015).....	66

Figure 15: Spatial distribution of TA, DIC, and pH in the Delaware Estuary .....	67
Figure 16: DIC versus TA in the Delaware Estuary.....	68
Figure A1. Simulated surface water $p\text{CO}_2$ against salinity grouped by temperature bins. ....	93

## ABSTRACT

Distributions of surface water partial pressure of carbon dioxide ( $p\text{CO}_2$ ), dissolved inorganic carbon (DIC), total alkalinity (TA), and pH were measured along the Delaware Estuary (USA) from June 2013 to April 2015. In addition, DIC, TA, and pH were periodically examined from March to October 2015 in the non-tidal freshwater Delaware, Schuylkill, and Christina Rivers. The Delaware River was highly supersaturated in  $p\text{CO}_2$  with respect to the atmosphere during all seasons while the Delaware Bay was undersaturated in  $p\text{CO}_2$  during spring and late summer and moderately supersaturated during mid-summer, fall, and winter. While the tidal freshwater Delaware River was a strong  $\text{CO}_2$  source ( $27.1 \pm 6.4 \text{ mol-C m}^{-2} \text{ yr}^{-1}$ ), the much larger bay was a weak source ( $1.2 \pm 1.4 \text{ mol-C m}^{-2} \text{ yr}^{-1}$ ), the latter of which had a much greater area than the former. In turn, the Delaware Estuary acted as a relatively weak  $\text{CO}_2$  source ( $2.4 \pm 4.8 \text{ mol-C m}^{-2} \text{ yr}^{-1}$ ), which is in great contrast to many other estuarine systems that serve as strong  $\text{CO}_2$  sources to the atmosphere. Seasonally,  $p\text{CO}_2$  changes were greatest at low salinities ( $0 \leq S < 5$ ) with  $p\text{CO}_2$  values in the summer nearly three-fold greater than those observed in the spring and fall. Undersaturated  $p\text{CO}_2$  was observed over the widest salinity range ( $7.5 \leq S < 30$ ) during spring. Near to supersaturated  $p\text{CO}_2$  was generally observed in mid- to high salinity waters ( $20 \leq S < 30$ ) except during spring and late summer. Strong seasonal trends in internal estuarine production and consumption of  $\text{CO}_2$  were observed throughout both the upper tidal river and lower bay. Comparably, positive correlations between river-borne and air-water  $\text{CO}_2$  fluxes in the upper estuary emphasize the significance of river-borne  $\text{CO}_2$  degassing to overall  $\text{CO}_2$  fluxes. While river-borne  $\text{CO}_2$  degassing heavily influenced  $\text{CO}_2$  dynamics in the tidal freshwater Delaware River, it was largely compensated by internal biological processes within the extensive bay system of the lower estuary.

DIC and TA exhibited large spatial and seasonal variations throughout the Delaware Estuary (975-2015 and 915-2225  $\mu\text{mol kg}^{-1}$ , respectively). Along the Delaware, Schuylkill, and Christina Rivers, DIC and TA were highest after periods of low discharge and were lowest after periods of high discharge. In the Schuylkill River, during extremely low discharge, DIC and TA values exceeded those at the ocean end-member ( $> 2100 \mu\text{mol kg}^{-1}$ ). Strong negative relationships between river TA and discharge suggest that changes in  $\text{HCO}_3^-$  concentrations or TA reflect the dilution of the weather derived products in the drainage basin. Furthermore, changes in the DIC to TA ratio at the freshwater end-member may reflect inputs of soil organic matter respiration due to seasonal variations in river discharge. While the reasons remain unclear, mixing of relatively high carbonate freshwater due to eroded limestone and dolomite bedrock minerals from the lower Schuylkill River drainage basin may lead to increased DIC and TA values near the Philadelphia region. In addition to variations in river discharge and mixing from multiple tributaries, internal biological processes within the bay system also led to seasonal shifts in DIC concentrations. Annual DIC input flux to the estuary and export flux to the ocean are estimated to be about  $15.4 \pm 8.0 \times 10^9 \text{ mol C yr}^{-1}$  and  $17.0 \pm 10.6 \times 10^9 \text{ mol C yr}^{-1}$ , respectively. Based on a  $\text{CO}_2$  mass balance model, internal estuarine produced  $\text{CO}_2$  flux is small ( $5.8 \times 10^9 \text{ mol C yr}^{-1}$ ) when compared to total riverine flux. Moreover, 36% of the internally produced  $\text{CO}_2$  is exported to the coastal ocean. In the case of the Delaware Estuary and other coastal systems with long freshwater residence times, much of the DIC produced by net ecosystem production is most likely removed to the atmosphere rather than exported to the sea.

## Chapter 1

### INTRODUCTION

Over the past 60 years, human activities, mainly the burning of fossil fuels and land-use practices such as deforestation, have steadily increased carbon dioxide (CO<sub>2</sub>) levels in the atmosphere. However, less than half of the anthropogenic CO<sub>2</sub> emission remains in the atmosphere (IPCC, 2013; Sabine et al., 2004; Sunda and Cai, 2012). At present, it is estimated that about 30% of anthropogenic CO<sub>2</sub> released by fossil fuels into the atmosphere is taken up by the oceans (Le Quéré et al., 2014; Sabine et al., 2004). Increased uptake of anthropogenic CO<sub>2</sub> is rapidly acidifying surface ocean waters via the production of carbonic acid (H<sub>2</sub>CO<sub>3</sub>) (Doney, 2010; Sunda and Cai, 2012).

Moreover, the terrestrial organic carbon (OC) that is transported by large and fast-transit river systems generally bypasses decomposition in estuaries and contributes to respiration along coastal ocean margins (Cai, 2011). Consequently, rapid increases in atmospheric CO<sub>2</sub> concentrations reduce the amount of CO<sub>2</sub> released along ocean margin systems, especially in low latitude zones where a majority of the terrestrial OC is delivered (Cai, 2011). In turn, by the end of the century, recent studies suggest that pH in surface ocean waters is predicted to drop by an additional 0.2-0.3 units (Orr et al., 2005; Freely et al., 2009; Millero et al., 2009).

Human perturbations and land-use activities have significantly influenced the transport of carbon across the land and ocean continuum and have created imbalances to

present-day carbon fluxes and storage reservoirs (Aumont et al., 2001; Cotrim da Cunha et al., 2007; Quinton et al., 2010; Bauer et al., 2013; Regnier et al., 2013). In the terrestrial biosphere, organic carbon is fixed via photosynthesis by plants, removed into soil waters, and transported down aquatic conduits into the coastal and open oceans (Regnier et al., 2013). Similarly, phytoplankton in surface waters play a substantial role in the biogeochemical cycle of aquatic systems by converting CO<sub>2</sub> and nutrients into particulate organic and inorganic matter and releasing oxygen (O<sub>2</sub>) in the water column via the same photosynthetic process (Doney, 2010). In comparison, in the inorganic carbon cycle, chemical weathering of silicate and carbonate minerals removes atmospheric CO<sub>2</sub> as dissolved inorganic carbon is transported to the ocean via river and estuarine systems. Ultimately, this carbon is recycled back into the atmosphere through oceanic carbonate sedimentation and volcanic activity (Regnier et al., 2013). As carbon is transported horizontally along the land and ocean continuum, various environmental processes impact the total carbon fluxes between reservoirs.

Recent studies suggest that 10% of CO<sub>2</sub> emitted in estuaries is sustained by freshwater inputs while 90% of the CO<sub>2</sub> released is from local net heterotrophy (Regnier et al., 2013). Although the surface area of estuarine systems is roughly 4% that of continental shelves, CO<sub>2</sub> degassing fluxes of estuarine waters (0.10-0.45 Pg C yr<sup>-1</sup>) is equal to the CO<sub>2</sub> uptake by the continental shelf (0.30-0.40 Pg C yr<sup>-1</sup>) (Borges, 2005; Borges et al., 2005; Cai et al., 2006; Chen and Borges, 2009; Cai, 2011). Such high CO<sub>2</sub> degassing fluxes suggest that much of the terrestrial organic carbon is respired into CO<sub>2</sub> during transport through the estuarine mixing zone (Borges and Abril, 2011; Cai, 2011).

The heterotrophic system of estuaries is supported by terrestrial and riverine organic carbon inputs from phytoplankton and soil carbon as well as inputs from waste water discharges (Chen and Borges, 2009). Moreover, salt marsh and mangrove estuarine

waters are strong CO<sub>2</sub> sources. These systems are sustained by inputs from various autochthonous and allochthonous organic carbon sources, CO<sub>2</sub> enriched pore waters during ebbing, and high concentrations of dissolved inorganic carbon from inter-tidal and sub-tidal benthic communities (Cai et al., 2003; Neubauer and Anderson, 2003; Wang and Cai, 2004; Ferrón et al., 2007; Chen and Borges, 2009). Thus, overall estuarine systems serve as a major source of CO<sub>2</sub> to the atmosphere, with partial pressures of CO<sub>2</sub> (*p*CO<sub>2</sub>), in the absence of strong primary production, ranging from 400 to 10,000 μatm (Raymond et al., 1997; Cai and Wang, 1998; Frankignoulle et al., 1998; Borges, 2005; Borges et al., 2006; Cai, 2011).

The Delaware Estuary system is a typical river-dominated coastal plain estuarine environment. With the discharge of anthropogenic waste concentrated upstream of the salinity gradient and a relatively simple drainage pathway, the Delaware Estuary is fairly easy to characterize, and because of this, it has served as a model estuary for biogeochemical study (Cifuentes et al., 1988; Sharp et al., 2009). In the past, the tidal freshwater reach of the Delaware Estuary received large quantities of municipal and industrial waste that later flowed into the Delaware Bay (Sharp et al., 2009; Sharp, 2010). The amount of discharged waste has significantly been reduced since the enactment of the Clean Water Act in the 1970s and tertiary treatment developments (Sharp et al., 2009; Sharp, 2010). Moreover, the Delaware Bay is a large shallow enclosed embayment surrounded by partially undeveloped salt marshes (Cifuentes et al., 1988). Substantial phytoplankton production occurs as nutrients from the Delaware River, as well as from municipal waste, is released and diluted into the bay region. During spring seasons when river discharge is high, much of the central portion of the estuary becomes stratified, confining phytoplankton in surface, and increasing total biomass (Culberson, 1988).

With increasing urbanization and industrial activity, the biogeochemistry of the Delaware Estuary may respond differently to the rapidly changing environment than it did in the past. Extensive coastal surveys provide the opportunity to obtain high quality data that deepen our understanding of the physical and biological processes that control coastal systems. Except for a few recent studies and the pioneering work of Jonathan Sharp and Charles Culberson, (Culberson, 1988; Sharp, 2009), research on inorganic carbon in the Delaware Estuary has been limited. In Chapter 2, I report the first seasonal distribution of  $p\text{CO}_2$  and air-water  $\text{CO}_2$  flux in the Delaware Estuary from 2013 through 2014. I further assess the temperature and biological effects on  $p\text{CO}_2$  distributions as well as the overall contribution of internal versus riverine sources on  $\text{CO}_2$  inputs to the estuarine system. In Chapter 3, I examine how input from multiple tributaries contribute to total DIC and TA riverine and export fluxes. In addition, I investigate the seasonal variation of the inorganic carbon system in the Delaware Estuary from 2013 to 2015. Lastly, in Chapter 4 we summarize our findings and emphasize the importance that extensive coastal surveys and research studies have to our overall understanding of oceanic systems.

## Chapter 2

### AIR-WATER FLUXES AND SOURCES OF CARBON DIOXIDE IN THE DELAWARE ESTUARY: SPATIAL AND SEASONAL VARIABILITY

#### Introduction

While, globally, the surface area of estuaries is only about 4% that of continental shelves, recent studies have concluded that the carbon dioxide (CO<sub>2</sub>) degassing flux from estuarine waters is as large as the CO<sub>2</sub> uptake by the continental shelf (Borges, 2005; Borges et al., 2005; Cai et al., 2006; Chen and Borges, 2009; Cai, 2011). Global estuarine waters are estimated to emit 0.10-0.45 Pg C yr<sup>-1</sup> while continental shelves take up 0.20-0.40 Pg C yr<sup>-1</sup> (Borges, 2005; Borges et al., 2005; Cai, 2011; Chen et al., 2013; Regnier et al., 2013; Laruelle et al., 2015). Such large estuarine CO<sub>2</sub> degassing suggests that much of the terrestrial organic carbon, including that from coastal wetlands, is respired to CO<sub>2</sub> during transport through the estuarine zone, though the relative importance of river supplied CO<sub>2</sub> and organic carbon versus those from the coastal wetlands is debatable (Borges and Abril, 2011; Cai, 2011). In turn, estuarine waters are a major source of CO<sub>2</sub> to the atmosphere, with partial pressures of CO<sub>2</sub> (*p*CO<sub>2</sub>) ranging from 350 to 10,000 μatm and air-water CO<sub>2</sub> fluxes ranging from -5 to 80 mol C m<sup>-2</sup> yr<sup>-1</sup> (Raymond et al., 1997; Cai and Wang, 1998; Frankignoulle et al., 1998; Borges, 2005; Borges et al., 2006; Borges and Abril, 2011; Cai 2011).

There is rising concern that global estuarine CO<sub>2</sub> degassing flux may be overestimated (Cai, 2011). Although substantial progress has been achieved over the past decade (Borges and Abril, 2011; Chen et al., 2013; references therein), our knowledge of CO<sub>2</sub> degassing fluxes and their controlling processes in estuaries remains insufficient. Globally, the majority of past estuarine CO<sub>2</sub> studies have been conducted on small estuarine systems, which typically have high *p*CO<sub>2</sub>. (Chen and Borges, 2009; Cai, 2011;

Borges and Abril, 2011). Specifically, in the U.S. east coast, high  $p\text{CO}_2$  was found in estuaries along the southeastern (Cai and Wang, 1998; Jiang et al., 2008) and northeastern (Salisbury et al., 2008; Hunt et al., 2011) coastal regions. While high  $p\text{CO}_2$  was also found in small estuaries along the U.S. Mid-Atlantic coast (Raymond et al., 1997; Raymond et al., 2000), only a few estuarine  $\text{CO}_2$  studies have been conducted in this region, such as Crosswell et al., (2012) in the Neuse River, NC, Raymond et al., (1997) in Hudson River, NY, and Raymond et al., (2000) in the York River, VA. Thus, there is limited research on  $\text{CO}_2$  dynamics in large estuaries or bay systems with long freshwater residence times in the U.S. Mid-Atlantic coast (most notably the Chesapeake and Delaware estuaries). Presumably, these large estuaries have lower  $p\text{CO}_2$  than small estuaries or bay systems with rapid freshwater transit times (Borges and Abril, 2011; Cai, 2011). Except for a few recent studies and the pioneering work of Sharp and Culberson, over the past 30 years there have been few inorganic carbon studies in the Delaware Estuary (Culberson, 1988; Sharp, 2009). Air-water  $\text{CO}_2$  fluxes, total DIC fluxes, and ongoing evaluations of water acidification have not been consistently (via annual and seasonal surveys) studied. Overall, there is a lack of data and pressing need to synthesize and expand global research to larger estuaries. Furthermore, of past estuarine  $\text{CO}_2$  studies, many lack spatial and seasonal coverage of surface water  $p\text{CO}_2$  and air-water  $\text{CO}_2$  fluxes, making flux estimates highly uncertain.

The Delaware Estuary is composed of a 100-km-long tidal Delaware River and the Delaware Bay (Figure 1) (Sharp, 2010). With a relatively simple hydrology, the Delaware Estuary is fairly easy to characterize, and because of this, it has served as a model estuary for biogeochemical studies (Cifuentes et al., 1988; Sharp et al., 2009). The tidal freshwater portion of the Delaware River flows from the head of the tide near Trenton, NJ through the greater Philadelphia area, the sixth largest municipal region of

the U.S., before passing into the saline Delaware Bay (Figure 1) (Sharp et al., 2009; Sharp, 2010). In turn, the upper Delaware River is heavily influenced by major industrial activity and continuously responding to a rapidly changing environment. For example, in the mid-20<sup>th</sup> century, the urban river of the Delaware Estuary suffered from severe hypoxia with average summer dissolved oxygen (DO) concentrations near zero value (Sharp, 2010). Fortunately, the implementation of the Clean Water Act (CWA) in the early 1970s helped promote efforts to improve water quality conditions in the Delaware River. With major upgrades to large sewage treatment plants, DO concentrations since the early 1990s have consistently been above the CWA standard of 3.5 mg L<sup>-1</sup> (~219  $\mu\text{mol L}^{-1}$ ) (Sharp, 2010). Nonetheless, high  $p\text{CO}_2$  is still expected to associate with strong respiratory O<sub>2</sub> consumption in the upper estuary. In contrast, the Delaware Bay is a large shallow embayment surrounded by salt marshes with minimal industrial or municipal inputs (Cifuentes et al., 1988). Thus, the Delaware Estuary is governed by the dynamic interaction between a river-dominated upper estuary and an ocean-dominated lower bay. This feature, typical for other large estuaries, and depending on river flow and geomorphology, smaller estuarine systems as well, provides us the opportunity to examine how contrasting geographical settings, physical mixing processes, and ecosystem metabolism in an extensive bay system can affect CO<sub>2</sub> gas exchange.

In this paper, we report the first seasonal distribution of  $p\text{CO}_2$  and air-water CO<sub>2</sub> flux in the Delaware Estuary, which was surveyed nine times via various day- to week-long surveys from 2013 through 2014. We further assess the temperature and biological effects on  $p\text{CO}_2$  distributions as well as the overall contribution of internal versus riverine sources on CO<sub>2</sub> inputs to the estuarine system. Finally, we present a summarized  $p\text{CO}_2$  distribution over the study area and provide a conceptual model to illustrate the control mechanisms on surface water CO<sub>2</sub> dynamics in the Delaware Estuary.

## Methods

### *Field Measurements*

The Delaware Estuary was surveyed on nine cruises: 08-10 June 2013, 08-15 August 2013, 17 October 2013, 17-22 November 2013, 23-24 March 2014, 03 July 2014, 27 of August to 01 of September 2014, 30 of October to 02 November 2014, and 05 December 2014. Distributions of  $p\text{CO}_2$ , dissolved inorganic carbon (DIC), total alkalinity (TA), and pH were measured from the mouth of the bay to the near zero salinity of the estuary in five of the nine cruises. During the August and October 2013 cruises, only surface water  $p\text{CO}_2$  was measured.

To monitor levels of  $p\text{CO}_2$ , surface water was directly pumped from 1 to 2 meters below the sea level through an underway  $p\text{CO}_2$  analyzer (AS-P2, Apollo Scitech) installed in the shipboard laboratory (Huang et al., 2015). Surface water flowed into a 1 L volume shower head equilibrator at a minimum rate of  $1.7 \text{ L min}^{-1}$  to facilitate rapid gas exchange. A specifically designed water-drain system is attached to the equilibrator to insure that the pressure inside and outside remains balanced (Jiang et al., 2008b). The equilibrated gas was pumped through a water trap (Peltier cooler), which removed most of the water vapor, and then into a drying tube packed with magnesium perchlorate [ $\text{Mg}(\text{ClO}_4)_2$ ] or Nafion tubing. Surface water  $\text{CO}_2$  (mole fraction of dry air [ $x\text{CO}_2$ ]) was measured approximately every one and a half minutes using an underway flow-through system equipped with a non-dispersive infrared (NDIR) gas analyzer (Li-Cor Model Li-7000, Lincoln, NE, USA). This LICOR 7000 was calibrated, every 3-6 hours, against three or four  $\text{CO}_2$  gas standards (151.5, 395.4, 982.6, and 1969 ppm  $\text{CO}_2$  in air) referenced against standards traceable to those of the National Institute of Standards and Technology (NIST). Atmospheric  $x\text{CO}_2$  was measured every 3-6 hours using the same  $\text{CO}_2$  system. In order to avoid contamination from the ship's stack gases or other possible

sources of air pollution, the inlet of the atmospheric CO<sub>2</sub> pipe was installed on the highest platform in the front of the ship. An on-board Sea-bird thermosalinograph (SBE-45) measured surface water temperature and salinity. To calculate surface water and atmospheric  $p\text{CO}_2$  values, all  $x\text{CO}_2$  measurements were corrected to 100% saturation of water vapor pressure and the in situ surface water temperature (Dickson et al., 2007).

DIC and TA water samples were collected throughout the salinity gradient. Multiple samples were taken at near salinity zero and at the mouth of the bay to obtain river and ocean end-member values. Samples for DIC and TA measurements were filtered through a cellulose acetate filter (0.45  $\mu\text{m}$ ) into 250 ml borosilicate bottles and then fixed with 100  $\mu\text{l}$  of saturated mercury bichloride solution (Cai and Wang, 1998; Jiang et al., 2008a). When collecting water, all bottles were overflowed for at least twice its volume to minimize contact with the atmosphere. Afterwards, sample bottles were kept in 4 to 10°C for future analysis. DIC was determined by acidifying 0.5-1.0 ml samples with phosphoric acid. The extracted CO<sub>2</sub> gas was subsequently quantified via an infrared gas analyzer (AS-C3 Apollo Scitech). TA was measured by Gran titration (Gran, 1952) using the open cell method with a semi-automatic titration system (AS-ALK2, Apollo Scitech) (Cai et al., 2010a; Huang et al., 2012). Both DIC and TA measurements were calibrated against certified reference material (CRM, provided by A.G. Dickson from Scripps Institution of Oceanography) at a precision level of about  $\pm 2 \mu\text{mol kg}^{-1}$  (Huang et al., 2012).

### ***Air-water CO<sub>2</sub> Flux Estimation***

In this study, air-water CO<sub>2</sub> fluxes ( $F$ ,  $\text{mmol m}^{-2} \text{d}^{-1}$ ) at pixel  $i$  of a 0.01 longitude x 0.01 latitude grid were calculated as follows:

$$F_i = k_i \cdot K_{oi} \cdot (p\text{CO}_{2(\text{water})i} - p\text{CO}_{2(\text{air})i}) \quad (1)$$

where  $k_i$  ( $\text{cm h}^{-1}$ ) is the gas transfer velocity of  $\text{CO}_2$ ,  $K_{oi}$  is the solubility coefficient of  $\text{CO}_2$  ( $\text{mol L}^{-1} \text{atm}^{-1}$ ), which can be calculated from in situ temperature and salinity (Weiss, 1974), and  $p\text{CO}_{2(\text{water})i}$  and  $p\text{CO}_{2(\text{air})i}$  ( $\mu\text{atm}$ ) are the partial pressure of  $\text{CO}_2$  in the water and the air, respectively. The mean atmospheric  $x\text{CO}_2$  during each cruise and the sea surface temperature, salinity, and pressure were used to calculate the  $p\text{CO}_{2(\text{air})i}$ . A positive  $F$  value indicates  $\text{CO}_2$  transfer from water to the atmosphere.

Generally, two main issues arise when trying to accurately determine air-water  $\text{CO}_2$  fluxes in coastal waters: how to accurately represent surface turbulence and obtaining spatial and temporal heterogeneity of  $p\text{CO}_2$  distributions. One of the greatest uncertainties when calculating air-water  $\text{CO}_2$  fluxes is estimating gas transfer velocities (Wanninkhof et al., 2009). While gas transfer velocities primarily depend on wind regime in the open ocean, in coastal and shallower estuaries it is probably more complicated as other factors such as tidal currents, bottom stress, wave slope, turbidity, surface films, and fetch limitation can also influence gas exchange rates (Raymond and Cole, 2001; Borges et al., 2004; Zappa et al., 2007; Jiang et al., 2008a; Abril et al., 2009). Unfortunately, because there have not been many studies on gas transfer velocities in estuaries, we relied on wind speed dependence to estimate gas exchange rates. Moreover, limited research has been conducted at wind speeds less than  $4 \text{ m s}^{-1}$ . In turn, quadratic relationships that estimate  $k$  often extrapolate to zero at low wind speeds (Wanninkhof et al., 2009). Increasing evidence suggests that  $k$  does not approach zero at low wind speeds but rather asymptotes to a finite value due to various external factors such as buoyancy effects, chemical enhancements, and physical mixing processes (McGillis et al., 2001; McGillis et al., 2004; Wanninkhof et al., 2009). To avoid gas transfer velocities of zero in river and inland waters where wind speeds are typically low, we adopted the gas transfer relationship as proposed by Wanninkhof et al., (2009):

$$k_{660} = 3 + 0.1 \cdot U_{10} + 0.064 \cdot U_{10}^2 + 0.011 \cdot U_{10}^3 \quad (2)$$

where  $k_{660}$  is the gas transfer velocity at the Schmidt number of 660, which can be calculated from in situ sea surface temperature (Wanninkhof, 1992), and  $U_{10}$  is the wind speed at 10 meters above the water surface. Another challenge to accurately determining air-water CO<sub>2</sub> fluxes is obtaining reliable spatial and temporal  $p\text{CO}_2$  distributions.

Unfortunately, while seasonal distributions of  $p\text{CO}_2$  were measured from the mouth of the bay to near zero salinity of the estuary (north to south), our lack of cross bay transects (east to west) limits our knowledge of CO<sub>2</sub> dynamics in shallow water regions of the estuary. Thus, there is a pressing need to conduct more research near these shallow water boundaries.

In addition, because the relationship between  $k$  and mean wind speeds is nonlinear, temporal distributions of wind speeds influence gas transfer velocities (Wanninkhof, 1992; Wanninkhof et al., 2002). To accurately determine the effect of variability of winds over a month, Wanninkhof (1992) introduced the nonlinearity coefficient of the wind speeds ( $C_2$ ), which is calculated as follows (Wanninkhof et al., 2002; Jiang et al., 2008b):

$$C_2 = \left( \frac{1}{n} \sum_{j=1}^n U_j^2 \right) / U_{\text{mean}}^2 \quad (3)$$

where  $C_2$  is the nonlinearity coefficient for quadratic terms of gas transfer relationships,  $U_j$  is the high-frequency wind speed collected at the buoys,  $U_{\text{mean}}$  is the monthly mean wind speed, and  $n$  is the total number of available wind speeds during that month. We used high-frequency wind speed data (measured every six minutes) obtained from four National Oceanic and Atmospheric Administration (NOAA) buoys (LWSD1, CMAN4, SJSN4, and DELD1) to calculate the nonlinearity coefficients at each buoy and extrapolate them to the entire estuary. Using the calculated nonlinearity coefficients, gas

transfer relationships were corrected to obtain the most accurate relationship between gas transfer velocities and wind speeds during each month.

In order to calculate area-averaged CO<sub>2</sub> flux throughout the Delaware Estuary, the system was divided into five geographic zones as defined by Sharp et al. (2009).

However, due to rapid change in *p*CO<sub>2</sub> values across the mid-bay, this region was split into an upper and mid-bay zone to allow for a more robust comparison of *p*CO<sub>2</sub> and CO<sub>2</sub> fluxes throughout the system (Figure 1). Surface water *p*CO<sub>2</sub>, temperature, salinity, wind speed, and pressure were interpolated onto 0.01 x 0.01 grid. Following the same method as presented in Jiang et al., (2008b), flux *F*<sub>*i*</sub> at each pixel was calculated:

$$S_i = \frac{\Delta\text{Lon}}{2\pi} \cdot 2 \cdot \pi \cdot R^2 \cdot [\sin(\text{Lat}_i + \frac{1}{2}\Delta\text{Lat}) - \sin(\text{Lat}_i - \frac{1}{2}\Delta\text{Lat})] \quad (4)$$

where *S*<sub>*i*</sub> is the total area surrounding pixel *i*; ΔLon and ΔLat are the longitude and latitude intervals of the grid respectively, Lat<sub>*i*</sub> is the latitude at pixel *i*, and *R* is the radius of the earth. The area-averaged CO<sub>2</sub> flux was calculated as followed (Jiang et al., 2008b):

$$F_{\text{area-averaged}} = \frac{1}{S_1 + S_2 + \dots S_n} \cdot \sum_{i=1}^n F_i \cdot S_i \quad (5)$$

Because there is no precise method to account for the uncertainties of air-water CO<sub>2</sub> fluxes, we followed the same approach as described in Jiang et al., (2008b). Atmospheric measurements for each cruise and gas transfer velocities of Wanninkhof et al., (2009) and Wanninkhof (2014) were used to estimate standard deviations of the atmospheric CO<sub>2</sub> and CO<sub>2</sub> flux, respectively.

### ***Temperature-normalized pCO<sub>2</sub> Estimation***

Temperature changes are important as they influence surface water *p*CO<sub>2</sub> by governing the thermodynamic equilibrium of the inorganic carbon system (Takahashi et al., 1993). If only controlled by temperature change and no other physical (mixing) or biogeochemical changes, *p*CO<sub>2</sub> in surface seawater would double for every 16°C increase

( $\partial \ln p\text{CO}_2 / \partial T = 0.0423^\circ\text{C}^{-1}$ ) (Takahashi et al., 1993). The temperature constant above determined by Takahashi et al., (1993) works well for open ocean waters with salinities between 34 and 36 as physical mixing with freshwater is generally minor. After temperature normalization, one may attribute the remaining  $p\text{CO}_2$  change to non-thermal processes (mostly biological activity but possibly also mixing processes). However, in coastal oceans mixing is often serious and influences the interpretations of observed temperature dependences. For example, Jiang et al., (2008a) found that values of ( $\partial \ln p\text{CO}_2 / \partial T$ ) in river- and marine-dominated estuaries were less (about  $0.027\text{-}0.042^\circ\text{C}^{-1}$ ) than that determined by Takahashi et al., (1993). We suggest that a thermodynamic prediction for estuarine water should be used for such comparisons. Calculated temperature derived coefficients are discussed in detail in Appendix A and in Bai et al., (2015). Similar to the results found in Jiang et al., (2008a), temperature derived constants were lower than the isochemical seawater constant  $0.0423^\circ\text{C}^{-1}$  determined by Takahashi et al., (1993). Thus, knowing the extensively complex nature of estuarine systems, it is important to note that derived variances in temperature-normalized  $p\text{CO}_2$  provide only a relatively simple analysis of seasonal  $p\text{CO}_2$  fluctuations due to temperature and biological processes as it neglects the impact that various physical processes, turbulent forces, and tidal mixing scenarios have on  $p\text{CO}_2$  dynamics.

Using a similar approach as in Takahashi et al., (2002), we also attempted to separate the temperature effect from other non-thermal effects on seasonal  $p\text{CO}_2$  change. We first normalized the  $p\text{CO}_2$  at in-situ temperature to the 10-year (2004-2014) annual mean temperature of  $13.3^\circ\text{C}$  via the following (Takahashi et al., 2002):

$$(p\text{CO}_{2\text{obs}} \text{ at } T_{\text{mean}}) = (p\text{CO}_{2\text{obs}}) \cdot \exp[C_s(T_{\text{mean}} - T_{\text{obs}})] \quad (6)$$

where  $T$  is temperature ( $^\circ\text{C}$ ),  $C_s$  is the averaged ( $\partial \ln p\text{CO}_2 / \partial T$ ) value for the salinity interval, and subscripts “mean” and “observed” indicate the annual mean and observed

values, respectively. Through this approach, we attributed any differences between calculated and observed  $p\text{CO}_2$  values to be the result of biological activity and/or physical mixing processes (non-thermal). Because salinity gradients down the estuary vary greatly depending on the season, river discharge, tidal cycle, precipitation, and other circulation processes, salinity-binned climatologies can provide crucial insight and a different perspective to the various physical and biological controls behind observed  $p\text{CO}_2$  distributions that geographic boundaries may not. In turn,  $p\text{CO}_2$  values from each survey were constructed into salinity-binned climatologies (intervals of five units from 0-30) to better isolate and interpret the thermal versus non-thermal effects on seasonal  $p\text{CO}_2$  fluctuations. Observed  $p\text{CO}_2$  values during months with no surveys were estimated by linearly regressing data from adjacent months with sample measurements. In contrast, to best analyze the effect of temperature changes on observed  $p\text{CO}_2$  values, annual mean  $p\text{CO}_2$  values across each salinity interval were used in conjunction with the mean and observed temperatures via the following equation (Takahashi et al., 2002):

$$(p\text{CO}_{2\text{mean}} \text{ at } T_{\text{obs}}) = (p\text{CO}_2)_{\text{mean}} \cdot \exp[C_s(T_{\text{obs}} - T_{\text{mean}})] \quad (7)$$

Using this method, we attributed any differences between calculated mean versus observed  $p\text{CO}_2$  values as a result of seasonal temperature changes. To remove the temperature effect from observed in situ  $p\text{CO}_2$ , the observed  $p\text{CO}_2$  values were normalized to a constant temperature of 13.3°C, which was the 10-year annual mean water temperature measured in the Delaware Estuary from 2004 to 2014.

### ***Estuarine and River CO<sub>2</sub> Contributions***

Due to various CO<sub>2</sub> sources such as the degradation of organic matter, discharge of sewage effluents, soil induced respiration, freshwater runoff, and addition of humic substances, river water flowing into estuarine systems are typically supersaturated in CO<sub>2</sub>

with respect to the atmosphere (Raymond et al., 2000; Abril and Borges, 2004; Borges et al., 2006). To investigate the influence of river-borne CO<sub>2</sub> input to overall air-water CO<sub>2</sub> fluxes, we used similar methods as performed in Jiang et al., (2008a). In situ DIC and TA measurements were coupled using the Excel macro CO2SYS (Pierrot, 2006) and inorganic carbon dissociation constants from Millero et al. (2006) for estuarine waters to calculate dissolved CO<sub>2</sub> concentrations. We first estimated the contribution of the ocean end-member to the estuarine DIC alone as follows (Jiang et al., 2008a):

$$\text{DIC}_{\text{mixing w/o}} = \frac{S_i}{S_{\text{ocean}}} \cdot \text{DIC}_{\text{ocean}} \quad (8)$$

where  $\text{DIC}_{\text{mixing w/o}}$  is the DIC concentration after the ocean end-member is diluted by fresh water with zero DIC and  $S_i$  and  $S_{\text{ocean}}$  are in situ and ocean end-member salinities, respectively (Figure 2A). When DIC inputs from both the river and the ocean end-members were considered, estuarine DIC was estimated using a two end member mixing model as follows (Jiang et al., 2008a):

$$\text{DIC}_{\text{mixing w/R}} = \frac{S_i}{S_{\text{ocean}}} \cdot \text{DIC}_{\text{ocean}} + \left(1 - \frac{S_i}{S_{\text{ocean}}}\right) \cdot \text{DIC}_{\text{river}} \quad (9)$$

where  $\text{DIC}_{\text{mixing w/R}}$  is the DIC concentration after mixing of river and ocean end-members and  $\text{DIC}_{\text{river}}$  is the river end-member (Figure 2A). With much of the DIC pool dominated by carbonate and bicarbonate ions, Sharp et al., (2009) observed small seasonal influences on DIC concentrations due to temperature affects and biological activity. They suggest that the majority of variability in DIC in the upper tidal river of the Delaware Estuary is due to the combined interaction of varying precipitation rates and prior meteorological conditions. This is expected as river DIC and TA are largely a dilution of weathering production by rain (Cai et al., 2008). However, at higher salinities, any drawdown of DIC relative to salinity is small since less than 1% of the DIC pool exists as  $p\text{CO}_2$  (Sharp et al., 2009). Thus, while total DIC concentrations illustrate some fluctuations in biological activity (which occurred mostly at the highly productive mid-

bay), it is an integrated measurement of freshwater and seawater mixing (Sharp et al., 2009).  $TA_{\text{mixing w/o}}$  and  $TA_{\text{mixing w/R}}$  were also estimated using similar equations by replacing DIC with TA (Figure 2B). Because  $CO_2$  concentrations do not change linearly during mixing, they were estimated using corresponding DIC and TA mixing values (Figure 2C) (Jiang et al., 2008a). Moreover, since  $CO_2$  concentrations fluctuate with temperature change, the 10-year (2004-2014) annual mean temperature of 13.3 °C was used in this work. Thus, the  $CO_2$  contribution due to river input ( $\Delta[CO_2]_{\text{riv}}$ ) was estimated as follows:

$$[CO_2]_{\text{riv}} = [CO_2]_{\text{mixing w/R}} - [CO_2]_{\text{mixing w/o}} \quad (10)$$

Calculated river  $CO_2$  inputs ( $[CO_2]_{\text{riv}}$ ) and combined river discharges from the Schuylkill and Delaware Rivers for each month were used to compute river-borne  $CO_2$  fluxes in the upper tidal river.

To further investigate the influence of  $CO_2$  inputs from the river (external) versus production from within the estuary (internal), we used a similar but modified method as performed in Jiang et al., (2008a). The  $CO_2$  contribution from within the estuarine zone ( $[CO_2]_{\text{est}}$ ) was estimated as follows:

$$[CO_2]_{\text{est}} = [CO_2]_i - [CO_2]_{\text{mixing w/R}} + (\tau_i \cdot F_i) \quad (11)$$

where ( $[CO_2]_i$ ) is the in situ  $CO_2$  concentration,  $\tau_i$  is the flushing time, and  $F_i$  is the air-water  $CO_2$  flux. Specifically, ( $[CO_2]_i$ ) was calculated using in situ DIC and TA concentrations and  $\tau_i$  was estimated using river discharge rates and volume of each region (Table 2) (Sheldon and Alber, 2002). Surveys that did not contain sufficient river end-member DIC and TA measurements were excluded. Alternatively, Eq. (11) suggests that integrated  $CO_2$  degassing ( $\tau_i \cdot F_i$ ) is supported by the deficit or excess  $CO_2$  concentration ( $[CO_2]_{\text{mixing w/R}} - [CO_2]_i$ ) plus the internal estuarine  $CO_2$  production or consumption ( $[CO_2]_{\text{est}}$ ) exhibited across each region.

## Results

### *Hydrographic Conditions*

Measured surface water temperatures and river discharge during each cruise were compared with the 10-year (2004-2014) and 30-year (1980-2014) monthly averages for surface water temperatures and Delaware River discharge rates, respectively. Water temperatures were slightly cooler than the 10-year average during March 2014, June 2013, and July 2014, while water temperatures during the rest of the cruises were slightly warmer (Figure 3A) (USGS gauge 01463500). Discharge conditions during each survey were compared with the 30-year average discharges from 1980 to 2014 (Figure 3B) (USGS gauge 01463500). The Delaware River discharge was greatest during March 2014 and June 2013. Discharges were smallest during August 2014, October 2013, November 2013, and November 2014. Of the four low-flow months, all of them except for August 2014 had discharge rates less than one standard deviation of the 30-year average.

The surface water salinity distributions confirm the various river discharge conditions recorded throughout each survey (Figure 4A-I). Salinity  $< 1.0$  was reached on six of the nine cruises (Figure 4A, 4B, 4C, 4E, 4G, and 4H). The July 2014, August 2013 and October 2013 cruises only transected as far north as the Chesapeake-Delaware Canal (about  $39.55^{\circ}\text{N}$ ) (Figure 1). Salinity  $< 1.0$  (a minimum of 0.98) was only observed during the July 2014 excursion, which had the highest river discharge of the three partial surveys (Figure 4C). Generally, high salinity waters (25-32.5) were observed in the lower bay and salinities around 20 to 25 in the mid-bay. The upper bay had a much broader scale ranging from salinities 10 to 20 and during the high flow months of March 2014 and June 2013 salinities  $< 10$  were observed (Figure 4A and 4B). Salinities did not reach less than 0.25 in the turbidity maximum zone. Salinity distributions in the urban river were limited due to the lack of surveys conducted in this region.

### *Surface Water $p\text{CO}_2$*

Generally, surface water  $p\text{CO}_2$  in the Delaware Estuary increased from the ocean to the river end-member with  $p\text{CO}_2$  values ranging from about 150 to over 4000  $\mu\text{atm}$  (Figure 5A-I). Moreover,  $p\text{CO}_2$  exhibited strong seasonal variations across both river and bay portions. The most pronounced shifts in surface water  $p\text{CO}_2$  were observed within the lower urban river and turbidity maximum river zones of the Delaware River with  $p\text{CO}_2$  being lowest in the cool months (March, October, and November) and highest in the warm months (June, July, and August) (Table 1). During all months, the turbidity maximum zone was supersaturated in  $\text{CO}_2$  with respect to the atmosphere (atmospheric  $p\text{CO}_2$ : 375-398  $\mu\text{atm}$ ) except during March 2014 (Figure 5A). Throughout the summer and early fall (June, July, and August),  $p\text{CO}_2$  ranged from about 650  $\mu\text{atm}$  to over 4000  $\mu\text{atm}$  across the turbidity and lower urban river zones (Figure 5B-E). In late fall (October and November),  $p\text{CO}_2$  dropped to as low as 500  $\mu\text{atm}$  in the turbidity maximum zone and reached 1400  $\mu\text{atm}$  within the lower urban river zone (Figure 5F-H). However, the decrease in  $p\text{CO}_2$  values were not always observed as temperatures cooled. During the winter (December), surface water  $p\text{CO}_2$  values increased across the turbidity maximum zone ranging from about 650 to 1000  $\mu\text{atm}$  (Figure 5I). As discussed later, this shift in  $p\text{CO}_2$  during winter is likely a result of opposing timing of seasonal temperature cycles and respiration versus that of river discharge rates.

Surface water  $p\text{CO}_2$  exhibited strong seasonal variations in the Delaware Bay as well (Figure 5A-I). In March 2014, most likely due to a strong biological bloom and low temperature (Figure 3A), the entire bay system (upper, mid-, and lower) was under-saturated in  $\text{CO}_2$  with respect to the atmosphere (Table 1). In particular,  $p\text{CO}_2$  reached as low as 160  $\mu\text{atm}$  in the mid-bay (Figure 5A). During the warmer summer months (June, July, and August),  $p\text{CO}_2$  in the bay remained around 400 to 500  $\mu\text{atm}$  with occasional

undersaturation occurring in the mid-bay region (Figure 5B-E). In August 2014, low  $p\text{CO}_2$  ranging from about 200 to 350  $\mu\text{atm}$  was observed throughout much of the mid- and lower bay regions (Figure 5E). In contrast, during the late fall  $p\text{CO}_2$  values were fairly homogenous throughout the mid- and lower bay (400-450  $\mu\text{atm}$  in October 2013 and 2014 and 375-415  $\mu\text{atm}$  in November 2013) and slightly higher  $p\text{CO}_2$  occurring in the upper bay (Figure 5F-H). In December 2014,  $p\text{CO}_2$  increased throughout all regions of the bay with  $p\text{CO}_2$  values ranging from 500 to 650  $\mu\text{atm}$  (Figure 5I). While reasons to support the elevated  $p\text{CO}_2$  values remain unclear, stratification of subsurface waters in late fall followed by strong winter mixing during winter (December 2014) and a two-fold increase in river discharge could explain the elevated  $p\text{CO}_2$  values observed throughout the mid- and the lower bay systems (Figure 3B).

#### ***Air-water CO<sub>2</sub> Fluxes***

The urban river and turbidity maximum zone served as strong sources of  $\text{CO}_2$  to the atmosphere and was positive during all months (Table 1). Across the upper to lower bay portions of the estuary, uptake of  $\text{CO}_2$  from the atmosphere was greatest during spring (March) ranging from  $F_{\text{CO}_2} = -12.1$  to  $-20.0 \text{ mmol m}^{-2} \text{ d}^{-1}$  (Table 1). The  $\text{CO}_2$  uptake flux was highest in March 2014 in the mid-bay ( $-20.0 \text{ mmol m}^{-2} \text{ d}^{-1}$ ), while the highest  $\text{CO}_2$  degassing flux occurred in June 2014 in the urban river ( $144.8 \text{ mmol m}^{-2} \text{ d}^{-1}$ ) (Table 1). Air-water  $\text{CO}_2$  fluxes in the upper to lower bay regions decreased in early winter (December) to a minimum in early spring (March), followed by an increase to an annual maximum in early summer (June). In the turbidity maximum zone and urban river, area-averaged  $\text{CO}_2$  fluxes followed the same seasonal decrease in spring and increase in summer but reached an annual minimum in late fall instead of early spring. In

winter (December), the mid- and lower bays, which were typically sinks or weak sources of CO<sub>2</sub>, exhibited relatively strong CO<sub>2</sub> fluxes to the atmosphere.

### ***CO<sub>2</sub> Distribution across the Salinity Gradient***

To further investigate  $p\text{CO}_2$  variations along the Delaware Estuary, we examined distributions of  $p\text{CO}_2$  across the salinity gradient. Due to limited area and salinity coverage, surveys conducted in August and October 2013 were excluded for this assessment. In all months,  $p\text{CO}_2$  versus salinity followed a concave upward trend towards the river end-member (Figure 6). The seasonal variation between  $p\text{CO}_2$  values was largest at low salinities around 0 to 5 with  $p\text{CO}_2$  values in the summer (June, July, and August) nearly two-fold greater than those observed in the spring (March) and fall (October and November) seasons (Figure 6). In all seasons,  $p\text{CO}_2$  was supersaturated with respect to the atmosphere from salinities 0 to 5. In spring, undersaturated  $p\text{CO}_2$  was observed over the widest salinity range from 7.5 to 30. In summer, undersaturated  $p\text{CO}_2$  was generally not observed except at moderate salinities around 17 to 28 in August. In fall,  $p\text{CO}_2$  values were near atmospheric concentrations around mid-salinity waters and were only undersaturated at salinities greater than 25. In winter (December),  $p\text{CO}_2$  values were always supersaturated with respect to the atmosphere across the entire salinity range. Seasonally, the Delaware Estuary served as a strong CO<sub>2</sub> sink ( $-5.0 \pm 6.0 \text{ mol-C m}^{-2} \text{ yr}^{-1}$ ) in the spring, a strong source ( $4.9 \pm 8.1 \text{ mol-C m}^{-2} \text{ yr}^{-1}$ ) in the summer, a weak source ( $1.0 \pm 2.4 \text{ mol-C m}^{-2} \text{ yr}^{-1}$ ) in the fall, and a strong source ( $5.7 \pm 1.9 \text{ mol-C m}^{-2} \text{ yr}^{-1}$ ) in the winter. While low salinity waters were strong CO<sub>2</sub> sources, proportionally these upper regions ( $0 \leq S < 10$ ) were small in comparison to the total estuarine study area. In turn, their area-averaged contribution ( $27.1 \pm 6.4 \text{ mol-C m}^{-2} \text{ yr}^{-1}$ ) to overall regional flux ( $2.4 \pm 4.8 \text{ mol-C m}^{-2} \text{ yr}^{-1}$ ) is minor. Thus, the Delaware Estuary as a whole acts as a

relatively weak CO<sub>2</sub> source ( $2.4 \pm 4.8 \text{ mol-C m}^{-2} \text{ yr}^{-1}$ ), which is in great contrast to many river estuaries that are strong CO<sub>2</sub> sources ( $26 \pm 21 \text{ mol-C m}^{-2} \text{ yr}^{-1}$ ) (Borges and Abril, 2011).

### ***Seasonal Variations in Temperature-normalized pCO<sub>2</sub>***

Seasonal distributions of  $p\text{CO}_{2\text{obs}}$  at 13.3 °C, which indicate impacts of non-thermal processes (biological and mixing), varied noticeably throughout the year and across salinity intervals (Figure 7). Typically,  $p\text{CO}_{2\text{obs}}$  at 13.3 °C was greatest during early and mid-winter season (December and January) except in the 0-5 salinity interval (mostly turbidity maximum zone and urban river) when  $p\text{CO}_{2\text{obs}}$  at 13.3 °C reached its maximum in June. Coupled with decreasing flow, in the 0-5 salinity interval,  $p\text{CO}_{2\text{obs}}$  at 13.3 °C decreased from June to an annual minimum in October. In the mid- salinity waters ( $5 \leq S \leq 20$ ),  $p\text{CO}_{2\text{obs}}$  at 13.3 °C decreased from mid-winter to an annual minimum in March, followed by an increase to a secondary maximum in June. In contrast, in the high salinity waters ( $20 \leq S \leq 30$ ) of the lower bay where biological removal of CO<sub>2</sub> was generally strong, annual minimums were observed in August. The annual distribution of  $p\text{CO}_{2\text{mean}}$  at  $T_{\text{obs}}$ , which indicates the impact of the seasonal thermal cycle, followed typical bell shaped curves across all salinity intervals with the lowest values occurring in winter and an annual maximum occurring in July.

### **Discussion**

The seasonal and spatial distributions of estuarine  $p\text{CO}_2$  is governed by the dynamic interaction between water temperature, horizontal and vertical mixing processes, biological processes, and CO<sub>2</sub> contributions from the river, ocean, and estuarine zone (Jiang et al., 2008a; Borges and Abril, 2011; Hunt et al., 2014). In the estuarine zone, the addition or removal of CO<sub>2</sub> include net ecosystem metabolism, DIC exchange with

intertidal marshes, sediments, groundwater inputs, air-water gas exchanges, and other estuarine contributing processes (Jiang et al., 2008a). In the following sections, we evaluate the impact that seasonal temperature changes and river discharge rates have on surface water  $p\text{CO}_2$  distributions, river and estuarine  $\text{CO}_2$  inputs, and river-borne  $\text{CO}_2$  fluxes throughout the Delaware Estuary.

### ***Temperature vs. Biological Effects on $p\text{CO}_2$***

Similar to other estuaries (Borges and Abril, 2011), seasonal temperature changes provided a first control on the observed seasonal changes in  $p\text{CO}_{2\text{obs}}$  (low in the winter and high in the summer, Figure 3A and 6). This is further reflected in the fact that temperature-normalized  $p\text{CO}_2$  was always higher than in situ  $p\text{CO}_2$  in the winter but lower than in situ  $p\text{CO}_2$  in the summer (Figure 7). Presumably, then, seasonal patterns of the temperature-normalized  $p\text{CO}_2$  reflect how non-thermal processes (mixing and biological) influence in situ  $p\text{CO}_2$ . For example, in the urban river and turbidity maximum zones ( $S < 5$ ), high  $p\text{CO}_{2\text{obs}}$  at 13.3 °C in the spring and winter may reflect both river inputs and strong respiratory  $\text{CO}_2$  production. Low  $p\text{CO}_{2\text{obs}}$  at 13.3 °C during the warmer months likely reflect the removal of  $\text{CO}_2$  due to various non-thermal processes. During the warmer months from May to October, Yoshiyama and Sharp (2006) found elevated nitrite ( $\text{NO}_2$ ) concentrations in the urban river when nitrification and primary production were highest. In addition, high  $\text{NO}_2$  concentrations were observed in the mid-bay in summer when primary production was maximal (Pennock and Sharp, 1994). Comparably,  $p\text{CO}_{2\text{mean}}$  at  $T_{\text{obs}}$  (changes due to the seasonal thermal cycle) trends were opposite to that of  $p\text{CO}_{2\text{obs}}$  at 13.3 °C with lower than  $p\text{CO}_{2\text{obs}}$  values in the winter and higher than  $p\text{CO}_{2\text{obs}}$  values in the summer. These opposing signals suggest that increases in surface water  $p\text{CO}_2$  due to winter-to-summer warming are partially

compensated by the reduction of surface water  $p\text{CO}_2$  due to mixing processes and/or biological removal of  $\text{CO}_2$  (Takahashi et al., 2002). Sharp et al. (2009) found that during the March-April period ammonium ( $\text{NH}_4$ ), phosphate ( $\text{PO}_4$ ), and silicate (Si) concentrations were heavily depleted in the mid- and lower bay regions due to extensive spring blooms. Similarly, but in the opposite direction, the reduction in surface water  $p\text{CO}_2$  due to fall-to-winter cooling is partially compensated by the elevation of surface water  $p\text{CO}_2$  caused by various non-thermal processes (Figure 7).

We further examine the relative importance of the temperature and biological effects in each salinity interval by calculating the ratio of  $\Delta p\text{CO}_{2\text{temp}}$  to  $\Delta p\text{CO}_{2\text{bio}}$  ( $T/B$ ) (for methods please refer to Appendix B). Based on our results, temperature was a dominant factor in controlling surface water  $p\text{CO}_2$  in low salinity waters ( $0 \leq S \leq 10$ ) (mainly the urban river and turbidity maximum zone) with  $T/B$  ratios ranging from 1.30 to 1.68 (Table 3). As salinity increased, both  $\Delta p\text{CO}_{2\text{thermal}}$  and  $\Delta p\text{CO}_{2\text{non-thermal}}$  decreased (Table 3). The decrease in  $\Delta p\text{CO}_{2\text{thermal}}$  may be attributed to the reduction in river water temperatures at the ocean end-member (Hunt et al., 2014). In comparison to the upper tidal river, low  $T/B$  ratios ranging from 0.69 to 0.80 were observed in mid-salinity waters ( $15 \leq S \leq 25$ ) (mainly the mid- and lower bay) suggesting that  $p\text{CO}_2$  distributions in the Delaware Bay are largely governed by biological and/or mixing processes.

### ***Influence of River-borne $\text{CO}_2$ on Estuarine Degassing***

The potential emission of river-borne  $\text{CO}_2$  was estimated based on the concept of excess  $\text{CO}_2$ , the difference between the in-situ DIC at zero salinity and a theoretical DIC value at atmospheric equilibrium ( $\Delta\text{DIC}$ ) (Abril et al., 2000; Borges et al., 2006). The theoretical DIC was computed using in-situ TA values and an atmospheric  $p\text{CO}_2$  of 395  $\mu\text{atm}$ . River-borne  $\text{CO}_2$  fluxes were calculated as the product of  $\Delta\text{DIC}$  and the combined

river discharges from the Schuylkill and Delaware Rivers for each month divided by the estuarine surface area. Generally, as freshwater residence time increases (river discharge decreases) river-borne CO<sub>2</sub> fluxes decrease (Borges et al., 2006). As more river-borne CO<sub>2</sub> is released into the atmosphere in the upper estuary due to increased residence time, leaving less river-borne CO<sub>2</sub> for degassing in the lower estuary, the overall contribution of CO<sub>2</sub> emissions are largely shaped by the net community production in the mixed layer (ML NCP) in the mid- to high salinity estuarine zones (Abril et al., 2000; Borges et al., 2006). In comparison, as freshwater residence time decreases (river discharge increases), DIC enrichment from ML NCP is reduced and river-borne CO<sub>2</sub> fluxes increase. In certain cases, such as the Rhine estuary or other systems with extremely rapid flushing times, residence time is so short that not all of the river-borne CO<sub>2</sub> is ventilated to the atmosphere in the estuarine zone (Borges and Frankignoulle, 2002; Borges et al., 2006). In turn, the potential emission of river-borne CO<sub>2</sub> is higher than the actual observed air-water CO<sub>2</sub> fluxes from the estuary (Borges et al., 2006).

Positive correlations between river-borne and air-water CO<sub>2</sub> fluxes illustrate the importance of river inputs to CO<sub>2</sub> degassing fluxes (Figure 8). In the Delaware Estuary, the largest river-borne CO<sub>2</sub> flux was observed during the highest flow month of June 2013 with river CO<sub>2</sub> flux accounting for 119% and 60% of the overall CO<sub>2</sub> degassing flux in the urban river and turbidity maximum zone, respectively (Figure 8). Moreover, during the high flow month of March 2014, river-borne CO<sub>2</sub> fluxes exceeded 200% and 150% of the overall CO<sub>2</sub> degassing fluxes in the urban river and turbidity maximum zone, respectively (Figure 8). Presumably, the higher river-borne to overall CO<sub>2</sub> fluxes in March are due to the combined influence of increased river discharge coupled with large CO<sub>2</sub> consumption in the estuary (Figure 3B and 4A). This is consistent with the observed low *p*CO<sub>2</sub> and high O<sub>2</sub> values (Figure 5A) (Cai unpublished data). In contrast, in July and

August 2014, air-water CO<sub>2</sub> fluxes exceeded river-borne CO<sub>2</sub> fluxes indicating strong estuarine CO<sub>2</sub> production. Such internal estuarine CO<sub>2</sub> production is most likely due to respiration in the water column, but may also include other inputs such as benthic respiration and net respiration from surrounding intertidal marshes. In turn, while correlations between river-borne and air-water CO<sub>2</sub> fluxes were exhibited, differences between the two fluxes suggest that the input of CO<sub>2</sub> from other estuarine sources is important.

### ***Internal Estuarine Production vs. River CO<sub>2</sub> Input***

Our results illustrate that both the river and the estuarine zone contribute to CO<sub>2</sub> inputs in the Delaware Estuary (Figure 9). Combined river CO<sub>2</sub> input and internal estuarine production were highest in the urban river (87.8 to 255.4 μmol L<sup>-1</sup>) and smallest in the lower bay (-38.8 to 7.0 μmol L<sup>-1</sup>) (Figure 9). In the tidal river, internal estuarine production exhibited clear seasonal trends with CO<sub>2</sub> contributions being lowest in the spring (March), highest in the summer (June and August), and medium in the fall (October and November). Strong seasonal trends in internal estuarine production were also observed in the bay regions. During spring and late summer (March and August 2014), internal estuarine CO<sub>2</sub> signals were negative in the mid- and lower bay zones and reached as much as eight folds greater than total river CO<sub>2</sub> inputs, ranging from -22.9 to -100.4 μmol L<sup>-1</sup> (Figure 9). Thus, the majority of river CO<sub>2</sub> input was heavily compensated by the biological removal of CO<sub>2</sub> in the bay waters. In addition, during spring season (March) high CO<sub>2</sub> consumption was also observed in the upper bay with internal estuarine CO<sub>2</sub> signals (-30.7 μmol L<sup>-1</sup>) exceeding total river CO<sub>2</sub> contribution (25.7 μmol L<sup>-1</sup>) (Figure 9). Depending on river discharge rates, the freshwater residence time in the Delaware Estuary ranges from about 40-90 days (Ketchum, 1952). Due to

smaller physical sizes, freshwater residence time in the upper tidal river is much shorter (Table 2). Thus, the percentage of river-borne CO<sub>2</sub> in the upper Delaware Estuary is large (Figure 9), and that percentage decreases in the mid- and lower bays, which have longer residence times and high biological CO<sub>2</sub> removal (Sharp, 1983).

### ***Assumptions and Limitations***

While this study serves as the first air-water CO<sub>2</sub> flux product in the Delaware Estuary, there are several limitations. First, the lack of cross-bay transects (east to west), except in December 2014, limits our knowledge of surface water *p*CO<sub>2</sub> distributions in shallow waters regions of the bay system. Due to various biological and physical processes (i.e. influence from nearby tidal marshes, tributaries, or estuarine circulation forces), surface water *p*CO<sub>2</sub> may vary from within the main channel to the perimeters of the estuary. Jiang et al., (2008a) found that surface water *p*CO<sub>2</sub> and air-water CO<sub>2</sub> flux in the marine-dominated Sapelo and Doboy sounds paralleled seasonal temperature changes and net CO<sub>2</sub> inputs from within the estuarine zone. Due to intense productivity of vegetation in the surrounding salt marshes, extensive accumulation of organic carbon occurs during spring and early summer (Dai and Wiegert, 1996; Jiang et al., 2008a). During late summer and early fall, increased surface water temperatures coupled with tidal flushing of intertidal marsh waters and the decomposition of dead plants contribute to high CO<sub>2</sub> degassing in these estuaries (Dai and Wiegert, 1996; Cai and Wang, 1998; Cai et al., 1999; Neubauer and Anderson, 2003; Wang and Cai, 2004). However, due to the much broader geographic size of the Delaware Bay compared to the marine-dominated Sapelo and Doboy sounds, in-water biological processes are most likely important. In turn, the impact from the growth and decay of marsh plants on surface water *p*CO<sub>2</sub> and CO<sub>2</sub> flux dynamics may not be as influential in the Delaware Bay except

near the shorelines where tides regularly flush marsh boundaries. Studies conducted by Culberson et al., (1987) and Lebo et al., (1990) performed several cross bay transects sampled at various depths, over diel cycles, within tributaries, and periodically offshore. Results showed that cross-bay gradients were inconsistent and relatively small, except in shallow waters near the shoreline where total suspended sediment and chlorophyll concentrations were frequently elevated (Culberson et al., 1987; Lebo et al., 1990; Sharp et al., 2009). Thus, the impact from marsh input of DIC to the Delaware Bay on overall  $p\text{CO}_2$  distributions and associated  $\text{CO}_2$  degassing fluxes are most likely small. During December 2014,  $p\text{CO}_2$  measurements were not only collected in the main channel, but also near the Delaware and New Jersey perimeters of the bay (Figure 5I). While slight variability was observed across the bay,  $p\text{CO}_2$  values from the lower to upper bay regions remained within about 150  $\mu\text{atm}$  (Figure 5I and Table 1).

In addition to the lack of cross bay transects, there is a pressing need to conduct more winter and early spring surveys to fully cover seasonal ranges in key properties such as temperature and river discharge rates. Moreover, cruises or moored sensor studies at or around large discharge events are needed. Recent study by Voynova and Sharp (2012) found that in the past century there have been a recorded 54 extreme discharges (defined by the average daily discharge as recorded in Trenton, NJ from 1 Oct 1912 to 30 Sept 2011 plus 10 standard deviations); 46% of these occurring in the past decade (Voynova and Sharp, 2012). With increasing evidence suggesting that extreme weather events will occur more frequently with climate change, it is important to maintain routine seasonal surveys to learn how such subsequent conditions (i.e. increased summer stratification, riverine  $\text{CO}_2$  fluxes, removal of oxygen in bottom waters) impact various coastal environments (Allan and Soden, 2008; Yoana and Sharp, 2012). Furthermore, more research is needed in the urban and upper river sections of the estuary to better

understand CO<sub>2</sub> dynamics throughout the whole estuarine gradient. The lack of inorganic carbon data in these upper regions limits syntheses of regional CO<sub>2</sub> fluxes and generalizations to underlying mechanisms. Routine sampling along small tributaries and river systems could provide crucial insight to the biogeochemistry in the upper tidal river.

There are also several limitations to the temperature-normalized and end-member mixing models that need to be addressed. First, knowing the extensively complex nature of estuarine systems, it is important to note that derived variances in temperature-normalized  $p\text{CO}_2$  provide only a relatively simple analysis of seasonal  $p\text{CO}_2$  fluctuations due to thermal and non-thermal processes as it neglects the impact that various physical processes, turbulent forces, and tidal mixing scenarios have on  $p\text{CO}_2$  dynamics. However, as mentioned before, since salinity fluctuates greatly depending on factors such as season, river discharge, and tidal cycle, salinity-binned climatologies can provide crucial insight to various physical and biological controlling mechanisms behind  $p\text{CO}_2$  distributions that geographic boundaries may not. Unfortunately, due to the lack of winter surveys and unusually high  $p\text{CO}_2$  values in December, interpolated temperature-normalized  $p\text{CO}_2$  during cooler months may be biased and slightly overestimated. Moreover, the temperature derived constants ( $\partial \ln p\text{CO}_2 / \partial T$ ) derived in this study were based on river and ocean end-member TA and DIC concentrations collected in the Delaware Estuary over the past two years. Thus, it is important to note that derived temperature constants here are applicable for general estuarine systems and may not be suitable for coastal environments with different hydrological and/or geochemical characteristics.

In situ DIC and TA measurements were coupled using the Excel macro CO2SYS (Pierrot, 2006) and inorganic carbon dissociation constants from Millero et al. (2006) for estuarine waters to calculate dissolved CO<sub>2</sub> concentrations. While river and ocean end-

members were obtained at near zero salinity and at the mouth of the bay, respectively, no fixed end-member sampling locations were established. This marginal difference in end-member location could slightly increase or decrease estimated CO<sub>2</sub> concentrations. In the chemical model of the CO<sub>2</sub>SYS, NH<sub>3</sub>, NH<sub>4</sub><sup>+</sup>, and organic matter contribution to TA were not included (Cai et al., 1998; Cai et al., 2010b), which were likely high in low salinity waters. Thus, lower calculated CO<sub>2</sub> than observed CO<sub>2</sub> was expected as the observed TA included other acid-base components (Figure 2C). However, due to the very high pCO<sub>2</sub>, such uncertainty is deemed unimportant in our consideration. Another factor that may contribute to the lower calculated CO<sub>2</sub> than observed CO<sub>2</sub> could be the use of mercuric chloride as a preservative in low salinity samples (S < 10) (Trabalka and Reichle, 2013). Excess alkalinity generated via the dilution of mercuric chloride could contribute to conservative CO<sub>2</sub> flux estimates (Trabalka and Reichle, 2013) although due to the relatively high TA in the Delaware River we believe this effect is small.

### **Summary and Concluding Remarks**

While the urban river and turbidity maximum zone are strong CO<sub>2</sub> sources to the atmosphere, these upper regions are small in comparison to the bay regions of the Delaware Estuary. Thus, overall the Delaware Estuary acts as a relatively weak CO<sub>2</sub> source ( $2.4 \pm 4.8 \text{ mol-C m}^{-2} \text{ yr}^{-1}$ ) in comparison to many other estuarine systems that serve as strong CO<sub>2</sub> sources to the atmosphere ( $26 \pm 21 \text{ mol-C m}^{-2} \text{ yr}^{-1}$ ) (Borges and Abril, 2011). Of the 62 estuaries compiled in Borges and Abril (2011), only the Aby Lagoon, a permanently stratified system, served as a sink for atmospheric CO<sub>2</sub>. Seasonal temperature cycles influence the rise and fall of surface water pCO<sub>2</sub> throughout the Delaware Estuary, but these effects are partially compensated by opposing cycles of biological removal and addition of CO<sub>2</sub>. Moreover, positive correlations between river-

borne degassing to overall CO<sub>2</sub> fluxes in the upper sub-sections of the estuary (the urban river and turbidity maximum zone). Such features are typical for rapidly flushing river-dominated estuaries. While river-borne CO<sub>2</sub> degassing fluxes heavily impact CO<sub>2</sub> dynamics throughout the upper Delaware Estuary, these forces are largely compensated by internal biological processes within the extensive bay system of the lower estuary.

Along the eastern Georgia (USA) coast, Jiang et al., (2008a) identified the Altamaha Sound as a river-dominated estuary with CO<sub>2</sub> fluxes driven by river discharge. Comparably, the Kennebec estuary, located on the central Maine (USA) coast, exhibited high river CO<sub>2</sub> inputs and short freshwater residence times (~ 4 days) suggesting that CO<sub>2</sub> sources in the estuary were mainly controlled by the degassing of river-borne DIC (Hunt et al., 2014). The upper Delaware Estuary showed similar results with high river CO<sub>2</sub> contributions and rapid freshwater transit times during all months (Figure 9 and Table 2). In contrast, in systems with long freshwater residence times (i.e. the Delaware Bay and Scheldt estuary), much, if not all, of the river-borne CO<sub>2</sub> is released into the atmosphere (Abril et al., 2000; Borges et al., 2006). In turn, overall CO<sub>2</sub> emission from the estuary is largely controlled by net community production in the mixed layer (ML NCP) (Borges et al., 2006). In the case of the European Scheldt estuary, long freshwater residence time (30 - 90 days) leads to extensive DIC enrichment in the water column and high CO<sub>2</sub> emissions to the atmosphere (Abril et al., 2000; Borges et al., 2006). Similarly, and in contrast to the rapidly flushing Altamaha Sound, Jiang et al., (2008a) identified the marsh surrounded Sapelo Sound as a marine-dominated estuary with CO<sub>2</sub> fluxes driven by seasonal temperature and metabolic cycles.

With its extensive geographic size, the Delaware Estuary features both a river-dominated upper estuary and an ocean-dominated lower bay. In this case, air-water CO<sub>2</sub> fluxes in the heterotrophic upper estuary are significantly influenced by intense river-

borne CO<sub>2</sub> degassing akin to the river-dominated Altamaha Sound and Kennebec estuary. The autotrophic lower estuary is governed by water-column biological processes and seasonal temperature cycles akin to the marine-dominated Sapelo Sound and Scheldt estuary (though the Delaware Estuary and other large estuarine systems are on orders of magnitude more productive than smaller marine-dominated estuaries).

## TABLES

Table 1. Area-averaged, standard deviation, and range of  $p\text{CO}_2$  and  $\text{CO}_2$  flux ( $F_{\text{CO}_2}$ ) in five of the six zones in the Delaware Estuary during each cruise.

		Mar 2014	Jun 2013	Jul 2014*	Aug 2013*	Aug 2014	Oct 2013*	Oct 2014	Nov 2013	Dec 2014*	Annual Average
Average $p\text{CO}_2$ ( $\mu\text{atm}$ )											
Lower Bay	Mean $\pm$ SD	230 $\pm$ 23	477 $\pm$ 11	473 $\pm$ 52	384 $\pm$ 42	315 $\pm$ 59	421 $\pm$ 6	405 $\pm$ 8	387 $\pm$ 3	596 $\pm$ 11	410
	Range	194 – 267	456 – 528	397 – 648	317 – 491	243 – 432	413 – 437	395 – 419	380 – 393	570 – 627	
Mid-Bay	Mean $\pm$ SD	198 $\pm$ 8	540 $\pm$ 66	559 $\pm$ 97	530 $\pm$ 36	250 $\pm$ 16	465 $\pm$ 22	422 $\pm$ 2	390 $\pm$ 8	590 $\pm$ 21	438
	Range	187 - 232	464 – 759	402 – 777	464 – 607	223 – 310	429 – 516	417 – 431	378 – 415	566 – 654	
Upper Bay	Mean $\pm$ SD	289 $\pm$ 47	919 $\pm$ 192	917 $\pm$ 97	680 $\pm$ 58	470 $\pm$ 98	566 $\pm$ 39	463 $\pm$ 19	434 $\pm$ 11	658 $\pm$ 26	599
	Range	225 - 401	645 – 1374	768 – 1149	594 – 846	312 – 697	508 – 651	428 - 483	411 – 461	597 – 744	
Turbidity Maximum Zone	Mean $\pm$ SD	595 $\pm$ 121	2087 $\pm$ 499	1473 $\pm$ 162	1237 $\pm$ 139	1102 $\pm$ 317	726 $\pm$ 34	575 $\pm$ 79	542 $\pm$ 61	786 $\pm$ 39	1014
	Range	397 - 854	1327 – 2981	1141 – 1680	837 – 1370	689 – 1866	645 – 754	481 – 737	457 – 709	711 – 1000	
Urban River	Mean $\pm$ SD	868 $\pm$ 48	3287 $\pm$ 163	2994 $\pm$ N/A	2542 $\pm$ N/A	2310 $\pm$ 589	1199 $\pm$ N/A	816 $\pm$ 133	880 $\pm$ 179	878 $\pm$ N/A	1753
	Range	762 – 945	3007 – 3600	N/A	N/A	1822 – 4000	N/A	640 – 1330	615 – 1450	N/A	
Average $F_{\text{CO}_2}$ ( $\text{mmol m}^{-2} \text{d}^{-1}$ )											
Lower Bay	Mean $\pm$ SD	-15.4 $\pm$ 2.3	3.8 $\pm$ 0.5	4.4 $\pm$ 2.5	3.8 $\pm$ 1.9	-3.0 $\pm$ 2.7	1.6 $\pm$ 0.4	0.8 $\pm$ 0.6	-1.2 $\pm$ 0.3	13.5 $\pm$ 1.0	0.9
	Range	-19.4 - (-12.0)	2.8 – 6.2	0.5 – 13.1	0.8 – 8.5	-6.4 – 2.5	1.1 – 2.6	0.1 – 1.8	-1.9 – (-0.7)	11.6 – 15.7	
Mid-Bay	Mean $\pm$ SD	-20.0 $\pm$ 0.6	6.8 $\pm$ 3.2	11.1 $\pm$ 6.8	10.2 $\pm$ 1.6	-6.7 $\pm$ 0.7	4.8 $\pm$ 1.8	2.0 $\pm$ 0.1	-1.1 $\pm$ 0.7	13.5 $\pm$ 2.0	2.3
	Range	-21.0 - (-17.8)	3.2 – 17.4	0.8 – 27.8	7.3 – 13.6	-8.0 – (-3.9)	2.1 – 9.0	1.6 – 2.7	-2.1 – 1.3	11.2 – 19.3	
Upper Bay	Mean $\pm$ SD	-12.1 $\pm$ 4.9	25.3 $\pm$ 9.5	39.5 $\pm$ 7.3	16.8 $\pm$ 2.6	5.7 $\pm$ 6.0	13.0 $\pm$ 2.9	5.0 $\pm$ 1.4	3.4 $\pm$ 1.2	19.7 $\pm$ 2.0	12.9
	Range	-18.4 – (-0.5)	11.8 – 48.0	26.9 – 54.7	13.0 – 24.3	-3.8 – 19.0	8.4 – 18.6	2.5 – 6.5	0.9 – 5.9	14.2 – 25.1	
Turbidity Maximum Zone	Mean $\pm$ SD	15.9 $\pm$ 9.6	83.9 $\pm$ 25.2	63.5 $\pm$ 2.9	42.2 $\pm$ 6.9	37.1 $\pm$ 13.9	21.1 $\pm$ 0.9	12.3 $\pm$ 5.1	10.1 $\pm$ 3.0	26.7 $\pm$ 1.9	34.8
	Range	-0.9 – 36.9	45.6 – 129.1	54.3 – 65.5	23.9 – 47.6	18.6 – 71.9	18.3 – 21.7	6.3 – 23.6	5.6 – 19.7	23.3 – 44.8	
Urban River	Mean $\pm$ SD	38.3 $\pm$ 4.3	144.8 $\pm$ 8.1	131.0 $\pm$ N/A	109.8 $\pm$ N/A	98.9 $\pm$ 25.9	52.1 $\pm$ N/A	30.2 $\pm$ 8.6	31.0 $\pm$ 8.1	32.1 $\pm$ N/A	74.2
	Range	33.6 – 45.5	130.4 – 160.0	N/A	N/A	83.0 – 175.4	N/A	17.8 – 64.1	20.9 – 66.4	N/A	

\*Months when surveys did not extend into Urban River. Area-averaged was estimated by linearly regressing data from adjacent months with sample measurements. Standard deviation and range not available.

Table 2. Flushing time in five of the six zones in the Delaware Estuary during each cruise.

	Mar 2014	Jun 2013	Jul 2014	Aug 2013	Aug 2014	Oct 2013	Oct 2014	Nov 2013	Dec 2014	Annual Average
Flushing Time (day)										
Lower Bay	14.5	11.7	26.5	23.8	36.2	21.9	18.5	21.9	16.1	21.2
Mid-Bay	29.9	22.9	54.5	38.1	64.1	41.3	30.9	40.0	28.3	38.9
Upper Bay	15.1	13.3	26.6	23.9	32.8	25.5	27.6	27.2	16.6	23.2
Turbidity Maximum Zone	7.6	7.5	11.9	13.3	18.5	19.9	16.1	16.9	11.3	13.7
Urban River	2.5	2.3	3.7	6.1	6.9	6.5	6.5	6.5	5.9	5.2

Table 3. Calculated  $\Delta p\text{CO}_{2\text{thermal}}$ ,  $\Delta p\text{CO}_{2\text{non-thermal}}$ ,  $T - B$ , and  $T/B$  values for each salinity interval in the Delaware Estuary.

	0-5	5-10	10-15	15-20	20-25	25-30
$\Delta p\text{CO}_{2\text{thermal}}$ ( $\mu\text{atm}$ )	1005	800	635	514	417	431
$\Delta p\text{CO}_{2\text{non-thermal}}$ ( $\mu\text{atm}$ )	773	477	615	635	604	473
$T - B$ ( $\mu\text{atm}$ )	232	323	20	-121	-187	-42
$T/B$	1.30	1.68	1.03	0.80	0.69	0.91

## FIGURES

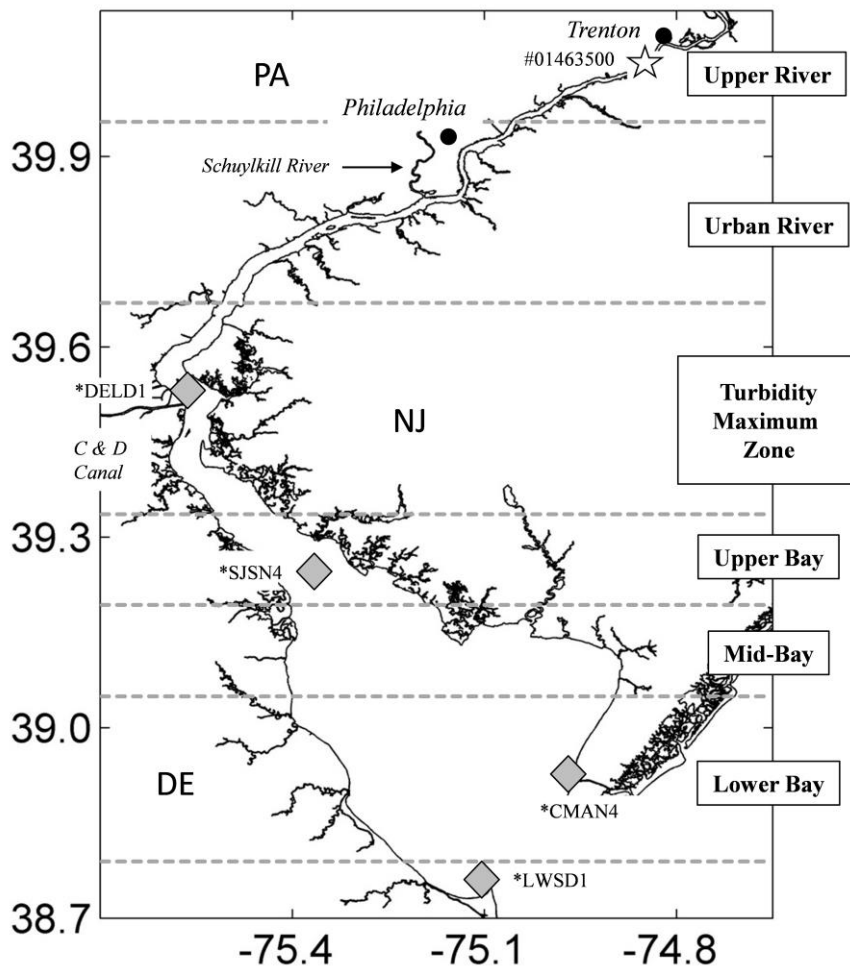


Figure 1: Map of the Delaware Estuary divided into six zones from the head of the tide in Trenton, NJ to the mouth of the bay. The gray diamonds indicate the position of four NOAA buoys (LWSD1, CMAN4, SJSN4, and DELD1). The white star shows the location of the USGS gauging station (#01463500).

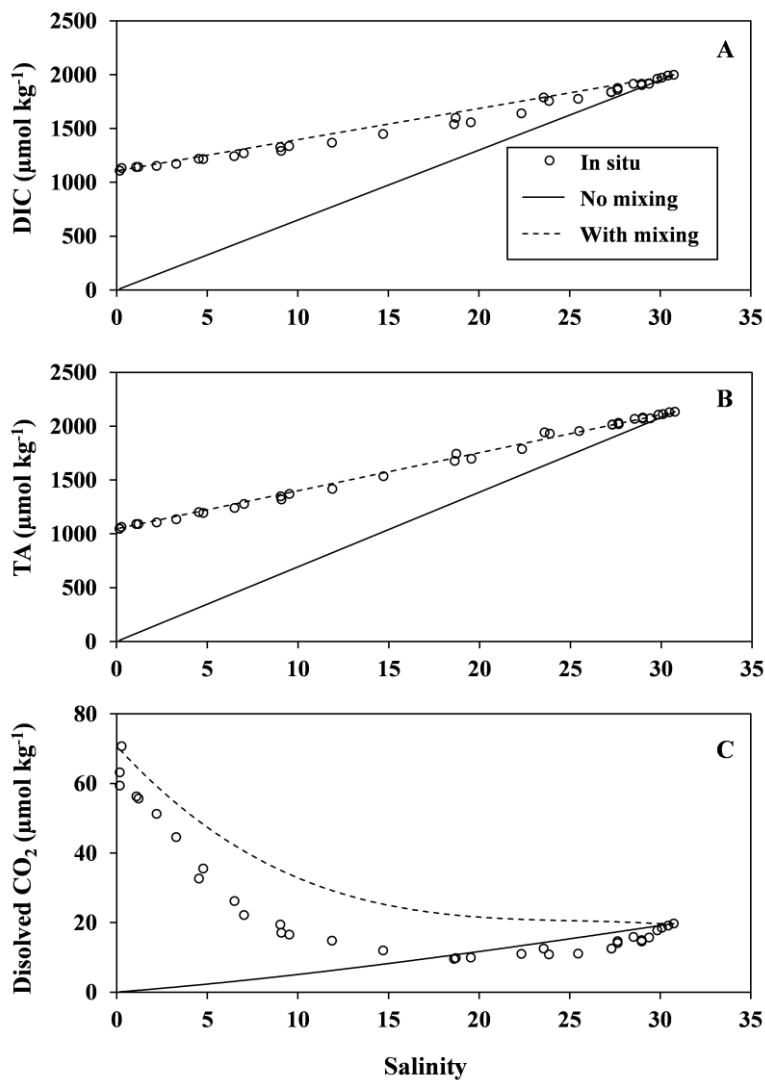


Figure 2. Concentrations of (A) DIC, (B) TA, and (C) dissolved  $\text{CO}_2$  in the Delaware Estuary during March 2014. Open circles represent in situ concentrations. Solid lines represent values after the ocean end-member is diluted by freshwater with a concentration of zero units. Dotted lines represent concentration after mixing of river and ocean end-members. CO2SYS was used to calculate  $p\text{CO}_2$  from measured DIC and TA.

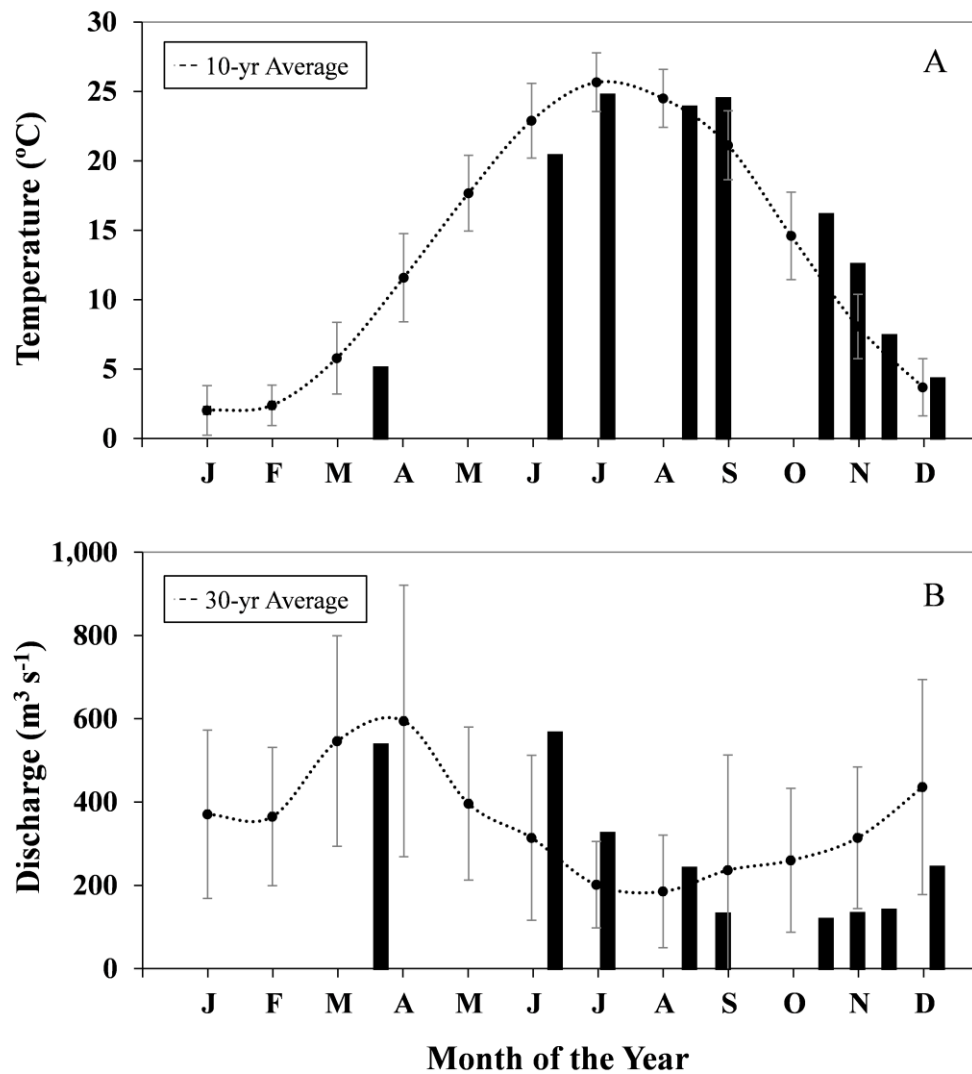


Figure 3. Measured (A) surface water temperatures and (B) Delaware River discharge in the Delaware Estuary during each sampling month. Error bars represent standard deviations of the 10-year (2004-2014) and 30-year (1980-2014) monthly averages for surface water temperatures and Delaware River discharge rates, respectively.

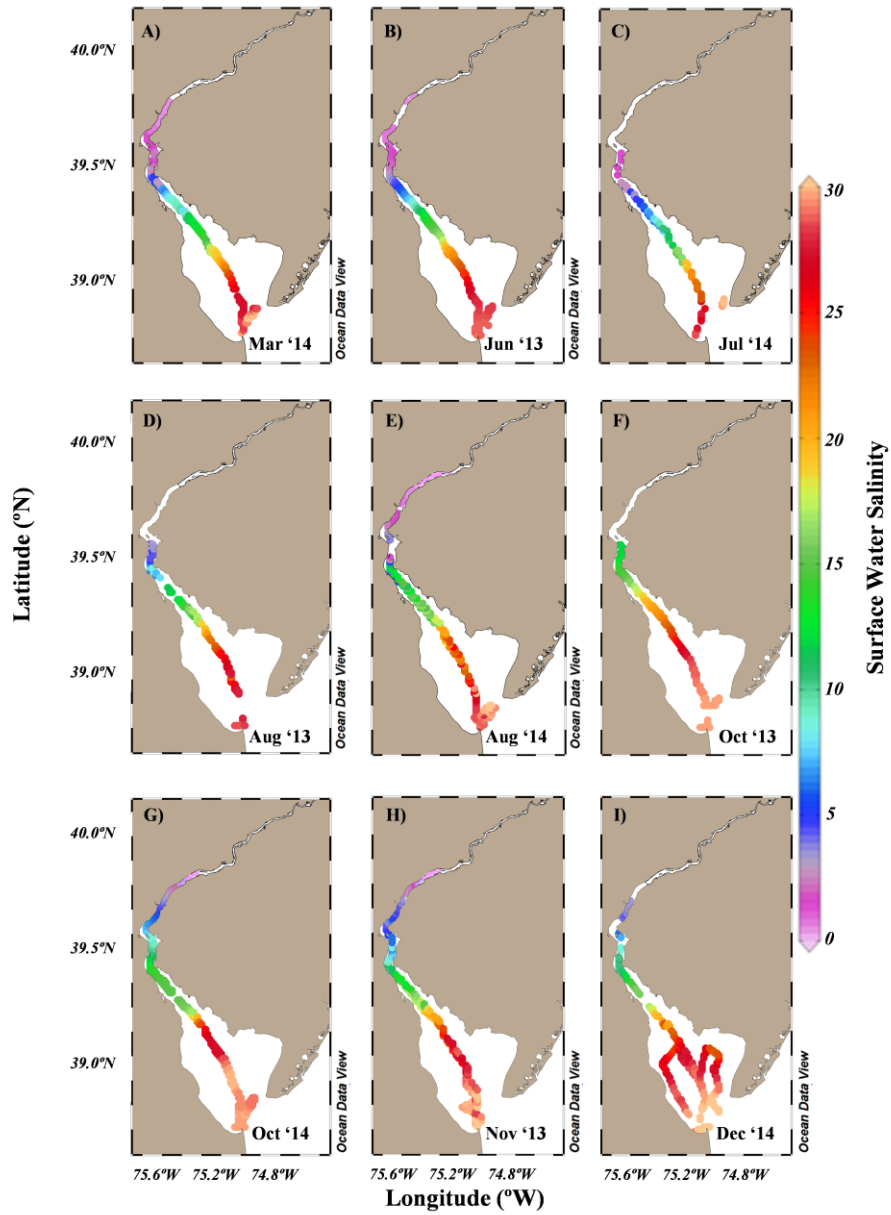


Figure 4. Spatial distributions of surface water salinity in the Delaware Estuary measured during each sampling month. The map was designed with the ODV software by R. Schlitzer (Ocean Data View software, 2015, <http://odv.awi.de/>).

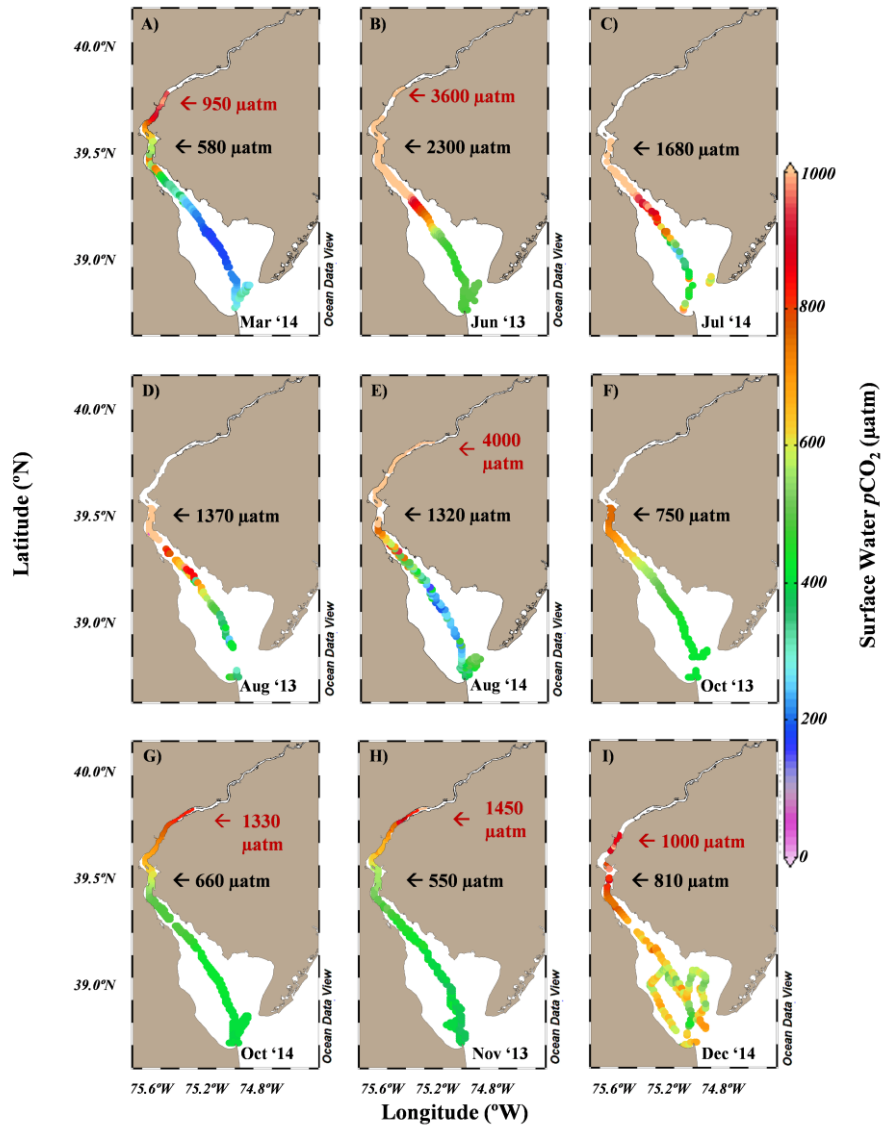


Figure 5. Spatial distributions of surface water  $p\text{CO}_2$  in the Delaware Estuary measured during each sampling month. Black and red arrows show surface water  $p\text{CO}_2$  values at the Chesapeake-Delaware Canal and the northern end member of each survey, respectively. The map was designed with the ODV software by R. Schlitzer (Ocean Data View software, 2015, <http://odv.awi.de/>).

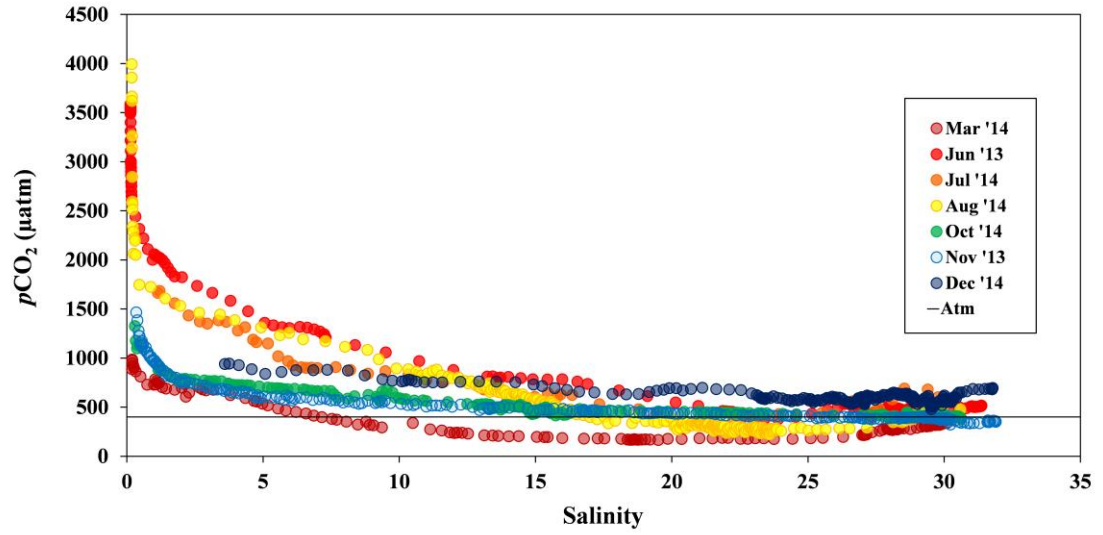


Figure 6. Measured surface water  $p\text{CO}_2$  against the salinity gradient during each sampling month in the Delaware Estuary.

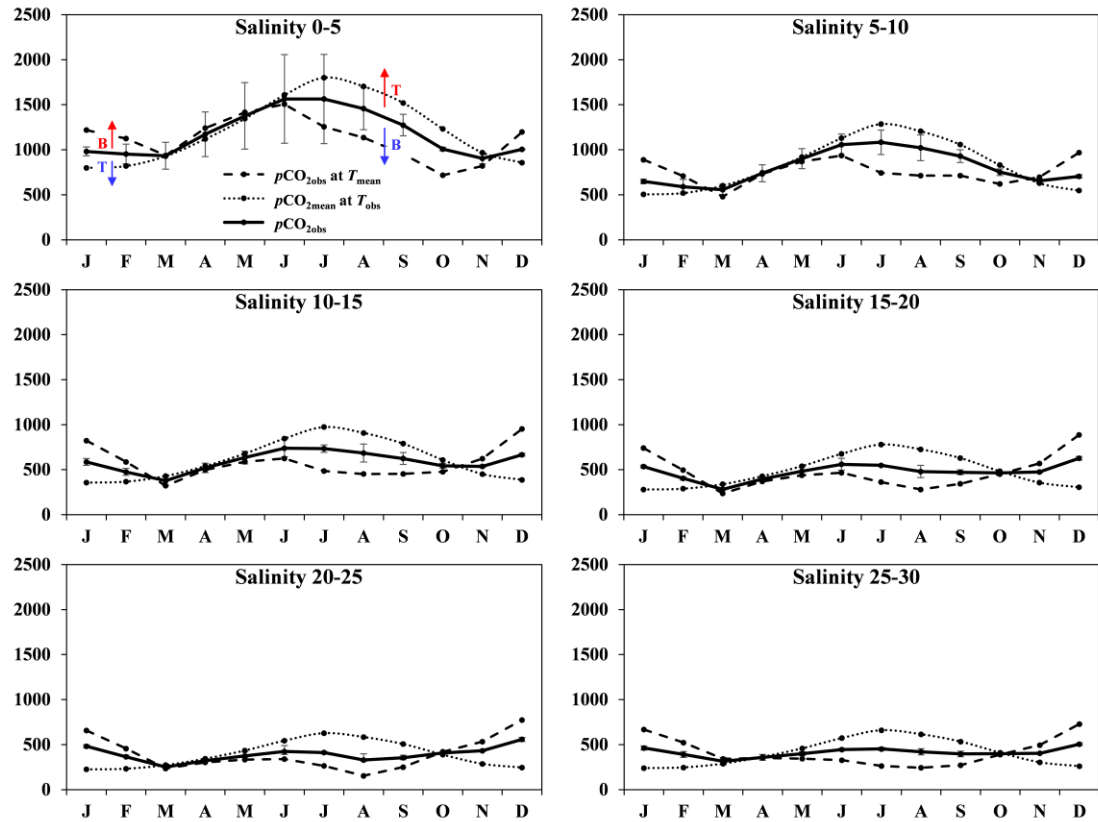


Figure 7. Salinity-binned intervals of temperature-normalized observed  $p\text{CO}_2$  values at  $13.3^\circ\text{C}$ , annual mean, area-averaged  $p\text{CO}_2$  values at in situ temperature, and observed  $p\text{CO}_2$  values in the Delaware Estuary over the year. Red arrows indicate increases in  $p\text{CO}_2$  and blue arrows indicate decreases in  $p\text{CO}_2$ . The symbol T represents changes in  $p\text{CO}_2$  due to thermal processes and the symbol B represents fluctuations in  $p\text{CO}_2$  due to non-thermal processes. Error bars represent one standard deviation of the mean value for each month.

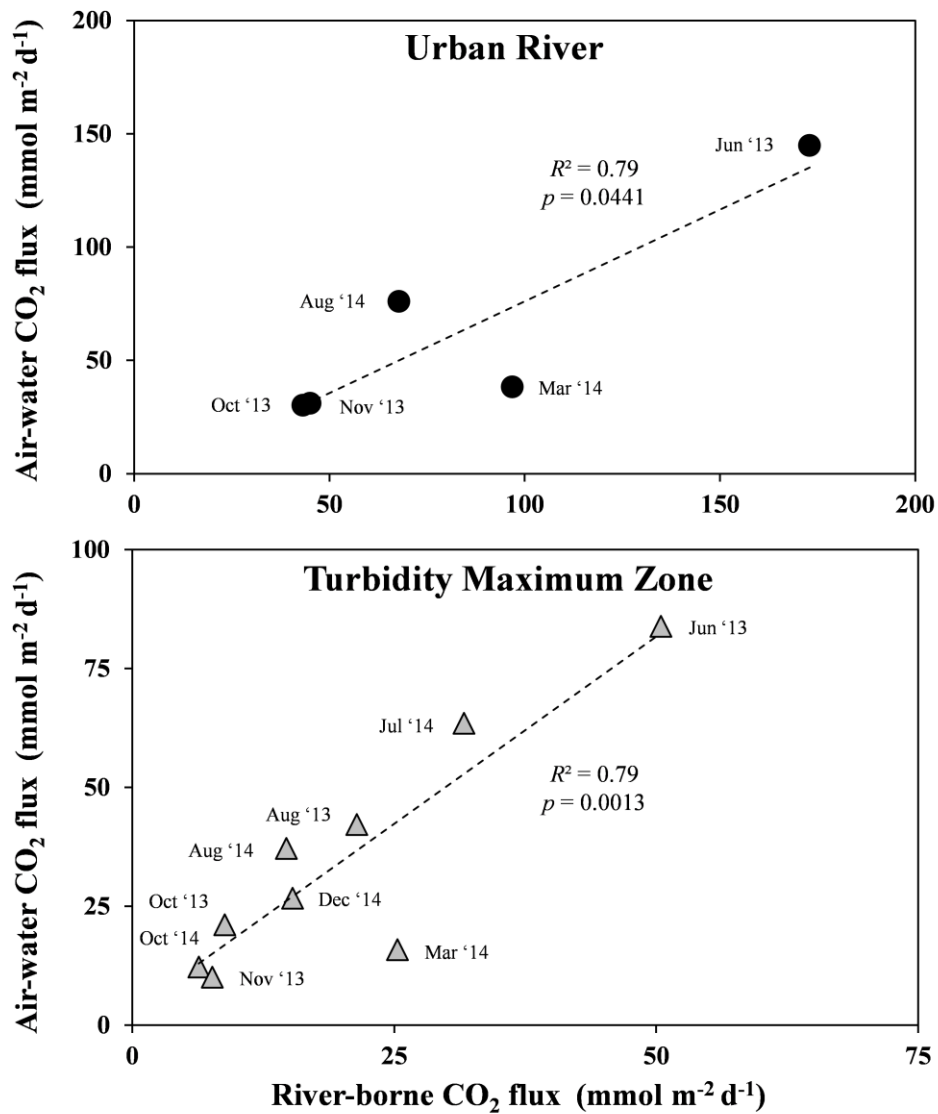


Figure 8: Air-water CO<sub>2</sub> fluxes against river-borne CO<sub>2</sub> fluxes in the urban river and turbidity maximum zone of the Delaware Estuary. Note the different axes used for the urban river and turbidity maximum zone.

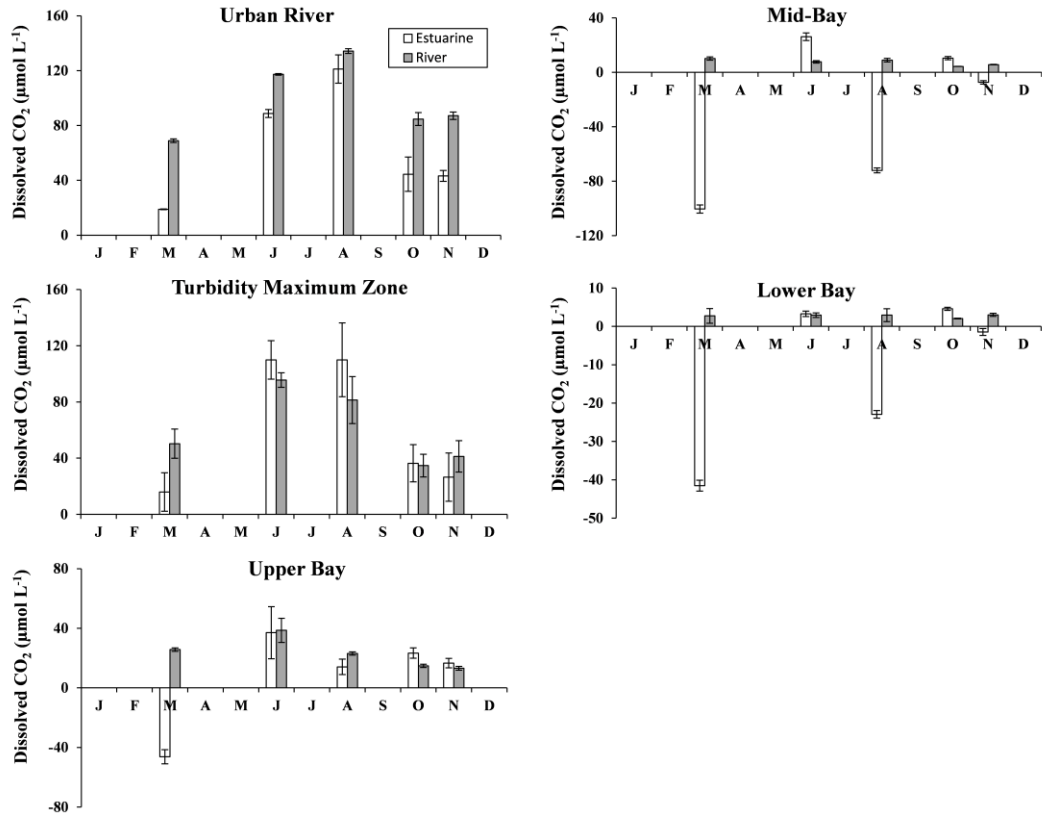


Figure 9: Dissolved CO<sub>2</sub> concentrations (normalized to 13.3 °C, area-averaged) due to river inputs and internal estuarine sources in each region of the Delaware Estuary. Note the different axes used across all regions of the estuary. Error bars represent one standard deviation of the mean value for each month.

## Chapter 3

### SEASONAL VARIABILITY OF THE INORGANIC CARBON SYSTEM IN THE DELAWARE ESTUARY

#### Introduction

The global carbon cycle is a complex dynamic interplay of processes involving the exchange of carbon between the earth's atmosphere, land, vegetation, coastal zones, and oceans. Over the past few centuries, human perturbations and land-use changes have significantly modified the transport of carbon across the land and ocean continuum and have resulted in imbalances to present-day carbon fluxes and storage reservoirs (Aumont et al., 2001; Cotrim da Cunha et al., 2007; Quinton et al., 2010; Bauer et al., 2013; Regnier et al., 2013). The total carbon input to freshwaters is estimated to be about 2.7-2.9 Pg C yr<sup>-1</sup> (Battin et al., 2009; Tranvik et al., 2009; Regnier et al., 2013). The majority of carbon fluxes in inland waters involve inputs from soil-derived carbon, chemical weathering of carbonate and silicate minerals, dissolved carbon in sewage waste, and photosynthetic carbon fixed in surface waters (Battin et al., 2009; Tranvik et al., 2009; Regnier et al., 2013). To balance the influx of carbon, a large fraction is returned to the atmosphere due to decomposition within inland waters (Cole et al., 1994; Butman et al., 2015). Additionally, carbon is laterally transported to adjacent waters, buried in freshwater sediments, and in some cases released as methane (CH<sub>4</sub>) gas (Downing et al., 2008; Bastviken et al., 2011). In the inorganic carbon cycle, the weathering of silicate and carbonate minerals consumes atmospheric CO<sub>2</sub> and transports dissolved inorganic carbon and subsequent cation and anion products into oceanic systems. Eventually, this CO<sub>2</sub> is released back into the atmosphere via oceanic carbonate sedimentation and volcanic activity (Regnier et al., 2013).

The supply of inorganic carbon by rivers is typically governed by river discharge, weathering intensity, and the geology of the drainage basin (White and Blum, 1995; White, 2003; Guo et al., 2008). Large shifts in seasonal precipitation and weather rates can significantly impact dissolved inorganic carbon (DIC) and total alkalinity (TA) concentrations (Probst et al., 1992; Cai, 2003; Guo et al., 2008). Guo et al., (2008) found that in the Pearl River estuary substantially lower DIC and TA values were present during the wet season ( $\sim 1000$  and  $700 \mu\text{mol kg}^{-1}$ , respectively) than during the dry season ( $> 2700$  and  $> 2400 \mu\text{mol kg}^{-1}$ , respectively). They suggested that the much lower DIC and TA values measured in the wet season were a result of increased river discharge diluting overall weathering production. Moreover, similar results were found in the Mississippi River where a strong negative correlation between river  $\text{HCO}_3^-$  concentration and discharge rate was observed (Cai et al., 2008). While there have been a few inorganic carbon studies on large river systems such as in the Amazon (Milliman and Boyle, 1975; Edmond et al., 1981), the Yangtze River (Edmond et al., 1985), the Yellow River (Turner et al., 1990), and the Mississippi River (Cai, 2003), carbonate chemistry research in estuarine environments remains fairly limited (Ternon et al., 2000; Cai, 2003; Cai et al., 2004; Cai et al., 2008).

Through monthly sampling at the Delaware, Schuylkill, and Christina River, we examine how input from multiple tributaries contribute to total DIC and TA riverine to the Delaware Estuary and export fluxes to the ocean. In addition, we investigate the seasonal variation of the inorganic carbon system in the Delaware Estuary based on data collected from eight cruises (2013-2015).

## Methods

### *Study Area*

The Delaware Estuary is a 135 mile (217 km) long coastal plain estuary that extends from the head of the tidal Delaware River at Trenton, New Jersey to the mouth of the Delaware Bay between Cape Henlopen and Cape May (Culberson, 1988; Sharp, 2010) (Figure 10). The upper drainage basin encompasses regions of New York, New Jersey, and Pennsylvania (Sharp et al., 2009). With approximately 768 square miles (1773 km<sup>2</sup>) of surface water area, the Delaware Estuary is one of the largest estuaries along the U.S. east coast, exceeded only by the Chesapeake Bay, Long Island Sound, and the Albemarle/Pamlico Sounds (Frithsen, 1991; Sutton et al., 1996). Moreover, the Delaware River flows through the Philadelphia area, the nation's fifth largest metropolitan region, and supplies drinking water to over 8% of the total U.S. population (Sharp et al., 2009; Sharp, 2010).

As the major source of water to the system, the Delaware River provides the estuary with roughly 60% of the total freshwater input (Sharp et al., 1986; Marino et al., 1991). Under mean flow conditions, the Delaware River discharges about 320 m<sup>3</sup> s<sup>-1</sup> (Sutton et al., 1996). While many small rivers in New Jersey, Pennsylvania, and Delaware flow into the estuary, the Schuylkill River is the largest sub-tributary, contributing about 78 m<sup>3</sup> s<sup>-1</sup> (Sutton et al., 1996). Together, the Delaware and Schuylkill River in Pennsylvania, combine for about 70% of the total freshwater inflow (Sharp et al., 1986; Marino et al., 1991). Overall, the total mean freshwater flow into the estuary is estimated at 550 m<sup>3</sup> s<sup>-1</sup> (Smullen et al., 1984).

As the tidal freshwater river passes through the industrial Philadelphia and Wilmington regions, it rapidly discharges into the extensive Delaware Bay system, a large shallow embayment surrounded by intertidal salt marshes. Depending on

precipitation and discharge rates, freshwater residence time in the Delaware Bay can range from about 40 to 90 days (Ketchum, 1952). Exhibiting strong tidal excursions of about 10 km, the Delaware estuarine system is thus influenced by the dynamic interaction between freshwater inflow from the upper drainage area and saltwater intrusion from the Atlantic Ocean (Sutton et al., 1996; Sharp et al., 2009). This feature coupled with a relatively simple hydrology has allowed the Delaware Estuary to serve as a model estuary for past biogeochemical study (Cifuentes et al., 1988; Sharp et al., 2009).

### ***Field Measurements***

Dissolved inorganic carbon (DIC), total alkalinity (TA), and pH were measured along the axis of the Delaware Estuary on eight cruises: 08-10 June 2013, 17-22 November 2013, 23-24 March 2014, 02-03 July 2014, 27 August to 01 September 2014, 30 October to 02 November 2014, 05 December 2014, and 06 April 2015. Water column samples were collected with a SeaBird Electronics 911 (SBE 911) plus CTD rosette system. Discrete underway samples were taken from the outlet of an onboard SeaBird thermosalinograph (SBE-45), which measured ongoing surface water temperature and salinity. In addition to the eight cruises, DIC, TA, and pH were periodically collected from March to October 2015 at the Delaware (from hereafter referred to as Trenton), Schuylkill, and Christina River end-members (Figure 11 and Table 4). River discharge for the Delaware and Schuylkill Rivers were collected from fixed USGS gauging stations in Trenton, NJ and Philadelphia, PA, respectively (USGS gauges 01463500 and 01474500). Combined river discharge from the Christina, Brandywine, Red Clay Creek, and White Clay Creek rivers were used to represent total freshwater input for the Christina river system (USGS gauges 01478000, 01481500, 01480015, and 01479000).

### ***Analytical Methods***

DIC and TA samples were filtered through a cellulose acetate filter (0.45  $\mu\text{m}$ ) into 250 ml borosilicate bottles, fixed with 100  $\mu\text{l}$  of saturated mercury bichloride solution, and preserved in 4°C for future analysis (Cai and Wang, 1998; Jiang et al., 2008a). DIC was determined via acid extraction by quantifying the released  $\text{CO}_2$  using an infrared gas analyzer (AS-C3 Apollo Scitech). TA was measured by Gran titration (Gran, 1952) using an open cell semi-automatic titration system (AS-ALK2, Apollo Scitech) (Cai et al., 2010a; Huang et al., 2012). All measurements were calibrated against certified reference material (provided by A.G. Dickson from Scripps Institution of Oceanography) with a precision of  $\pm 2 \mu\text{mol kg}^{-1}$  (Huang et al., 2012). The pH of water samples was determined onboard (at 25°) using an Orion 3-Star Plus pH Benchtop Meter with a Ross pH electrode (Thermo Fisher Scientific Inc. Beverly, MA, USA) and calibrated using three National Bureau Standard (NBS) pH buffers of 4.01, 7.00, and 10.01.

### **Results**

#### ***Spatial Distributions of DIC, TA, and pH***

DIC and TA exhibited large spatial and seasonal variations (975-2015 and 915-2225  $\mu\text{mol kg}^{-1}$ , respectively) (Figure 12). DIC and TA values were lowest near zero salinity in the spring and summer season when river discharge was strong and highest in the fall and winter season when discharge was weak (Figure 12). At the bay mouth ( $S > 30$ ), DIC and TA concentrations remained fairly constant throughout all seasons (1920-1990 and 2095-2180  $\mu\text{mol kg}^{-1}$ , respectively). During spring and summer, reduced DIC and elevated pH (8.0-8.5) values from salinity 15-25 were observed suggesting biological consumption of  $\text{CO}_2$  in the mid- to lower bay waters. (Figure 12). In the fall and winter, DIC and TA were generally linear in relation to salinity with a steady but minimal

decline in pH value across the salinity gradient (Figure 12). At salinity < 2.5, pH decreased greatly, reaching as low as 7.09 in June. A small increase in DIC and TA concentrations was observed near zero salinity. This concave upward phenomenon was most pronounced during the late summer (August) and fall (October and November) surveys (Figure 12).

### ***DIC and TA Riverine Flux***

To account for inputs from the Schuylkill and Christina tributaries, riverine DIC and TA end-member samples were collected from March to October 2015 (Figure 11). Since the observed DIC and TA end-member concentrations in each tributary exhibit strong negative relationships with river discharge (Figure 13), we can estimate seasonal DIC and TA end-member concentrations based on measured discharge rates. Through this approach, we used discharge rates to estimate end-member concentrations and net DIC and TA input flux for each survey (Table 5). The annual DIC and TA riverine fluxes to the estuary are  $11.6 \pm 6.0 \times 10^9$  and  $11.3 \pm 5.5 \times 10^9$  mol C yr<sup>-1</sup>.

### ***DIC and TA Export Flux***

DIC and TA values varied linearly near the ocean end-member of the mixing zones, suggesting no net addition or removal of DIC and TA beyond conservative mixing. The effective concentrations of DIC and TA were calculated by extrapolating the DIC and TA conservative mixing lines from the high salinity waters to the river end-member ( $S = 0$ ) (Cai et al., 2004; Guo et al., 2008). The difference between the effective and actual (or composite) concentrations at the river end-member indicate the amount of DIC and TA added or removed during mixing and therefore not transported to the ocean (Boyle et al., 1974; Cai and Wang, 1998; Liu et al., 2014). Using the effective concentrations and combined river discharge rates from the Delaware, Schuylkill, and

Christina River, we estimate net DIC and TA export fluxes in each survey (Table 6). The estimated annual DIC and TA fluxes to the ocean are  $12.7 \pm 8.0 \times 10^9$  and  $13.3 \pm 8.6 \times 10^9$  mol C yr<sup>-1</sup>.

## **Discussion**

Many factors influence seasonal and spatial distributions of estuarine DIC and TA concentrations. Here, we discuss how discharge rates control freshwater end-member concentrations in the Delaware Estuary. Then, we investigate how mixing between multiple tributaries yield non-conservative DIC and TA mixing lines in the upper tidal river. Finally, we produce a rough CO<sub>2</sub> mass balance for the Delaware Estuary.

### ***Influence of River Discharge and Weathering Intensity***

Due to large changes in river discharge and strong tidal excursions of about 10 km, salinity ranges from the turbidity maximum zone to the mouth of the Delaware Estuary vary dramatically (Sharp et al., 2009). Under high river discharge conditions, fresh water can reach as low as the mid-bay region (Sutton et al., 1996). Depending on discharge conditions, DIC concentrations range from about 300 to 1,200  $\mu\text{mol kg}^{-1}$  at the head of the estuary at Trenton (Sharp et al., 2009). During our spring and summer surveys when discharge rates were high, DIC and TA concentrations were about 300  $\mu\text{mol kg}^{-1}$  lower than those observed in the fall when river discharge was low (Figure 12 and Table 6). DIC and TA varied even more at Trenton. Following 5-day average discharge of  $1127 \text{ m}^3 \text{ s}^{-1}$ , TA on July 2, 2015 was an average of  $410.4 \mu\text{mol kg}^{-1}$  (Table 4) about 500  $\mu\text{mol kg}^{-1}$  lower than the average TA in the river at discharge rates less than  $200 \text{ m}^3 \text{ s}^{-1}$  at the same location (Figure 13 and Table 4). DIC followed similar patterns. In addition, TA changed the most at the Schuylkill River as well. On July 2, 2015 after a high 5-day average discharge of  $271 \text{ m}^3 \text{ s}^{-1}$ , TA was  $1026.3 \mu\text{mol kg}^{-1}$  (Table 4).

However, when average river discharge in the Schuylkill River was less than  $50 \text{ m}^3 \text{ s}^{-1}$ , TA values were always higher than  $1500 \text{ } \mu\text{mol kg}^{-1}$  (Figure 13 and Table 4). Thus, it appears that variation in DIC and TA values is mainly a result of seasonal shifts in discharge rates. Such fluctuations in river DIC and TA is expected as they are primarily governed by the dilution of weathering production by rain (White and Blum, 1995; White, 2003; Cai et al., 2008).

A compilation of historical data from 1998 shows that TA for the Delaware River at Trenton was negatively correlated with river discharge (Figure 14A, USGS gauge 01463500). TA are highest during low flow seasons (summer and fall) and lowest during high flow seasons (spring and winter) (Figure 14C). TA and river discharge are also negatively correlated in the Mississippi, Changjiang, Pearl, Huanghe, Congo, and Indus River basins (Probst et al., 1992; Karim and Veizer, 2000; Cai, 2003; Li and Zhang, 2003; Chen et al., 2008; Guo et al., 2008). While TA is negatively correlated with river discharge, TA export flux is positively correlated to discharge rate (Figure 14B). The highest TA fluxes occur during peak flow season (spring) and the lowest TA fluxes occur during the lowest flow season (fall) (Figure 14D). Cai et al., (2008) observed strong correlations between TA flux and discharge in the Mississippi, Changjiang, Pearl, and Huanghe River basins as well (Cai 2003; Chen et al., 2008; Guo et al., 2008). While strong correlations between TA flux and river discharge are exhibited, it is important to note that flux is governed by both river discharge and concentration. In the case of extreme weathering events, estimated TA fluxes may be twice as large as the average flux. Under the same conditions, if river discharge is increased four-fold, concentrations must be reduced in half to yield a two-fold increase in TA flux. Cai et al., (2008) suggest that the dilution of weathering production by precipitation leads to lower concentrations during the wet season. Thus, while TA values may decrease with increasing discharge

during the wet season and high discharge periods, overall river TA flux still increases. In turn, the negative relationship between TA and river discharge in the Delaware River suggests that changes in  $\text{HCO}_3^-$  concentrations or TA reflect the dilution of the weather derived products in the drainage basin (Cai et al., 2008; Guo et al., 2008).

Another interesting but rarely reported phenomenon is the seasonal variation of the DIC to TA ratio at the freshwater end-members. At Trenton, the highest ratios (1.02 – 1.11) were observed after high discharge periods ( $> 200 \text{ m}^3 \text{ s}^{-1}$ ) and the lowest ratios (0.86 – 1.01) were observed after low discharge periods ( $< 150 \text{ m}^3 \text{ s}^{-1}$ ) (Table 4). Similar results were found in the Schuylkill River where DIC to TA ratios were highest (1.02 – 1.07) following high discharge rates ( $> 100 \text{ m}^3 \text{ s}^{-1}$ ) and the ratios were lowest (0.93 to 1.02) following low discharge rates ( $< 75 \text{ m}^3 \text{ s}^{-1}$ ) (Table 4). If only influenced by the weathering of carbonate minerals, the ratio of DIC to TA remains the same (Cai et al., 2004). On the other hand,  $\text{CO}_2$  production from soil organic matter respiration can increase DIC to TA ratios (Mayorga et al., 2005). During the wet season and high discharge periods, more  $\text{CO}_2$  from soil organic matter respiration stored in the drainage basin is brought along the river system. Thus, we suggest that changes in the DIC to TA ratio at the freshwater end-member may reflect inputs of soil organic matter respiration due to seasonal variations in river discharge. As the ratio of DIC to TA determines aquatic pH and the buffer capacity, our observations indicate that the variation of this ratio should be considered in future global carbon cycle models, in particular regarding wet and drought cycles in future climate scenarios and how coastal waters will respond to a changing terrestrial carbon export (Reginer et al., 2013; Bauer et al., 2013).

### ***Influence of River Mixing***

While TA in the Schuylkill River was nearly double than those for the Delaware River at Trenton, river discharge in the Delaware River was nearly four folds greater than discharge rates exhibited in the Schuylkill River (Table 4 and 6). Moreover, on average discharge in the Delaware River was more than 12-fold greater than discharge rates of the Christina River (Table 4 and 6). Despite mixing from multiple end-members, such differences in river discharge rates suggest that TA values are predominantly governed by carbonate concentrations in the Delaware River. However, during periods of low discharge, TA increased significantly at the Schuylkill River (Figure 13 and Table 4). On September 29, 2015 TA values were as high as the oceanic values at the bay mouth exceeding  $2100 \mu\text{mol kg}^{-1}$ . The mixing of high TA from the Schuylkill River may increase TA values at the confluence of the Delaware and Schuylkill River. Slight increases in TA values were observed at the northern most points (around 125-150 km upstream) during the August 2014, November 2013, and October 2014 cruises (Figure 15).

Serving as the only major sub-tributary to the Delaware River from Trenton, NJ to the mouth of the bay, the mineralogy of the Schuylkill River drainage basin may have a significant impact on TA patterns throughout the Delaware River estuarine system. Originating in the Blue Ridge Mountains and Great Valley Provinces of the Appalachians in Tuscarora, PA, the Schuylkill River flows southeast through the Pediment Limestone/Dolomite Lowlands and into the Atlantic Coastal Province at Philadelphia (Woods et al., 1999; Kauffman et al., 2009). The upper Blue Ridge Mountains are primarily underlain by sedimentary sandstone and shale on the ridges and limestone and dolomite in the valleys (Kauffman et al., 2009). In the Great Valley regions, a mixture of shale, slate, carbonate, and crystalline rocks are found with softer shales underlying lower

portions of the watershed (Kauffman et al., 2009). In contrast to the upper regions, the Piedmont Limestone/Dolomite Lowlands are developed primarily on limestone and dolomite rock (Sloto, 1990; Woods et al., 1999; Kauffman et al., 2009). Specifically, within this region, the Schuylkill River flows through the Valley Creek basin in eastern Chester County, PA. Here, 68% of the basin is underlain by carbonate rocks and 32% by noncarbonated rocks (Sloto, 1990). Moreover, the center of the basin, otherwise known as Chester Valley, is primarily underlain by easily eroded limestone and dolomite bedrock (Sloto, 1990). The erosion of such minerals would lead to increased TA values along the tributary. While most flow in the Valley Creek basin is released to nearby rivers and streams, regional flow in Chester Valley is discharged to the Schuylkill River (Sloto, 1990).

The Delaware River originates in the Catskill Mountains of New York. The rural upper watershed is heavily forested and thus exhibits very good to exceptional water quality (Kauffman et al., 2009). Similar to the Schuylkill River, the central region of the Delaware River basin in New Jersey and Pennsylvania extends through the Appalachian Plateaus, underlain by glacial till, sedimentary sandstone, and shale bedrock, and southward into the Blue Ridge Mountains and Great Valley Provinces (Woods et al., 1999). The lower region of the Delaware River basin is composed of the Piedmont Triassic Lowlands and Atlantic Coastal Province (Woods et al., 1999). Unlike in the Piedmont regions of the lower Schuylkill River drainage basin, the Piedmont Triassic Lowlands of the lower Delaware River basin are derived from Triassic sandstone, shale, siltstone, and argillite bedrock, and thus less influenced by easily eroded carbonate minerals (Woods et al., 1999). While more research and data is needed, especially at the confluence of the Schuylkill and Delaware River, increases in TA near the Philadelphia

region along the Delaware River may be in part due to the mixing of relatively high carbonate freshwater from the lower Schuylkill River drainage basin.

### ***Seasonal Variation in DIC***

Seasonal shifts in DIC were also observed across the estuarine mixing zone. Generally, nonlinear concentration-salinity trends indicate an in situ addition or removal of chemical species (Cai and Wang, 1998). In spring (March 2014 and April 2015) and summer (July 2014 and August 2014), DIC deviated from conservative lines from salinity 15 to 25 while TA distributions remained linear, suggesting high consumption of CO<sub>2</sub> in the water column (Figure 12). During the same time, pH was highest, further supporting the presence of a phytoplankton bloom (Figure 12). Nonlinear distributions were observed when plotting DIC against TA (Figure 16). The curvature (concave upward trend at both ends) pattern indicates DIC removal in the middle portion of the Delaware Bay. Joesoef et al., (2015) found that internal biological processes have significant impact on CO<sub>2</sub> dynamics within the Delaware Bay. In March 2014, the entire bay system was under-saturated in CO<sub>2</sub> with respect to the atmosphere, reaching as low as 160  $\mu\text{atm}$  (Joesoef et al., 2015). Moreover, in July and August 2014,  $p\text{CO}_2$  (200 – 350  $\mu\text{atm}$ ) was low throughout the mid- and lower bay regions (Joesoef et al., 2015). Thus, while not as significant as changes in weathering and precipitation rates on DIC variability, internal biological processes within the bay system can also lead to seasonal shifts in DIC concentrations. In addition, the flushing of intertidal marsh waters can influence DIC patterns in estuarine systems as well. CO<sub>2</sub> degassing fluxes were high in the marine-dominated Sapelo and Doboy Sounds due to the extensive accumulation, decomposition, and flushing of organic matter from surrounding salt marshes (Jiang et al., 2008a). However, recent studies suggest that except near the shorelines, the flushing

of intertidal marsh waters has a relatively small impact on overall surface water  $p\text{CO}_2$  and  $\text{CO}_2$  flux dynamics in the Delaware Bay system (Joesoef et al., 2015).

### ***CO<sub>2</sub> Mass Balance***

Here we present a rough  $\text{CO}_2$  mass balance for the Delaware Estuary. Using discharge rates from the Delaware, Schuylkill, and Christina River (Table 6), DIC input fluxes to the estuary were computed for each cruise based on the linear relationships shown in Figure 13. Combining total DIC fluxes for each river, we obtain an annual-averaged DIC input flux of  $11.6 \pm 6.0 \times 10^9 \text{ mol C yr}^{-1}$ . Using the effective concentrations extrapolated from the high salinity water, an annual-averaged DIC export flux to the ocean of  $12.7 \pm 8.0 \times 10^9 \text{ mol C yr}^{-1}$  was calculated. If we assume that the Delaware, Schuylkill, and Christina River provide the estuary with 75% (annual mean discharge of  $411 \text{ m}^3 \text{ s}^{-1}$  for all cruises) of its total freshwater input, we scale up to obtain an annual mean discharge rate of  $548 \text{ m}^3 \text{ s}^{-1}$ . Thus, by upward scaling, a final DIC input flux of  $15.4 \pm 8.0 \times 10^9 \text{ mol C yr}^{-1}$  and export flux of  $17.0 \pm 10.6 \times 10^9 \text{ mol C yr}^{-1}$  is obtained. Annual air-water  $\text{CO}_2$  flux to the atmosphere from the Delaware Estuary has recently been estimated as  $2.4 \pm 4.8 \text{ mol C m}^{-2} \text{ yr}^{-1}$  (Joesoef et al., 2015). Using the annual air-water  $\text{CO}_2$  flux and an estimated surface water area of  $1773 \text{ km}^2$  for the estuarine system (Sutton et al., 1996), the total  $\text{CO}_2$  flux to the air is estimated as  $4.3 \times 10^9 \text{ mol C yr}^{-1}$ . Thus, a rough  $\text{CO}_2$  mass balance for the estuary is formed as follows:

$$\begin{aligned} & \text{River input flux } (15.4 \times 10^9 \text{ mol C yr}^{-1}) \\ & \quad + \text{ Unknown estuarine source} \\ & \quad = \text{ Estuarine output flux } (17.0 \times 10^9 \text{ mol C yr}^{-1}) \\ & \quad \quad + \text{ Atmospheric flux } (4.3 \times 10^9 \text{ mol C yr}^{-1}) \end{aligned}$$

The unknown estuarine input term is therefore estimated as  $5.8 \times 10^9$  mol C yr<sup>-1</sup>. While primarily dominated by net ecosystem metabolism in the estuary, it is important to note that this unknown term includes CO<sub>2</sub> addition from intertidal marsh waters, wastewater effluents, small riverine systems, and other various external sources (Cai and Wang, 1998; Jiang et al., 2008a). From the mass balance model, the CO<sub>2</sub> flux produced within the estuary is small when compared to the total riverine flux. Moreover, it appears that only a small percentage of the internally produced CO<sub>2</sub> is exported to the coastal ocean as most of it is lost to the atmosphere. Lastly, while CO<sub>2</sub> consumption was large during the spring and late summer, the positive estuarine input term suggests that overall the bay serves as a net heterotrophic environment.

Similar trends were observed along the macrotidal well-mixed Scheldt Estuary where much of the DIC produced by net ecosystem production (NEP) was removed to the atmosphere rather than exported to the North Sea (Borges and Abril, 2011). Freshwater residence times in the Scheldt Estuary and Delaware Bay are long ranging from about 30 to 90 days and 40 to 90 days, respectively (Ketchum, 1952; Borges and Abril, 2011). In contrast, the Randers Fjord has a much shorter residence times (5-10 days). Here, CO<sub>2</sub> emission to the atmosphere is lower than the NEP in the mixed layer (Gazeau et al., 2005). Furthermore, total DIC export to the Baltic Sea is higher than riverine DIC inputs, suggesting that, due to the shorter freshwater residence time in the Randers Fjord, much of the DIC produced by NEP is exported rather than removed to the atmosphere (Gazeau et al., 2005). In the case of the Scheldt estuary, long freshwater residence time leads to extensive DIC enrichment in the water column and high CO<sub>2</sub> emissions to the atmosphere (Abril et al., 2000; Borges et al., 2006). Thus, in the Scheldt Estuary and other systems

with long freshwater residence times (i.e. the Delaware Bay), much of the DIC produced by NEP is most likely removed to the atmosphere rather than exported to the sea.

### **Summary and Concluding Remarks**

Variability of the inorganic carbon system in estuaries is largely governed by seasonal changes in river discharge, weathering intensity, and the geology of the drainage basin. Strong negative correlations between river TA and discharge at the Delaware, Schuylkill, and Christina river end-members suggest that changes in  $\text{HCO}_3^-$  concentrations largely reflect the dilution of the weather derived products in the drainage basin (Cai et al., 2008; Guo et al., 2008). Moreover, seasonal variations in the DIC to TA ratio at the freshwater end-members may reflect inputs of soil organic matter respiration due seasonal fluctuations in river discharge rates. While reasons remain unclear, elevated DIC and TA concentrations near the Philadelphia region may be partly due to the mixing of relatively high carbonate freshwater from the lower Schuylkill River drainage basin due to eroded limestone and dolomite bedrock minerals. In addition to strong seasonal variations in discharge and mixing from multiple end-members, internal biological processes within the bay system also contribute to shifts in DIC concentrations. Annually, total DIC input flux to the estuary is estimated to be  $15.4 \pm 8.0 \times 10^9 \text{ mol C yr}^{-1}$  while total export flux to the ocean is estimated to be  $17.0 \pm 10.6 \times 10^9 \text{ mol C yr}^{-1}$ . Moreover, from the proposed  $\text{CO}_2$  mass balance model,  $\text{CO}_2$  flux produced within the estuary is small ( $5.8 \times 10^9 \text{ mol C yr}^{-1}$ ) when compared to total DIC input flux, and 36% of this  $\text{CO}_2$  is exported to the coastal ocean. Thus, in the case of the Delaware Estuary and other estuarine systems with long freshwater residence times, much of the DIC produced by NEP is most likely emitted to the atmosphere rather than exported to the sea.

## TABLES

Table 4: Sampling dates, average discharge, pH, DIC, TA , and DIC to TA ratio measured at the Delaware (Trenton), Schuylkill, and Christina River.

Location	Date	Discharge (m <sup>3</sup> s <sup>-1</sup> )	pH	DIC (μmol kg <sup>-1</sup> )	TA (μmol kg <sup>-1</sup> )	DIC to TA Ratio
Trenton	3/10/2015	182	8.8	973.4	1038.8	0.94
	4/21/2015	442	7.8	745.2	723.7	1.03
	5/7/2015	190	8.8	856.5	902.9	0.95
	5/21/2015	148	8.0	1025.5	1015.9	1.01
	6/9/2015	199	8.2	857.8	869.2	0.99
	6/23/2015	425	7.7	783.5	765.5	1.02
	7/2/2015	1127	7.2	454.2	410.4	1.11
	9/15/2015	183	8.2	945.8	936.7	1.01
	9/29/2015	98	8.7	945.8	1103.9	0.86
10/12/2015	170	8.1	1095.2	1046.1	1.05	
Schuylkill	4/16/2015	52	8.9	1421.2	1525.7	0.93
	5/21/2015	32	8.1	1682.9	1655.9	1.02
	6/9/2015	105	7.9	1400.1	1371.3	1.02
	7/2/2015	271	7.7	1095.3	1026.3	1.07
	9/15/2015	60	7.8	1506.1	1472.2	1.02
	9/29/2015	19	8.1	2071.3	2107.8	0.98
	10/12/2015	34	8.3	1869.3	1851.4	1.01
Christina	4/16/2015	14	7.7	1056.5	1015.1	1.04
	4/28/2015	15	7.5	1076.4	1018.6	1.06
	5/21/2015	11	7.7	1134.1	1072.8	1.06
	6/9/2015	32	7.5	1089.4	1004.0	1.08
	9/15/2015	6	7.9	1326.9	1210.6	1.10
	9/29/2015	7	8.0	1188.6	1165.4	1.02
	10/12/2015	7	8.0	1199.6	1168.0	1.03

Table 5: TA and DIC in the Delaware (Trenton), Schuylkill, and Christina River and their input fluxes in the Delaware Estuary.

Survey	Trenton TA (DIC) ( $\mu\text{mol kg}^{-1}$ )	Schuylkill TA (DIC) ( $\mu\text{mol kg}^{-1}$ )	Christina TA (DIC) ( $\mu\text{mol kg}^{-1}$ )	TA input flux ( $10^9 \text{ mol yr}^{-1}$ )	DIC input flux ( $10^9 \text{ mol yr}^{-1}$ )
March 2014	TA = 700.3 DIC = 721.5	TA = 1341.8 DIC = 1366.8	TA = 935.3 DIC = 1004.8	15.55	16.02
April 2015	TA = 609.1 DIC = 647.6	TA = 1382.8 DIC = 1404.3	TA = 1030.1 DIC = 1093.7	16.71	17.58
June 2013	TA = 634.0 DIC = 667.8	TA = 995.4 DIC = 1050.5	TA = 870.7 DIC = 944.2	21.31	22.51
July 2014	TA = 901.6 DIC = 884.7	TA = 1565.3 DIC = 1571.0	TA = 1050.7 DIC = 1113.0	9.72	9.64
August 2014	TA = 1101.0 DIC = 1046.4	TA = 1977.9 DIC = 1947.8	TA = 1131.8 DIC = 1188.9	5.36	5.16
October 2014	TA = 1147.2 DIC = 1083.9	TA = 1860.7 DIC = 1840.8	TA = 1123.1 DIC = 1180.8	5.27	5.08
November 2013	TA = 1154.0 DIC = 1089.4	TA = 1929.7 DIC = 1903.7	TA = 1112.0 DIC = 1170.3	5.03	4.84
December 2014	TA = 998.9 DIC = 963.7	TA = 1548.0 DIC = 1555.1	TA = 1057.9 DIC = 1119.7	8.43	8.30
Annual Average	TA = 890.9 DIC = 876.1	TA = 1550.0 DIC = 1557.0	TA = 1031.9 DIC = 1095.3	11.31	11.55

Table 6: Effective TA and DIC values extrapolated from the high salinity section and their export fluxes to the ocean.

Survey	TA (DIC) ( $\mu\text{mol kg}^{-1}$ ) as a function of salinity	Effective concentration ( $\mu\text{mol kg}^{-1}$ )	Delaware discharge ( $\text{m}^3 \text{s}^{-1}$ )	Schuylkill discharge ( $\text{m}^3 \text{s}^{-1}$ )	Christina discharge ( $\text{m}^3 \text{s}^{-1}$ )	TA export flux ( $10^9 \text{ mol yr}^{-1}$ )	DIC export flux ( $10^9 \text{ mol yr}^{-1}$ )
March 2014	TA = $35.99 \times S + 1034$ , $R^2 = 0.97$ DIC = $35.59 \times S + 889$ , $R^2 = 0.97$	1034 889	456	104	37	19.46	16.73
April 2015	TA = $38.85 \times S + 1030$ , $R^2 = 0.99$ DIC = $33.43 \times S + 911$ , $R^2 = 0.96$	1030 911	629	93	18	24.02	21.25
June 2013	TA = $38.08 \times S + 974$ , $R^2 = 0.97$ DIC = $30.48 \times S + 992$ , $R^2 = 0.97$	974 992	576	258	61	27.51	28.01
July 2014	TA = $35.34 \times S + 933$ , $R^2 = 0.98$ DIC = $28.12 \times S + 980$ , $R^2 = 0.96$	933 980	224	57	15	8.74	9.18
August 2014	TA = $36.36 \times S + 981$ , $R^2 = 0.98$ DIC = $30.09 \times S + 949$ , $R^2 = 0.90$	981 949	111	19	8	4.29	4.15
October 2014	TA = $34.43 \times S + 1041$ , $R^2 = 0.99$ DIC = $27.44 \times S + 1123$ , $R^2 = 0.99$	1041 1123	94	26	9	4.25	4.58
November 2013	TA = $29.28 \times S + 1238$ , $R^2 = 0.99$ DIC = $21.48 \times S + 1326$ , $R^2 = 0.97$	1238 1326	92	22	10	4.83	5.17
December 2014	TA = $33.96 \times S + 1155$ , $R^2 = 0.99$ DIC = $25.25 \times S + 1217$ , $R^2 = 0.98$	1155 1217	159	60	14	8.51	8.97
Annual Average			305	84	23	13.30	12.73

## FIGURES

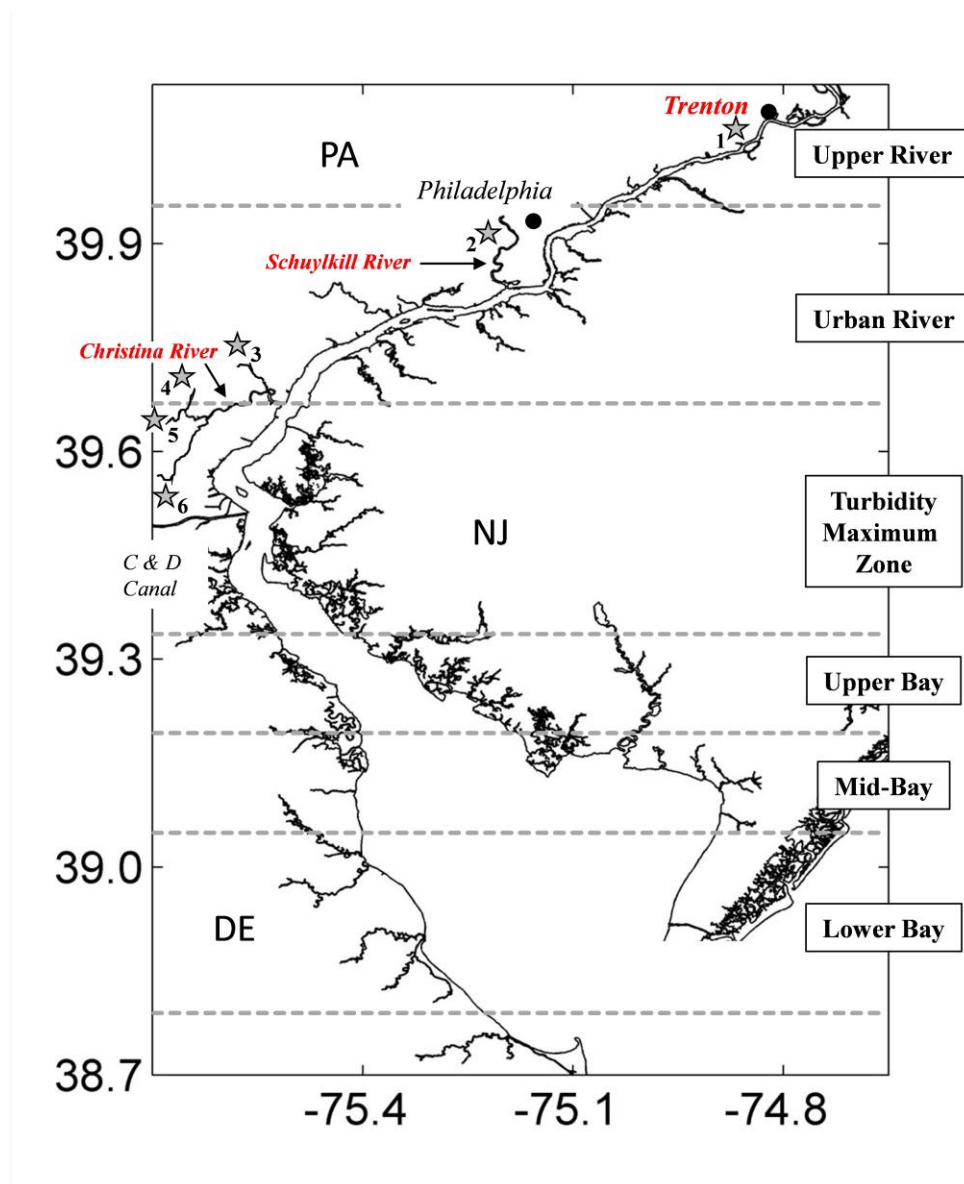


Figure 10: Map of the Delaware Estuary and river end-members. Gray stars indicate USGS gauging stations (1) #01463500, (2) #01474500, (3) #01481500, (4) #01480015, (5) #01479000, and (6) #01478000 at the Delaware (Trenton), Schuylkill, and Christina River.

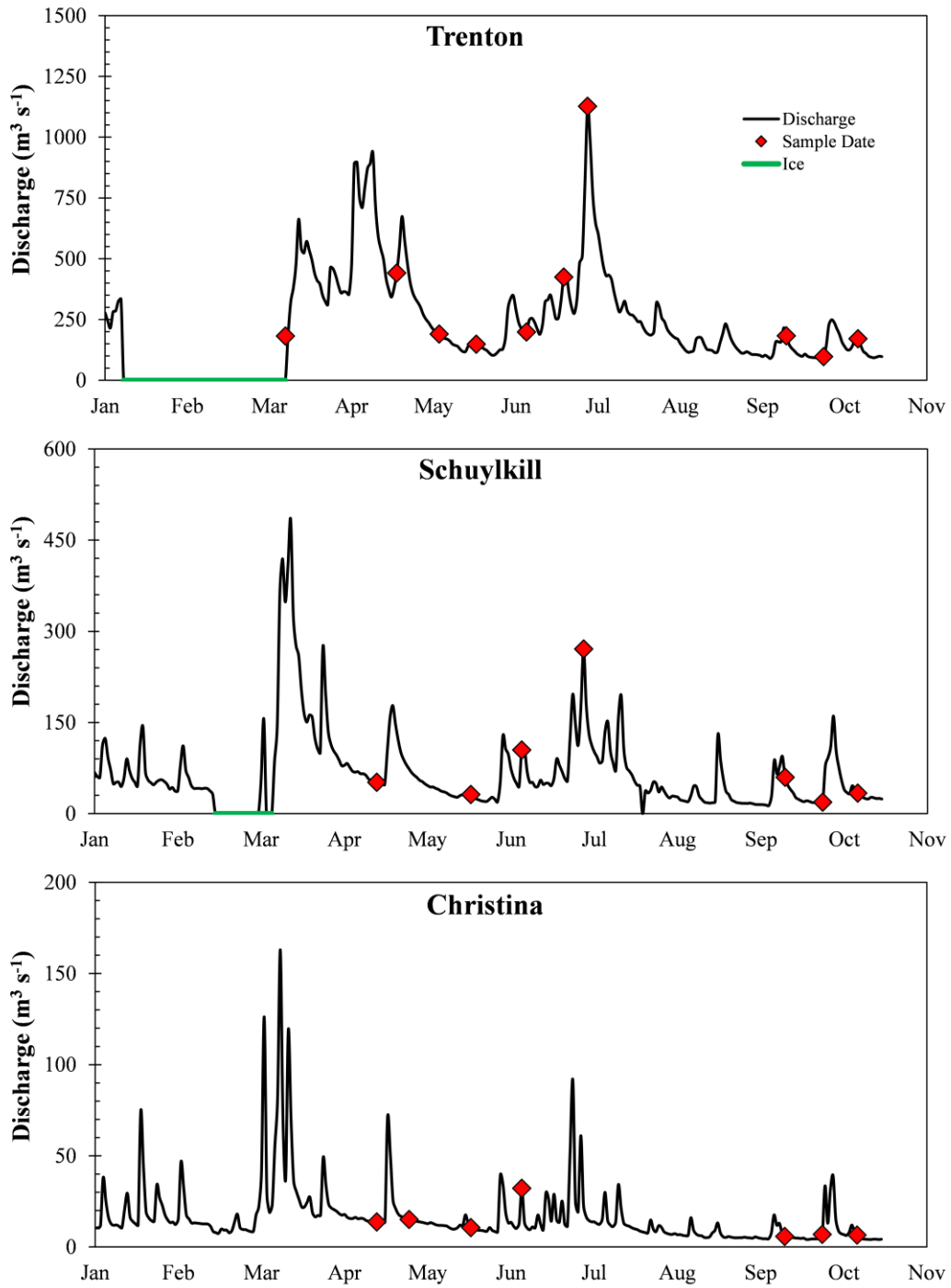


Figure 11: Discharge at the Delaware (Trenton), Schuylkill, and Christina River from March to October 2015. Note the different scales used for each river.

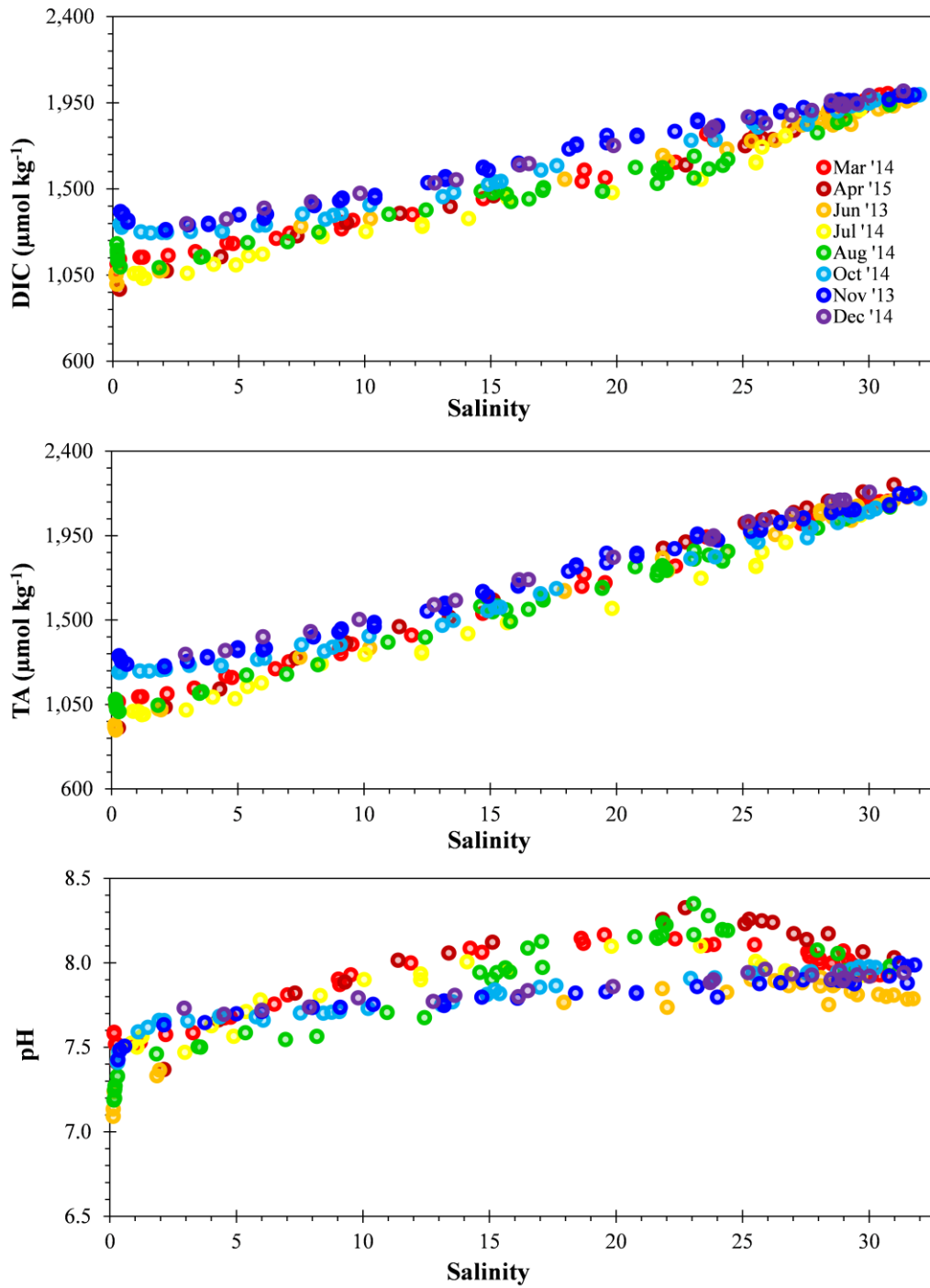


Figure 12: Salinity distributions of DIC, TA, and pH in the Delaware Estuary.

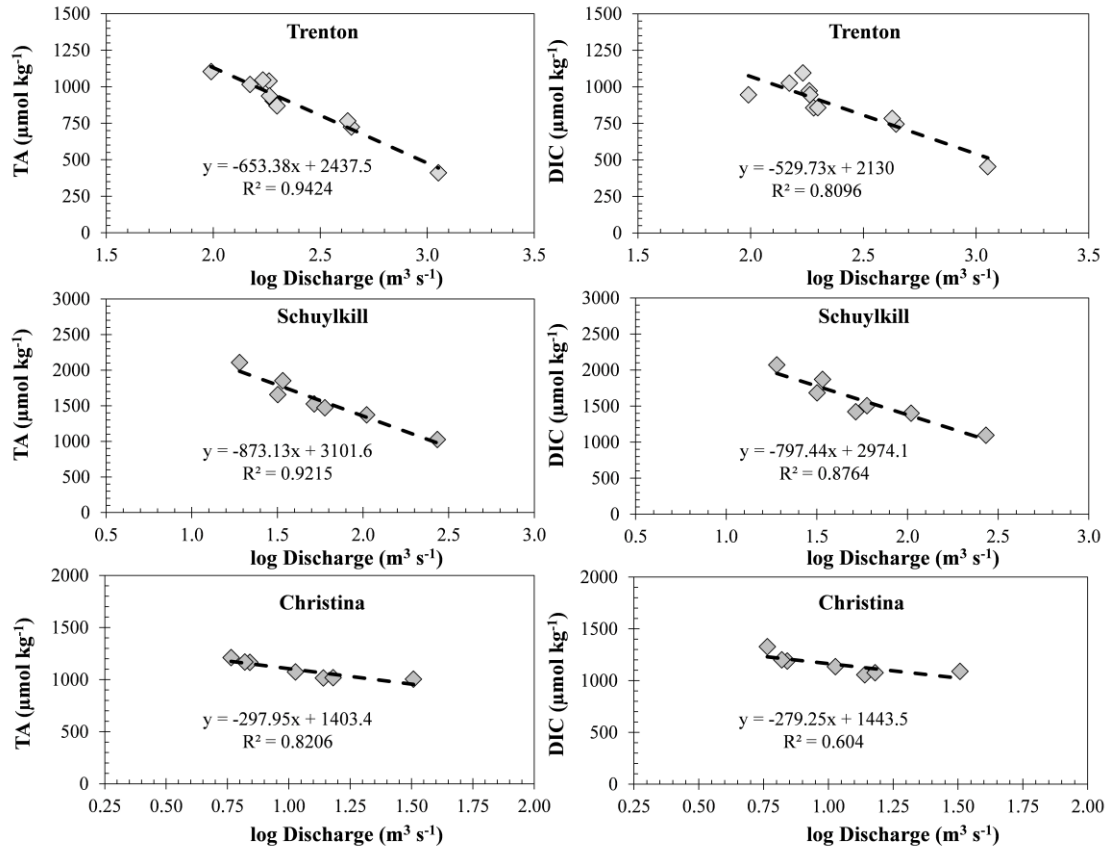


Figure 13: TA and DIC versus log discharge at the Delaware (Trenton), Schuylkill, and Christina River. Note the different scales used for each river.

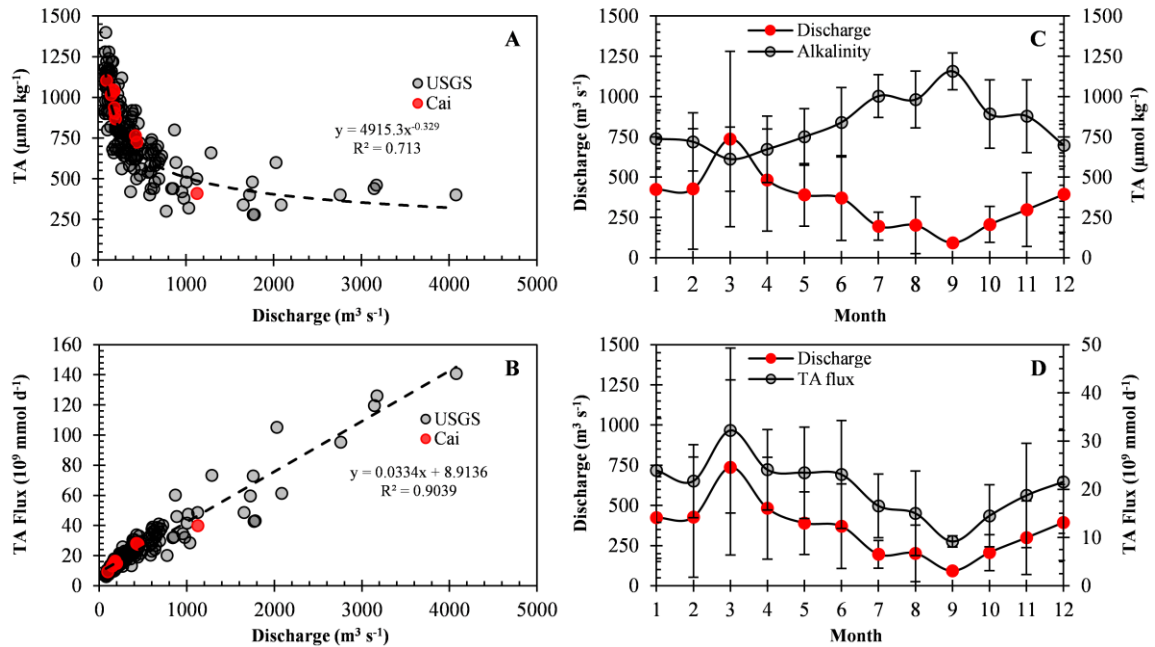


Figure 14: The relationship between TA and discharge (A), TA flux and discharge (B), as well as the time series of the Delaware River discharge and TA values (C) and TA flux (D) at Trenton, NJ (1998 – 2015) (USGS gauging station 01463500). In A and B, black circles indicate data obtained from the USGS gauging station while red circles indicate data measured in lab. In C and D, errors bars represent one standard deviation of the mean value for each month.

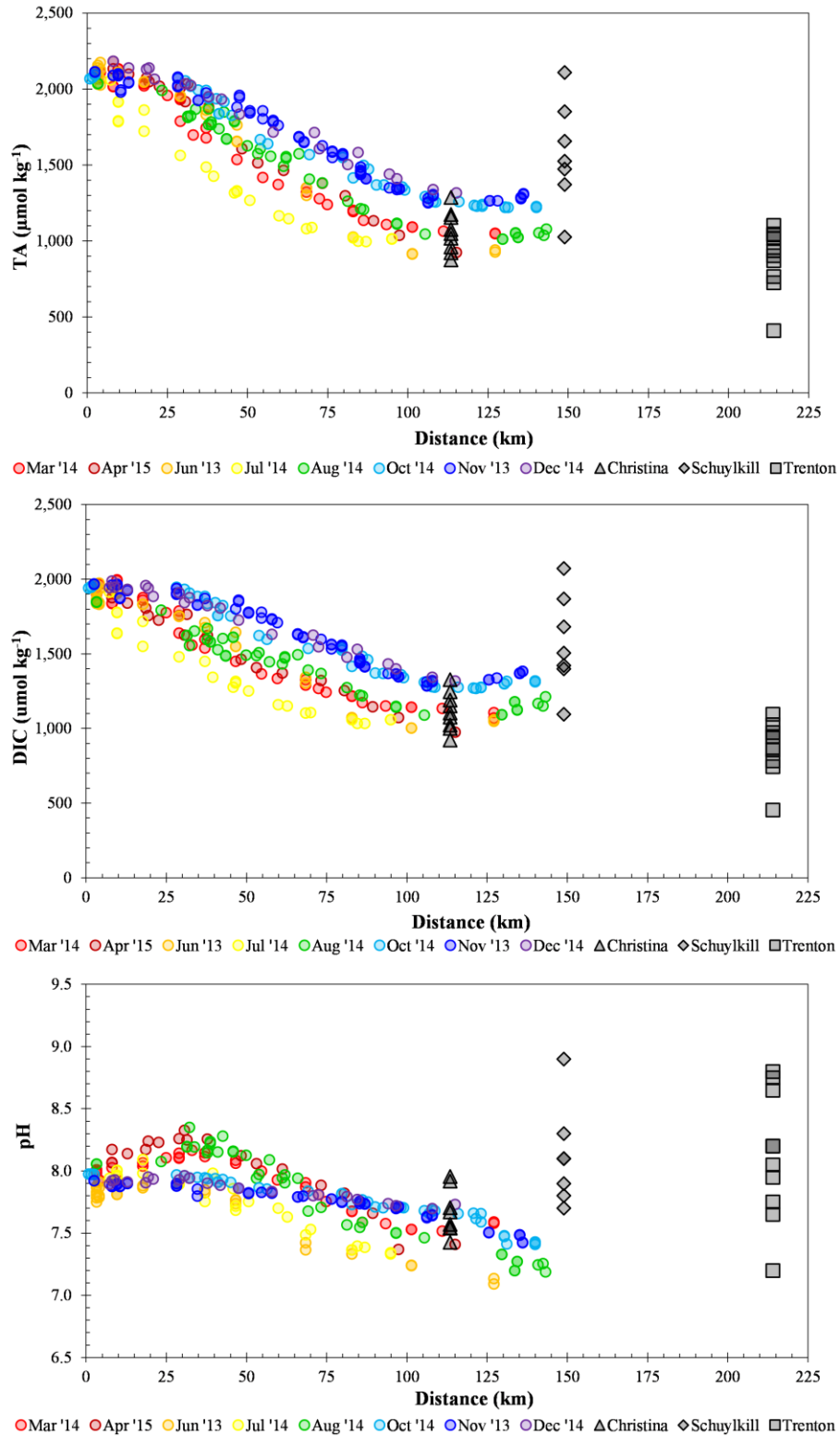


Figure 15: Spatial distribution of TA, DIC, and pH in the Delaware Estuary.

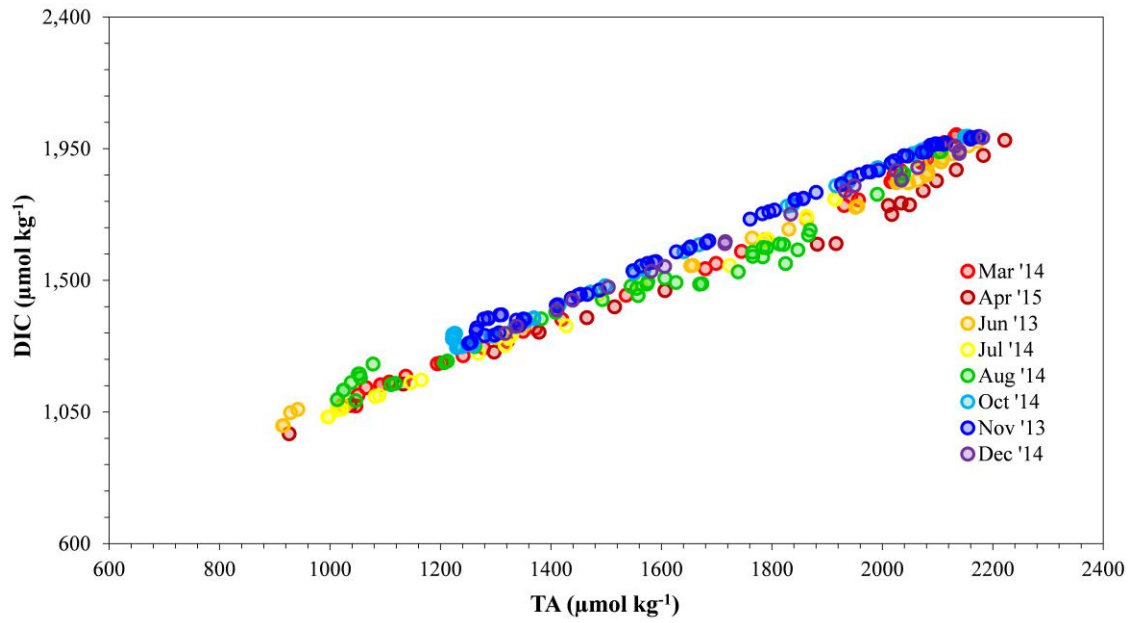


Figure 16: DIC versus TA in the Delaware Estuary.

## Chapter 4

### CONCLUSION

While the upper tidal river is a strong CO<sub>2</sub> source to the atmosphere, this region is small in comparison to the bay system of the Delaware Estuary. Thus, overall the Delaware Estuary serves as a relatively weak CO<sub>2</sub> source ( $2.4 \pm 4.8 \text{ mol-C m}^{-2} \text{ yr}^{-1}$ ) compared to many other estuarine systems that act as strong CO<sub>2</sub> sources to the atmosphere ( $26 \pm 21 \text{ mol-C m}^{-2} \text{ yr}^{-1}$ ) (Borges and Abril, 2011). Temperature influences the rise and fall of surface water *p*CO<sub>2</sub> throughout the Delaware Estuary, but these effects are partially compensated by opposing cycles of biological removal and addition of CO<sub>2</sub>. Moreover, positive correlations between river-borne degassing to overall CO<sub>2</sub> fluxes in the upper tidal river suggest the importance of river-borne CO<sub>2</sub> to overall to CO<sub>2</sub> degassing fluxes. Although river-borne CO<sub>2</sub> degassing fluxes heavily impact CO<sub>2</sub> dynamics throughout the upper Delaware Estuary, these forces are largely compensated by internal biological processes within the extensive bay system.

At the river end-member, strong negative correlations between river TA and discharge in the Delaware River suggest that changes in HCO<sub>3</sub><sup>-</sup> concentrations reflect the dilution of the weather derived products in the drainage basin (Cai et al., 2008; Guo et al., 2008). While the reasons remain unclear and more data is needed, especially at the confluence of the Schuylkill and Delaware River, high DIC and TA values near Philadelphia may be a result of the mixing of relatively high carbonate freshwater due to eroded limestone and dolomite bedrock minerals from the lower Schuylkill River drainage basin. In addition to seasonal variations in river discharge and mixing from multiple tributaries, internal biological processes within the bay system also contribute to shifts in DIC concentrations. Total DIC input flux to the estuary and export flux to the ocean are estimated to be about  $15.4 \pm 8.0 \times 10^9 \text{ mol C yr}^{-1}$  and  $17.0 \pm 10.6 \times 10^9 \text{ mol C}$

yr<sup>-1</sup>, respectively. Moreover, from the projected CO<sub>2</sub> mass balance model, internal estuarine produced CO<sub>2</sub> flux is small ( $5.8 \times 10^9$  mol C yr<sup>-1</sup>) when compared to total riverine flux. Thus, in the case of the Delaware Estuary and other coastal environments with long freshwater residence times, much of the DIC produced by NEP is most likely removed to the atmosphere rather than exported to the ocean.

Conclusions gained over this model study provide broad implications and future insights to the physics and biogeochemistry of other coastal systems. However, with increasing urbanization along its borders and the impacts of future climate changes, the Delaware Estuary and other estuarine zones may not respond to current environmental changes in the same way as they did in the past. Thus, the continuation of coastal surveys and research studies on estuarine and coastal margins are imperative to assessing the overall health and biogeochemistry of estuaries as well as to predicting and ultimately regulating the rise of current and future threats to our oceanic systems.

## BIBLIOGRAPHY

Abril, G., and Borges, A. V. (2005). Carbon dioxide and methane emissions from estuaries. In *Greenhouse gas emissions—fluxes and processes* (pp. 187-207). Springer Berlin Heidelberg.

Abril, G., Etcheber, H., Borges, A. V., and Frankignoulle, M. (2000). Excess atmospheric carbon dioxide transported by rivers into the Scheldt estuary. *Comptes Rendus de l'Academie des Sciences-Series IIA-Earth and Planetary Science*, 330(11), 761-768.

Abril, G., Commarieu, M. V., Sottolichio, A., Bretel, P., and Guerin, F. (2009). Turbidity limits gas exchange in a large macrotidal estuary. *Estuarine, Coastal and Shelf Science*, 83(3), 342-348.

Allan, R. P., and Soden, B. J. (2008). Atmospheric warming and the amplification of precipitation extremes. *Science*, 321(5895), 1481-1484.

Aumont, O., Orr, J. C., Monfray, P., Ludwig, W., Amiotte-Suchet, P., and Probst, J. L. (2001). Riverine-driven interhemispheric transport of carbon. *Global Biogeochemical Cycles*, 15(2), 393-405.

Bai, Y., Cai, W. J., He, X., Zhai, W., Pan, D., Dai, M., and Yu, P. (2015). A mechanistic semi-analytical method for remotely sensing sea surface  $p\text{CO}_2$  in river-dominated coastal oceans: A case study from the East China Sea. *Journal of Geophysical Research: Oceans*, 120(3), 2331-2349.

- Bastviken, D., Tranvik, L. J., Downing, J. A., Crill, P. M., and Enrich-Prast, A. (2011). Freshwater methane emissions offset the continental carbon sink. *Science*, 331(6013), 50-50.
- Battin, T. J., Luysaert, S., Kaplan, L. A., Aufdenkampe, A. K., Richter, A., and Tranvik, L. J. (2009). The boundless carbon cycle. *Nature Geoscience*, 2(9), 598-600.
- Bauer, J. E., Cai, W. J., Raymond, P. A., Bianchi, T. S., Hopkinson, C. S., and Regnier, P. A. (2013). The changing carbon cycle of the coastal ocean. *Nature*, 504(7478), 61-70.
- Borges, A. V. (2005). Do we have enough pieces of the jigsaw to integrate CO<sub>2</sub> fluxes in the coastal ocean? *Estuaries*, 28(1), 3-27.
- Borges, A. V., and Frankignoulle, M. (2002). Distribution of surface carbon dioxide and air-sea exchange in the upwelling system off the Galician coast. *Global Biogeochemical Cycles*, 16(2), 13-1.
- Borges, A., and Abril, G. (2011). 5.04-Carbon dioxide and methane dynamics in estuaries. *Treatise on Estuarine and Coastal Science, Volume 5: Biogeochemistry*.
- Borges, A. V., Delille, B., Schiettecatte, L. S., Gazeau, F., Abril, G., and Frankignoulle, M. (2004). Gas transfer velocities of CO<sub>2</sub> in three European estuaries (Randers Fjord, Scheldt, and Thames). *Limnology and Oceanography*, 49(5), 1630-1641.

Borges, A. V., Delille, B., and Frankignoulle, M. (2005). Budgeting sinks and sources of CO<sub>2</sub> in the coastal ocean: Diversity of ecosystems counts. *Geophysical Research Letters*, 32(14).

Borges, A. V., Schiettecatte, L. S., Abril, G., Delille, B., and Gazeau, F. (2006). Carbon dioxide in European coastal waters. *Estuarine, Coastal and Shelf Science*, 70(3), 375-387.

Boyle, E., Collier, R., Dengler, A. T., Edmond, J. M., Ng, A. C., and Stallard, R. F. (1974). On the chemical mass-balance in estuaries. *Geochimica et Cosmochimica Acta*, 38(11), 1719-1728.

Butman, D. E., Wilson, H. F., Barnes, R. T., Xenopoulos, M. A., and Raymond, P. A. (2015). Increased mobilization of aged carbon to rivers by human disturbance. *Nature Geoscience*, 8, 112-116.

Cai, W. J. (2003). Riverine inorganic carbon flux and rate of biological uptake in the Mississippi River plume. *Geophysical Research Letters*, 30(2).

Cai, W. J. (2011). Estuarine and coastal ocean carbon paradox: CO<sub>2</sub> sinks or sites of terrestrial carbon incineration? *Annual Review of Marine Science*, 3, 123-145.

Cai, W. J., and Wang, Y. (1998). The chemistry, fluxes, and sources of carbon dioxide in the estuarine waters of the Satilla and Altamaha Rivers, Georgia. *Limnology and Oceanography*, 43(4), 657-668.

Cai, W. J., Wang, Y., and Hodson, R. E. (1998). Acid-base properties of dissolved organic matter in the estuarine waters of Georgia, USA. *Geochimica et Cosmochimica Acta*, 62(3), 473-483.

Cai, W. J., Pomeroy, L. R., Moran, M. A., and Wang, Y. (1999). Oxygen and carbon dioxide mass balance for the estuarine-intertidal marsh complex of five rivers in the southeastern US. *Limnology and Oceanography*, 44(3), 639-649.

Cai, W. J., Wang, Y., Krest, J., and Moore, W. S. (2003). The geochemistry of dissolved inorganic carbon in a surficial groundwater aquifer in North Inlet, South Carolina, and the carbon fluxes to the coastal ocean. *Geochimica et Cosmochimica Acta*, 67(4), 631-639.

Cai, W.J., Dai, M., Wang, Y., Zhai, W., Huang, T., Chen, S., Zhang, F., Chen, Z. and Wang, Z. (2004). The biogeochemistry of inorganic carbon and nutrients in the Pearl River estuary and the adjacent Northern South China Sea. *Continental Shelf Research*, 24(12), 1301-1319.

Cai, W. J., Dai, M., and Wang, Y. (2006). Air-sea exchange of carbon dioxide in ocean margins: A province-based synthesis. *Geophysical Research Letters*, 33(12).

Cai, W.J., Guo, X., Chen, C.T.A., Dai, M., Zhang, L., Zhai, W., Lohrenz, S.E., Yin, K., Harrison, P.J. and Wang, Y. (2008). A comparative overview of weathering intensity and

HCO<sub>3</sub><sup>-</sup> flux in the world's major rivers with emphasis on the Changjiang, Huanghe, Zhujiang (Pearl) and Mississippi Rivers. *Continental Shelf Research*, 28(12), 1538-1549.

Cai, W. J., Hu, X., Huang, W. J., Jiang, L. Q., Wang, Y., Peng, T. H., and Zhang, X. (2010a). Alkalinity distribution in the western North Atlantic Ocean margins. *Journal of Geophysical Research: Oceans (1978–2012)*, 115(C8).

Cai, W. J., Luther III, G. W., Cornwell, J. C., and Giblin, A. E. (2010b). Carbon cycling and the coupling between proton and electron transfer reactions in aquatic sediments in Lake Champlain. *Aquatic Geochemistry*, 16(3), 421-446.

Chen, C. T. A., and Borges, A. V. (2009). Reconciling opposing views on carbon cycling in the coastal ocean: continental shelves as sinks and near-shore ecosystems as sources of atmospheric CO<sub>2</sub>. *Deep Sea Research Part II: Topical Studies in Oceanography*, 56(8), 578-590.

Chen, C. T. A., Zhai, W., and Dai, M. (2008). Riverine input and air–sea CO<sub>2</sub> exchanges near the Changjiang (Yangtze River) Estuary: status quo and implication on possible future changes in metabolic status. *Continental Shelf Research*, 28(12), 1476-1482.

Chen, C. T. A., Huang, T. H., Chen, Y. C., Bai, Y., He, X., and Kang, Y. (2013). Air–sea exchanges of CO<sub>2</sub> in the world's coastal seas. *Biogeosciences*, 10(10), 6509-6544.

Cifuentes, L. A., Sharp, J. H., and Fogel, M. L. (1988). Stable carbon and nitrogen isotope biogeochemistry in the Delaware estuary. *Limnology and Oceanography*, 33(5), 1102-1115.

Cole, J. J., Caraco, N. F., Kling, G. W., and Kratz, T. K. (1994). Carbon dioxide supersaturation in the surface waters of lakes. *Science*, 265(5178), 1568-1570.

Cotrim da Cunha, L., Buitenhuis, E. T., Le Quéré, C., Giraud, X., and Ludwig, W. (2007). Potential impact of changes in river nutrient supply on global ocean biogeochemistry. *Global Biogeochemical Cycles*, 21(4).

Crosswell, J. R., Wetz, M. S., Hales, B., and Paerl, H. W. (2012). Air-water CO<sub>2</sub> fluxes in the microtidal Neuse River Estuary, North Carolina. *Journal of Geophysical Research: Oceans (1978–2012)*, 117(C8).

Culberson, C. H. (1988). Dissolved oxygen, inorganic carbon, and the acid–base system in the Delaware Estuary. *Ecology and restoration of the Delaware River Basin. Pennsylvania Academy of Sciences*, 58-76.

Culberson, C. H., Biggs, R. B., Church, T. M., Lee, B. W., Sharp, J. H., and Pennock, J. R. (1987). *Data from the YABLED Cruises, September 1981-July 1984*.

Dai, T., and Wiegert, R. G. (1996). Estimation of the primary productivity of *Spartina alterniflora* using a canopy model. *Ecography*, 410-423.

Dickson, A. G., and Millero, F. J. (1987). A comparison of the equilibrium constants for the dissociation of carbonic acid in seawater media. *Deep Sea Research Part A. Oceanographic Research Papers*, 34(10), 1733-1743.

Dickson, A. G., Sabine, C. L., and Christian, J. R. (2007). Guide to best practices for ocean CO<sub>2</sub> measurements.

Doney, S. C. (2010). The growing human footprint on coastal and open-ocean biogeochemistry. *Science*, 328(5985), 1512-1516.

Downing, J.A., Cole, J.J., Middelburg, J.J., Striegl, R.G., Duarte, C.M., Kortelainen, P., Prairie, Y.T. and Laube, K.A. (2008). Sediment organic carbon burial in agriculturally eutrophic impoundments over the last century. *Global Biogeochemical Cycles*, 22(1).

Edmond, J. M., Boyle, E. A., Grant, B., and Stallard, R. F. (1981). The chemical mass balance in the Amazon plume I: the nutrients. *Deep Sea Research Part A. Oceanographic Research Papers*, 28(11), 1339-1374.

Edmond, J. M., Spivack, A., Grant, B. C., Ming-Hui, H., Zexiam, C., Sung, C., and Xiushau, Z. (1985). Chemical dynamics of the Changjiang estuary. *Continental Shelf Research*, 4(1), 17-36.

Feely, R. A., Doney, S. C., and Cooley, S. R. (2009). Ocean acidification: present conditions and future changes in a high-CO<sub>2</sub> world.

Ferrón, S., Ortega, T., Gómez-Parra, A., and Forja, J. M. (2007). Seasonal study of dissolved CH<sub>4</sub>, CO<sub>2</sub> and N<sub>2</sub>O in a shallow tidal system of the bay of Cádiz (SW Spain). *Journal of Marine Systems*, 66(1), 244-257.

Frankignoulle, M., Abril, G., Borges, A., Bourge, I., Canon, C., Delille, B., Libert, E. and Théate, J.M. (1998). Carbon dioxide emission from European estuaries. *Science*, 282(5388), 434-436.

Frithsen, J. B., Killam, K., and Young, M. (1991). *An assessment of key biological resources in the Delaware River estuary*. Versar, Incorporated.

Gazeau, F., Borges, A.V., Barrón, C., Duarte, C.M., Iversen, N., Middelburg, J.J., Delille, B., Pizay, M.D., Frankignoulle, M. and Gattuso, J.P. (2005). Net ecosystem metabolism in a micro-tidal estuary (Randers Fjord, Denmark): evaluation of methods. *Marine Ecology-Progress Series*, 301, 23-41.

Gran, G. (1952). Determination of the equivalence point in potentiometric titrations. Part II. *Analyst*, 77(920), 661-671.

Guo, X., Cai, W. J., Zhai, W., Dai, M., Wang, Y., and Chen, B. (2008). Seasonal variations in the inorganic carbon system in the Pearl River (Zhujiang) estuary. *Continental Shelf Research*, 28(12), 1424-1434.

Huang, W. J., Wang, Y., and Cai, W. J. (2012). Assessment of sample storage techniques for total alkalinity and dissolved inorganic carbon in seawater. *Limnology and Oceanography: Methods*, 10(9), 711-717.

Huang, W. J., Cai, W. J., Wang, Y., Lohrenz, S. E., and Murrell, M. C. (2015). The carbon dioxide system on the Mississippi River-dominated continental shelf in the northern Gulf of Mexico: 1. Distribution and air-sea CO<sub>2</sub> flux. *Journal of Geophysical Research: Oceans*, 120(3), 1429-1445.

Hunt, C. W., Salisbury, J. E., Vandemark, D., and McGillis, W. (2011). Contrasting carbon dioxide inputs and exchange in three adjacent New England estuaries. *Estuaries and Coasts*, 34(1), 68-77.

Hunt, C. W., Salisbury, J. E., and Vandemark, D. (2014). CO<sub>2</sub> Input Dynamics and Air-Sea Exchange in a Large New England Estuary. *Estuaries and Coasts*, 37(5), 1078-1091.

IPCC, A. (2007). Intergovernmental panel on climate change. *Climate change 2007: Synthesis report*.

Jiang, L. Q., Cai, W. J., and Wang, Y. (2008a). A comparative study of carbon dioxide degassing in river-and marine-dominated estuaries. *Limnology and Oceanography*, 53(6), 2603-2615.

Jiang, L. Q., Cai, W. J., Wanninkhof, R., Wang, Y., and Lüger, H. (2008b). Air-sea CO<sub>2</sub> fluxes on the US South Atlantic Bight: Spatial and seasonal variability. *Journal of Geophysical Research: Oceans (1978–2012)*, 113(C7).

Joesoef, A., Huang, W. J., Gao, Y., and Cai, W. J. (2015). Air–water fluxes and sources of carbon dioxide in the Delaware Estuary: spatial and seasonal variability. *Biogeosciences*, 12(20), 6085-6101.

Karim, A., and Veizer, J. (2000). Weathering processes in the Indus River Basin: implications from riverine carbon, sulfur, oxygen, and strontium isotopes. *Chemical Geology*, 170(1), 153-177.

Kauffman, G., Belden, A., and Homsey, A. (2009). Technical Summary: State of the Delaware Basin Report.

Ketchum, B. H. (1952). *The distribution of salinity in the estuary of the Delaware River*. Woods Hole Oceanographic Institution.

Laruelle, G. G., Lauerwald, R., Rotschi, J., Raymond, P. A., Hartmann, J., and Regnier, P. (2015). Seasonal response of air–water CO<sub>2</sub> exchange along the land–ocean aquatic continuum of the northeast North American coast. *Biogeosciences*, 12(5), 1447-1458.

Le Quéré, C., Moriarty, R., Andrew, R. M., Peters, G. P., Ciais, P., Friedlingstein, P., Jones, S. D., Sitch, S., Tans, P., Arneeth, A., Boden, T. A., Bopp, L., Bozec, Y., Canadell, J. G., Chini, L. P., Chevallier, F., Cosca, C. E., Harris, I., Hoppema, M., Houghton, R. A.,

House, J. I., Jain, A. K., Johannessen, T., Kato, E., Keeling, R. F., Kitidis, V., Klein Goldewijk, K., Koven, C., Landa, C. S., Landschützer, P., Lenton, A., Lima, I. D., Marland, G., Mathis, J. T., Metzler, N., Nojiri, Y., Olsen, A., Ono, T., Peng, S., Peters, W., Pfiel, B., Poulter, B., Raupach, M. R., Regnier, P., Rödenbeck, C., Saito, S., Salisbury, J. E., Schuster, U., Schwinger, J., Séférian, R., Segschneider, J., Steinhoff, T., Stocker, B. D., Sutton, A. J., Takahashi, T., Tilbrook, B., van der Werf, G. R., Viovy, N., Wang, Y. P., Wanninkhof, R., Wiltshire, A., and Zeng, N. (2015). Global carbon budget 2014. *Earth System Science Data*, 7(1), 47-85.

Lebo, M.L., L.A. Cifuentes, M.L. Fogel, M.P. Hoch, R.G. Keil, D.L. Kirchman, J.M. Ludlam, J.R. Pennock, J.H. Sharp, P.T. Spicer, and D.J. Velinsky. (1990). *Data from the Delaware Estuary Scenic Cruises, April 1986 – September 1988*.

Li, J. Y., and Zhang, J. (2003). Variations of solid content and water chemistry at Nantong station and weathering processes of the Changjiang watershed. *Resources and Environment in the Yangtze Basin*, 12(4), 363-369.

Liu, Z., Zhang, L., Cai, W. J., Wang, L., Xue, M., and Zhang, X. (2014). Removal of dissolved inorganic carbon in the Yellow River Estuary. *Limnology and Oceanography*, 59(2), 413-426.

Marino, G. R., DiLorenzo, J. L., Litwack, H. S., Najarian, T. O., and Thatcher, M. L. (1991). General water quality assessment and trend analysis of the Delaware Estuary. *Part one: Status and Trends. Delaware River Basin Commission. West Trenton, NJ*.

Mayorga, E., Aufdenkampe, A. K., Masiello, C. A., Krusche, A. V., Hedges, J. I., Quay, P. D., Richey, J. E. and Brown, T. A. (2005). Young organic matter as a source of carbon dioxide outgassing from Amazonian rivers. *Nature*, 436(7050), 538-541.

McGillis, W. R., Edson, J. B., Hare, J. E., and Fairall, C. W. (2001). Direct covariance air-sea CO<sub>2</sub> fluxes. *Journal of Geophysical Research: Oceans (1978–2012)*, 106(C8), 16729-16745.

McGillis, W.R., Edson, J.B., Zappa, C.J., Ware, J.D., McKenna, S.P., Terray, E.A., Hare, J.E., Fairall, C.W., Drennan, W., Donelan, M., DeGrandpre, M.D., Wanninkhof, R., and Feely, R. A. (2004). Air-sea CO<sub>2</sub> exchange in the equatorial Pacific. *Journal of Geophysical Research: Oceans (1978–2012)*, 109(C8).

Mehrbach, C., Culbertson, C. H., Hawley, J. E., and Pytkowicz, R. M. (1973). Measurement of the apparent dissociation constants of carbonic acid in seawater at atmospheric pressure. *Limnology and Oceanography*, 18(6), 897-907.

Millero, F. J. (2009). Effect of Ocean acidification on the speciation of metals in seawater. *Oceanography*, 22(4), 72.

Millero, F. J., Graham, T. B., Huang, F., Bustos-Serrano, H., and Pierrot, D. (2006). Dissociation constants of carbonic acid in seawater as a function of salinity and temperature. *Marine Chemistry*, 100(1), 80-94.

Milliman, J. D., and Boyle, E. 1975, Biological uptake of dissolved silica in the Amazon river estuary. *Science*, 189, 995-997.

Neubauer, S. C., and Anderson, I. C. (2003). Transport of dissolved inorganic carbon from a tidal freshwater marsh to the York River estuary. *Limnology and Oceanography*, 48(1), 299-307.

Officer, C. B. (1979). Discussion of the behaviour of nonconservative dissolved constituents in estuaries. *Estuarine and Coastal Marine Science*, 9(1), 91-94.

Orr, J. C., Fabry, V. J., Aumont, O., Bopp, L., Doney, S. C., Feely, R. A., Gnanadesikan, A., Gruber, N., Ishida, A., Joos, F. and Key, R. M., Lindsay, K., Maier-Reimer, E., Matear, R., Monfray, P., Mouchet, A., Naijar, R. G., Plattner, G. K., Rodgers, K. B., Sabine, C. L., Sarmiento, J. L., Schlitzer, R., Slater, R. D., Totterdell, I. J., Weirig, M. F., Yamanaka, Y., and Yool, A. (2005). Anthropogenic ocean acidification over the twenty-first century and its impact on calcifying organisms. *Nature*, 437(7059), 681-686.

Pennock, J. R. (1987). Temporal and spatial variability in phytoplankton ammonium and nitrate uptake in the Delaware Estuary. *Estuarine, Coastal and Shelf Science*, 24(6), 841-857.

Pierrot, D., Lewis, E., and Wallace, D. W. R. (2006). CO2SYS DOS Program developed for CO<sub>2</sub> system calculations. *ORNL/CDIAC-105. Carbon Dioxide Information Analysis Center, Oak Ridge National Laboratory, US Department of Energy, Oak Ridge, TN.*

Probst, J. L., NKoukou, R. R., Krempp, G., Bricquet, J. P., Thiébaux, J. P., and Olivry, J. C. (1992). Dissolved major elements exported by the Congo and the Ubangi rivers during the period 1987–1989. *Journal of Hydrology*, 135(1), 237-257.

Quinton, J. N., Govers, G., Van Oost, K., and Bardgett, R. D. (2010). The impact of agricultural soil erosion on biogeochemical cycling. *Nature Geoscience*, 3(5), 311-314.

Raymond, P. A., and Cole, J. J. (2001). Gas exchange in rivers and estuaries: Choosing a gas transfer velocity. *Estuaries and Coasts*, 24(2), 312-317.

Raymond, P. A., Caraco, N. F., and Cole, J. J. (1997). Carbon dioxide concentration and atmospheric flux in the Hudson River. *Estuaries*, 20(2), 381-390

Raymond, P. A., Bauer, J. E., and Cole, J. J. (2000). Atmospheric CO<sub>2</sub> evasion, dissolved inorganic carbon production, and net heterotrophy in the York River estuary. *Limnology and Oceanography*, 45(8), 1707-1717.

Regnier, P., Friedlingstein, P., Ciais, P., Mackenzie, F. T., Gruber, N., Janssens, I. A., Laruelle, G. G., Lauerwald, R., Luysaert, S., Andersson, A. J., Arndt, S., Arnosti, C., Borges, A. V., Dale, A. W., Gallego-Sala, A., Godderis, Y., Goossens, N., Hartmann, J., Heinze, C., Ilyina, T., Joos, F., LaRowe, D. E., Leifeld, J., Meysman, F. J. R., Munhoven, G., Raymond, P. A., Spahni, R., Suntharalingam, P., and Thullner, M. (2013). Anthropogenic perturbation of the carbon fluxes from land to ocean. *Nature Geoscience*, 6(8), 597-607.

Sabine, C. L., Feely, R. A., Gruber, N., Key, R. M., Lee, K., Bullister, J. L., Wanninkhof, R., Wong, C., Wallace, D. W., Tilbrook, B. and Millero, F. J., Peng, T. H., Kozyr, A., Ono, T., and Rios, A. F. (2004). The oceanic sink for anthropogenic CO<sub>2</sub>. *Science*, 305(5682), 367-371.

Salisbury, J. E., Vandemark, D., Hunt, C. W., Campbell, J. W., McGillis, W. R., and McDowell, W. H. (2008). Seasonal observations of surface waters in two Gulf of Maine estuary-plume systems: Relationships between watershed attributes, optical measurements and surface pCO<sub>2</sub>. *Estuarine, Coastal and Shelf Science*, 77(2), 245-252.

Sharp, J. H. (1983). The Delaware estuary: Research as background for estuarine management and development. *Univ. Delaware and New Jersey Mar. Sci. Consort.*

Sharp, J. H. (2010). Estuarine oxygen dynamics: What can we learn about hypoxia from long-time records in the Delaware Estuary? *Limnology and Oceanography*, 55(2), 535-548.

Sharp, J. H., Cifuentes, L. A., Coffin, R. B., Pennock, J. R., and Wong, K. C. (1986). The influence of river variability on the circulation, chemistry, and microbiology of the Delaware Estuary. *Estuaries*, 9(4), 261-269.

Sharp, J.H., Yoshiyama, K., Parker, A.E., Schwartz, M.C., Curless, S.E., Bearegard, A.Y., Ossolinski, J.E. and Davis, A.R. (2009). A biogeochemical view of estuarine eutrophication: seasonal and spatial trends and correlations in the Delaware Estuary. *Estuaries and Coasts*, 32(6), 1023-1043.

Sheldon, J. E., and Alber, M. (2002). A comparison of residence time calculations using simple compartment models of the Altamaha River Estuary, Georgia. *Estuaries*, 25(6), 1304-1317.

Sloto, R. A. (1990). *Geohydrology and simulation of ground-water flow in the carbonate rocks of the Valley Creek basin, eastern Chester County, Pennsylvania*. Department of the Interior, US Geological Survey.

Smullen, J. T., Sharp, J. H., Garvine, R. W., and Haskin, H. H. (1984). River flow and salinity. *Excerpts from The Delaware Estuary: Research as Background for Estuarine Management and Development*, 9-25.

Stocker, T.F., Qin, D., Plattner, G.K., Tignor, M., Allen, S.K., Boschung, J., Nauels, A., Xia, Y., Bex, B. and Midgley, B.M. (2013). IPCC, 2013: climate change 2013: the physical science basis. Contribution of working group I to the fifth assessment report of the intergovernmental panel on climate change.

Sunda, W. G., and Cai, W. J. (2012). Eutrophication Induced CO<sub>2</sub>-Acidification of Subsurface Coastal Waters: Interactive Effects of Temperature, Salinity, and Atmospheric pCO<sub>2</sub>. *Environmental Science and Technology*, 46(19), 10651-10659.

Sutton, C. C., O'Herron, J. C., and Zappalorti, R. T. (1996). *The Scientific Characterization of the Delaware Estuary: Y Clay C. Sutton, John C. O'Herron II, and Robert T. Zappalorti*. Delaware Estuary Program.

Takahashi, T., Olafsson, J., Goddard, J. G., Chipman, D. W., and Sutherland, S. C. (1993). Seasonal variation of CO<sub>2</sub> and nutrients in the high-latitude surface oceans: A comparative study. *Global Biogeochemical Cycles*, 7(4), 843-878.

Takahashi, T., Sutherland, S.C., Sweeney, C., Poisson, A., Metzl, N., Tilbrook, B., Bates, N., Wanninkhof, R., Feely, R.A., Sabine, C. Olafsson, J., and Nojin, Yukihiro. (2002). Global sea-air CO<sub>2</sub> flux based on climatological surface ocean pCO<sub>2</sub>, and seasonal biological and temperature effects. *Deep Sea Research Part II: Topical Studies in Oceanography*, 49(9), 1601-1622.

Ternon, J. F., Oudot, C., Dessier, A., and Diverres, D. (2000). A seasonal tropical sink for atmospheric CO<sub>2</sub> in the Atlantic Ocean: the role of the Amazon River discharge. *Marine Chemistry*, 68(3), 183-201.

Trabalka, J. R., and Reichle, D. E. (1983). The Changing Carbon Cycle: a Global Analysis. *Oak Ridge National Laboratory, Knoxville, TN*, 592.

Tranvik, L.J., Downing, J.A., Cotner, J.B., Loiselle, S.A., Striegl, R.G., Ballatore, T.J., Dillon, P., Finlay, K., Fortino, K., Knoll, L.B. Kortelainen, P.L., Kutser, T., Larsen, S., Laurion, I., Leech, D. M., McCallister, S. L., McKnight, D. M., Melack, J. M., Overholt, E., Porter, J. A., Prairie, Y., Renwick, W. H., Roland, F., Sherman, B. S., Schindler, D. W., Sobek, S., Tremblay, A., Vanni, M. J., Verschoor, A. M., Wachenfeldt, E., and Weyhenmeyer, G. A. (2009). Lakes and reservoirs as regulators of carbon cycling and climate. *Limnology and Oceanography*, 54(6part2), 2298-2314.

Turner, R. E., Rabalais, N. N., and Nan, Z. Z. (1990). Phytoplankton biomass, production and growth limitations on the Huanghe (Yellow River) continental shelf. *Continental Shelf Research*, 10(6), 545-571.

Voynova, Y. G., and Sharp, J. H. (2012). Anomalous biogeochemical response to a flooding event in the Delaware Estuary: a possible typology shift due to climate change. *Estuaries and Coasts*, 35(4), 943-958.

Wang, Z. A., and Cai, W. J. (2004). Carbon dioxide degassing and inorganic carbon export from a marsh-dominated estuary (the Duplin River): A marsh CO<sub>2</sub> pump. *Limnology and Oceanography*, 49(2), 341-354.

Wang, Z. A., Cai, W. J., Wang, Y., and Upchurch, B. L. (2003). A long pathlength liquid-core waveguide sensor for real-time pCO<sub>2</sub> measurements at sea. *Marine chemistry*, 84(1), 73-84.

Wanninkhof, R. (1992). Relationship between wind speed and gas exchange. *Journal of Geophysical Research*, 97(25), 7373-7382.

Wanninkhof, R. (2014). Relationship between wind speed and gas exchange over the ocean revisited. *Limnology and Oceanography: Methods*, 12(6), 351-362.

Wanninkhof, R., Doney, S. C., Takahashi, T., and McGillis, W. R. (2002). The Effect of Using Time-Averaged Winds on Regional Air-Sea CO<sub>2</sub> Fluxes. *Geophysical Monograph Series*, 27, 351-356.

Wanninkhof, R., Asher, W. E., Ho, D. T., Sweeney, C., and McGillis, W. R. (2009). Advances in quantifying air-sea gas exchange and environmental forcing. *Marine Science*, 1, 213-244.

Weiss, R. (1974). Carbon dioxide in water and seawater: the solubility of a non-ideal gas. *Marine Chemistry*, 2(3), 203-215.

White, A. F. (2003). Natural weathering rates of silicate minerals. *Treatise on Geochemistry*, 5, 133-168.

White, A. F., and Blum, A. E. (1995). Effects of climate on chemical weathering in watersheds. *Geochimica et Cosmochimica Acta*, 59(9), 1729-1747.

Woods, A. J., Omernik, J. M., and Brown, D. D. (1999). Level III and IV ecoregions of Delaware, Maryland, Pennsylvania, Virginia, and West Virginia. *US Environmental Protection Agency, National Health and Environmental Effects Research Laboratory, Corvallis, Oregon. Report with map supplement, Scale, 1, 1-000.*

Yoshiyama, K., and Sharp, J. H. (2006). Phytoplankton response to nutrient enrichment in an urbanized estuary: Apparent inhibition of primary production by overeutrophication. *Limnology and Oceanography*, 51(1part2), 424-434.

Zappa, C.J., McGillis, W.R., Raymond, P.A., Edson, J.B., Hints, E.J., Zemmelen, H.J., Dacey, J.W. and Ho, D.T. (2007). Environmental turbulent mixing controls on air-water gas exchange in marine and aquatic systems. *Geophysical Research Letters*, 34(10).

## Appendix A

### TEMPERATURE DERIVED COEFFICIENTS

We first derived temperature constants for a general estuarine system using the Excel macro CO2SYS (Pierrot, 2006) and inorganic carbon dissociation constants from Millero et al., (2006) for estuarine waters ( $S < 30$ ) and from Mehrbach et al., (1973) refit by Dickson and Millero (1987) for high salinity waters ( $S > 30$ ). Based on data collected over the past two years, river and ocean end-members of TA (900 and 2300  $\mu\text{mol kg}^{-1}$ , respectively) and of DIC (960 and 2000  $\mu\text{mol kg}^{-1}$ , respectively) were used. Calculated  $p\text{CO}_2$  varied among different temperatures, from 5 to 30°C, with the largest difference in low salinities (0 to 5) (Figure A1). In turn, when binning salinities to intervals of 5 units, the greatest variability in temperature constants was observed in salinities 0-5 and 5-10 (Table A1). Averaged values of  $(\partial \ln p\text{CO}_2 / \partial T)$  for salinity intervals between 0-35 ranged from 0.0332 to 0.0420  $^{\circ}\text{C}^{-1}$  (Table A1).

Table A1: Averaged temperature coefficients ( $\partial \ln p\text{CO}_2 / \partial T$ ) for each salinity bin.

Simulated surface water  $p\text{CO}_2$  values at varying salinities were computed using river and ocean end-member TA and DIC values of 900 and 960  $\mu\text{mol kg}^{-1}$  and 2300 and 2000, respectively.

Salinity	Coefficient
0 – 5	0.0332
5 – 10	0.0382
10 – 15	0.0411
15 – 20	0.0417
20 – 25	0.0417
25 – 30	0.0415
30 – 35	0.0420

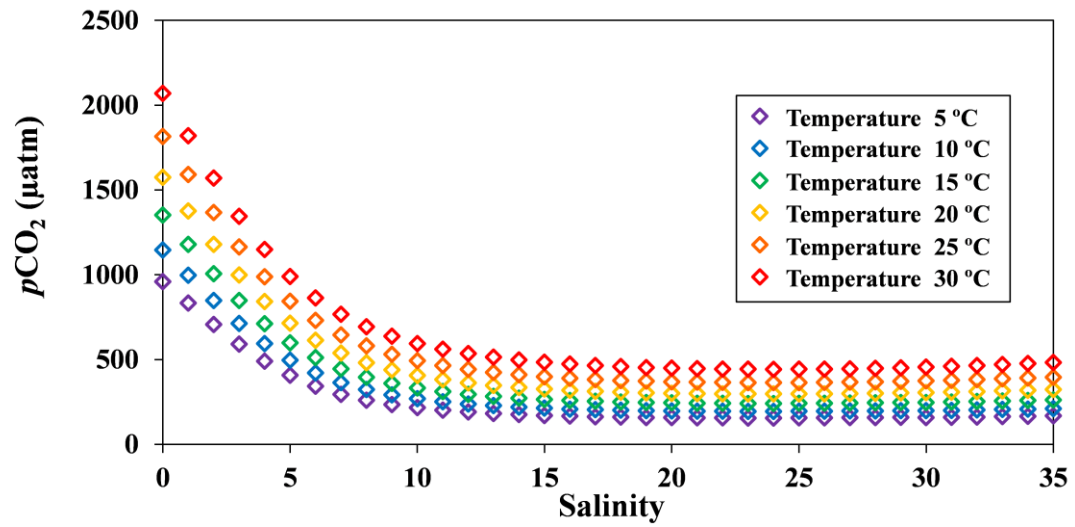


Figure A1. Simulated surface water  $p\text{CO}_2$  against salinity grouped by temperature bins. Surface water  $p\text{CO}_2$  values were calculated using river and ocean end-member TA and DIC values of 900 and 960  $\mu\text{mol kg}^{-1}$  and 2300 and 2000  $\mu\text{mol kg}^{-1}$ , respectively.

## Appendix B

### TEMPERATURE AND BIOLOGICAL EFFECT

Using similar methods as performed in Takahashi et al., (2002), we calculate the thermal effects on surface water  $p\text{CO}_2$  in each salinity interval as follows:

$$\Delta p\text{CO}_{2\text{thermal}} = (p\text{CO}_{2\text{mean}} \text{ at } T_{\text{obs}})_{\text{max}} - (p\text{CO}_{2\text{mean}} \text{ at } T_{\text{obs}})_{\text{min}} \quad (\text{B1})$$

where  $(p\text{CO}_{2\text{mean}} \text{ at } T_{\text{obs}})_{\text{max}}$  and  $(p\text{CO}_{2\text{mean}} \text{ at } T_{\text{obs}})_{\text{min}}$  are the maximum and minimum  $p\text{CO}_{2\text{mean}} \text{ at } T_{\text{obs}}$  values, respectively. In other words, the thermal effects on the mean annual  $p\text{CO}_2$  value is represented by the seasonal amplitude of  $(p\text{CO}_{2\text{mean}} \text{ at } T_{\text{obs}})$  values computed using Eq. (7). Likewise, the non-thermal effects (biological and mixing processes) on surface water  $p\text{CO}_2$  were calculated as follows (Takahashi et al., 2002):

$$\Delta p\text{CO}_{2\text{non-thermal}} = (p\text{CO}_{2\text{obs}} \text{ at } 13.3 \text{ }^\circ\text{C})_{\text{max}} - (p\text{CO}_{2\text{obs}} \text{ at } 13.3 \text{ }^\circ\text{C})_{\text{min}} \quad (\text{B2})$$

where  $(p\text{CO}_{2\text{obs}} \text{ at } 13.3 \text{ }^\circ\text{C})_{\text{max}}$  and  $(p\text{CO}_{2\text{obs}} \text{ at } 13.3 \text{ }^\circ\text{C})_{\text{min}}$  are the maximum and minimum  $p\text{CO}_{2\text{obs}} \text{ at } 13.3 \text{ }^\circ\text{C}$  values, respectively. Thus, the non-thermal thermal effects on surface water  $p\text{CO}_2$  ( $p\text{CO}_{2\text{obs}} \text{ at } 13.3 \text{ }^\circ\text{C}$ ) is represented by the seasonal amplitude of  $p\text{CO}_2$  values corrected to the 10-year (2004-2014) annual mean temperature using Eq. (6). The relative importance of these effects in each salinity interval can be expressed as the difference between  $\Delta p\text{CO}_{2\text{thermal}}$  and  $\Delta p\text{CO}_{2\text{non-thermal}}$  ( $T - B$ ) or the ratio of  $\Delta p\text{CO}_{2\text{thermal}}$  to  $\Delta p\text{CO}_{2\text{non-thermal}}$  ( $T/B$ ). In estuarine regions where thermal effects on surface water  $p\text{CO}_2$  exceed non-thermal effects, the ( $T/B$ ) ratio is greater than 1 or ( $T - B$ ) is positive, whereas in areas where non-thermal effects dominate, the ( $T/B$ ) ratio is less than 1 or ( $T - B$ ) is negative.